universität wien

DIPLOMARBEIT

Titel der Diplomarbeit

How to bridle a homeodomain protein: characterization of At KNB36 and At MPB2C

angestrebter akademischer Grad

Magister der Naturwissenschaften (Mag.rer.nat.)

Verfasser:	Gregor Kollwig
Studienrichtung/Studienzweig:	Biologie/Genetik - Mikrobiologie
Betreuer:	Univ. Doz. Dr. Friedrich Kragler

Wien, am 30.06.2010

TABLE OF CONTENTS

Ob du denkst daß du etwas tun kannst, oder ob du denkst daß du es nicht tun kannst -
in beiden Fällen hast du Recht. [Henry Ford]

ZUSAMMENFASSUNG

Selektiver, gerichteter Transport von Proteinen zwischen pflanzlichen Zellen erfolgt über symplasmische Verbindungungen, die Plasmodesmata. Die Präsenz von bestimmten Proteinen wie zum Beispiel den Homöotischen Transkriptionsfaktoren Zm KNOTTED1 (KN1) und At SHOOTMERISTMLESS (STM), ist maßgeblich für die korrekte Entwicklung und Aufrechterhaltung der unterschlichen Gewebe und definiert somit die Gestaltbildung der Pflanze. Einige dieser Faktoren können den symplasmischen Transportweg via Plasmodesmata nutzen um in benachbarte Zellen zu gelangen. Um eine korrekte Differenzierung und räumliche Anordnung der unterschiedlichen Gewebe zu gewährleisten, muß die Pflanze diesen Transport strikt regulieren.
KN1 aus *Zea Mays*, wie auch das homologe Protein STM aus *Arabidopsis thaliana*, sind essentiell für die Entwicklung und Aufrechterhaltung des Apikalmeristems, einem Reservoir von Stammzellen aus welchen jedes neue Organ hervorgebracht wird. In dieser Arbeit werden die Proteine At KNB36 und At MPB2C und ihr regulatives Potential in Bezug auf KN1 und STM charakterisiert.
Hierfür wurden transgene GUS-Reporterlinien etabliert welche die gewebespezifische Expression von MPB2C und KNB36 in *Arabidopsis* reflektieren. Anschließend wurden die resultierenden Expressionsmuster mit jenen von KN1 und STM verglichen, um die Frage zu beantworten ob die Gewebespezifität *in planta* korreliert. Wie KN1/STM werden auch KNB36 und MPB2C in Meristemen bzw deren Peripherie exprimiert. Um zu untersuchen, ob die so gefundene Korrelation der Expressionsmuster auch eine Kolokalisation der Proteine auf subzellulärer Ebene zur Folge hat, wurden transgene Pflanzenlinien generiert in welchen jeweils MPB2C-GFP/TAP oder KNB36-RFP/GFP/TAP überexprimiert werden. Konfokalmikroskopische Analysen zeigten KNB36-GFP/RFP als zellkern-lokalisiertes, und verifizierten MPB2C-GFP als cytoplasmisches, mikrotubuli-assoziertes Fusionsprotein. KN1-GFP/RFP Fusionsproteine welche in diesen Pflanzen transient überexprimiert wurden zeigten hier Colokalisation mit KNB36 im Nucleus und ebenfalls mit MPB2C an den Microtubuli.
Um eine Interaktion zwischen den untersuchten Proteinen und Homeodomän Transkriptionsfaktoren dezidiert zu verifizieren und deren Natur aufzuklären, wurden die MPB2C- und KNB36- fusionskonstrukte in einer trichomdefizienten Linie etabliert.
In dieser Linie fungiert eine KN1-domaine als zentrales Element für ein transport-abhängiges Phenotyp-komplementationsystem.
Durch statistische Trichomenerfassung und Konfokalmikroskopie konnte bewiesen werden, daß MPB2C KN1 bindet und an den Mikrotubuli arretiert. KNB36 hingegen, scheint den Abbau von KN1 zu induzieren.
Da KNB36 selbst KN1 nicht binden kann, postulieren wir die Bildung eines trimeren Komplexes aus KNB36, MPB2C und KN1/STM. Das Kalkül dieser These äußert sich in der Wildtyppflanze dahingehend daß MPB2C Homöotische Proteine, wie KN1 und STM, welche über die Ränder des Meristems hinaustransportiert werden, an den Mikrotubuli arretiert, wo, nach Bildung eines trimeren Komplexes, ihre Degradation durch KNB36 eingeleitet wird.

ABSTRACT

In plants, selective cell-to-cell transport of proteins is provided by the symplasmic pathway, the plasmodesmata. The presence of specific proteins, like the homeodomain transcription factors Zm KNOTTED1 (KN1) and At SHOOTMERISTEMLES (STM), is required for correct development and maintenance of different tissues and therefore essential for plant morphology.
Some distinct homeodomain proteins are able to use the symplasmic pathway via plasmodesmata to move into adjacent cells. To assure correct organ differentiation and spatial arrangement of organs, transport of these factors is strictly regulated.
KN1 from *Zea Mays* and its homolog STM from *Arabidopsis thaliana* are essential for development and maintenance of the shoot apical meristem, a pool of stem cells which represents the origin of new organs. This work is about the characterization of the proteins At KNB36 and At MPB2C and their regulative potential regarding KN1 and STM. To examine tissue specific expression of MPB2C and KNB36 in *Arabidopsis*, transgenic GUS-reporterlines were established. Subsequently the resulting expression patterns were compared to those of KN1 and STM to examine tissue specific correlations *in planta*. Like KN1/STM, KNB36 and MPB2C are expressed within, respectively around meristems. Transgenic lines expressing MPB2C-GFP/TAP and KNB36-RFP/GFP/TAP were established to find out if the proteins also colocalize on a subcelluar level. Confocal microscopy revealed KNB36-GFP/RFP as a nucleus localized protein and verifies MPB2C in the cytoplasm, associated with microtubules. For close investigations of the interaction between the investigated proteins and homeodomain transcription factors, MPB2C and KNB36 fusion proteins were established in a transgenic trichome rescue line. In this line, phenotypic complementation is facilitated through the transport of the KN1 homeodomain. Statistical aquisition of trichome numbers as well as microscopy analysis showed that MPB2C arrests KN1 at the microtubules. Furthermore, KNB36 seems to trigger degradation of KN1. Because KNB36 is not able to interact with the KN1 homeodomain, we predict the formation of a trimeric complex composed of KNB36, MPB2C and KN1/STM.
In summary, homeodomain proteins like KN1 and STM are transported beyond meristematic borders where MPB2C arrests them at the microtubules, followed by KNB36 dependend degradation.

I. INTRODUCTION

1. *Transport mechanisms in plant cells*

1.1 Plant cell versus animal cell

An arbitrary multicellular organism like the animal, human or plant one, is only able to develop proper and maintain functioning, if an interchange of material between single cells is provided. This interchange, or transport, and can proceed in a passive as well as in an active way. Transported material normally serves as nutrient, information – or energy carrier.

One of the probably most important differences between animal and plant tissue is given by the fact that the differentiation (specialization) of the animal cell depends on its ancestor. Through the principle of the so called cell linage, the tissues of the animal organism are defined early in development. As a general rule, the division of a single cell results in two daughter cells of the same kind as their ancestor.

In contrast to the animal cells, the fate of the plant cell is generally determined late in development. Not the character of the ancestor is crucial, but rather the position within the organism. Here, the exchange of so called “positional information” between the single cells, provides the means to sense the exact position within the plant organism and their fate.

Individual animal cells are linked via symplasmic channels. In 1967, Paul Revel and Morris Karnovsky were the first who made regular arranged proteinogenic channels with a diameter of 1,5 – 2 nm viewable. These so called GAP JUNCTIONS are composed of two kinds of proteins, pannexins and connexins, which facilitate an intercellular exchange of ions, second messengers and small metabolites (Mese et al., 2007; Robertson, 1963; Revel and Karnovsky, 1967).
Another connection system can be found in the recently discovered TUNNELING NANO TUBES (TNT). They have a diameter of 50 – 200 nm and their membranes appeared to be continuous between connected cells. This membrane bridges are suggested to form de novo during a 4-minute period between dislodging cells. They provide a cell-to-cell pathway for various cargo over an incredible length of up to 140µm (Figure 1). TNT-mediated interexchange is supposed to play a important, but unexplored role in the immune system and shows striking similarity to plasmodesmata present in the plant kingdom (Rustom et al., 2004; Gerdes et al., 07).

Figure1: Tunnelling Nano Tubes – electron micrograph

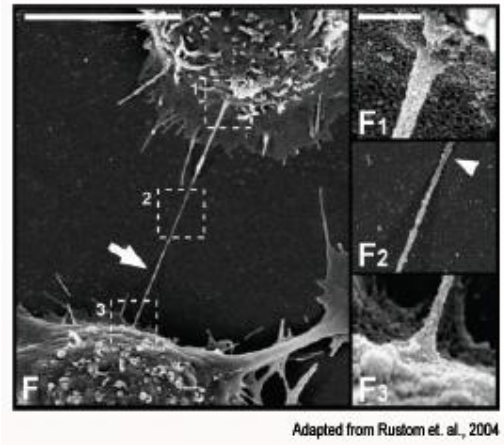

Note: (F) TNT between rat pheochromocytoma PC12 cells imaged by scanning electron microscopy. (F1-3) close-ups of a TNT (Adapted from Rustom et al., 2004)

Plants developed two mechanisms to transport material betwen cells. The symplasmic and the apoplasmic transport.
The cell nucleus, the cytoplasm and the cell organelles therein are bounded per definition by the plasma membrane, and represent the smallest functional unit, the protoplast. In plants, this protoplast is additionally coated by the cell wall which builds the apoplast. In contrast to the apoplast the symplast represents the continuum of all protoplasts connected via plasmodesmata (PD). So the plant could be conceived as a giant symplast wherein all cells share cytoplasm (Lucas et al., 1993 ; Haywood et al., 2002).

1.2 The symplasmic cell-to-cell transport via plasmodesmata

As mentioned before plasmodesmata (PD) constitute the symplasmic pathway. In principal PD can be seen as border crossings, in form of complex channels connecting each cell in the plant organism (Figure 2). PD represent not passive tubes, but build a dynamic transport system for molecules of appropriate size. To increase flexibility, they are able to change their form after triggering by oversized factors which are permitted to move from cell-to-cell. Thus, PD seem to be highly evolved passages between cells, which exhibit an very specific filter system.

Figure 2: Plasmodesmata – schemata and electron micrograph

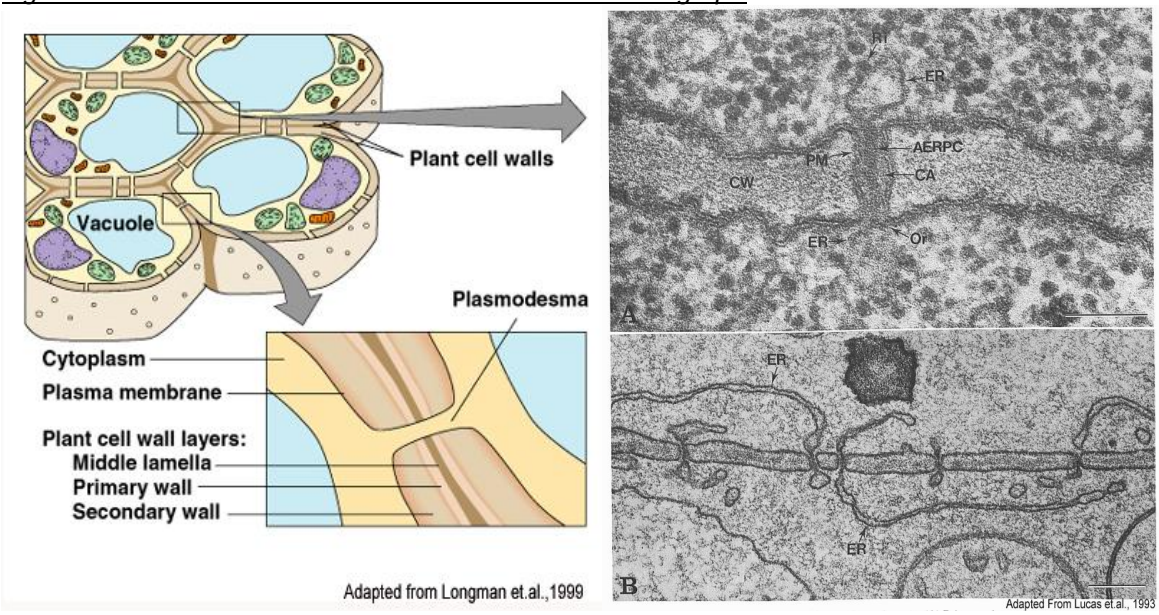

Note: (left) Schemata of plant tissue, symplasmically connected via PD (Adapted from Longman et al., 1990); (right) Electron micrographs of simple PD (A) root tip of phaselous vulgaris (OsO4 fixed) (B) root tip of Zea mays (KMnO4 fixed). ER (Endoplasmatic rediculum); CW (cell wall); CA (cytoplasmic annulus) Or (Orifice); AERPC (appressed ER-protein complex or desmotubule) (Adapted from Lucas et al., 1993)

2.2.1 Plasmodesma Structure

Plasmodesmata were discovered by Eduard Tangl in the end of the 19th century and named “Plasmodesmen” by Eduard Strassburger in the year 1901. Since these days improved techniques, like electron microscopy, revealed the complex composition and organisation of these cytoplasmic connections. As you can see in figure 3, the PD channels with a diameter (∅) of approximately 60 nm are composed of membranes and proteins (Robards et al., 1968; Lucas et al., 2001). Close investigation of this structure showed, that a single PD is comprised of 2 tubes. The outer tube (∅~60 nm) is formed by the plasma membrane (PM) which is seamlessly connected with those of linked cells. The inner tubes derive from the endoplasmatic reticulum (ER) (Hepler et al., 1982; Botha et al., 1993) which sidles through the outer tube. In the area of the PD the ER is termed appressed ER (desmotubule) (Robards et al., 1968). The space between these tubes, the cytoplasmic annulus (cytoplasmic sleeve) represents the major symplasmic conduit and appears filled with globular proteins forming elongated spokes, anchored to the 2 tubes. These create 10 micro

channels (MC) of a expected size of 2,5 nm (Ding et al., 1992). The outer protein ring which is connected with the PM, as well as the appressed ER, is assumed to represent Actin filaments (White et al., 1994; Ding et al., 1996) and Myosin motor proteins (Reichelt et al., 1999; Baluska et al., 2001). They are suggested to form a helically arranged contractile apperatus, providing the means for contraction and relaxation of the cytoplasmic annulus. This alters the aperture of the cytoplasmic sleeve increasing or restricting symplasmic transport (Ding et al., 1992; Lucas et al., 1993; Overall and Blackman et al., 1996; Zambryski and Crawford 2000).

Figure 3: Simplified Structure of Plasmodesmata

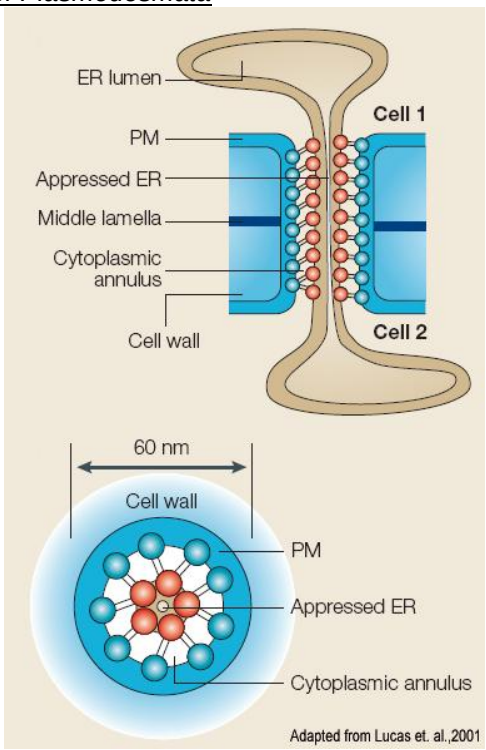

Note: Simplified structural model of primary PD regarding to prevailing opinions. (Adapted from Lucas et al., 2001; (PM) Plasma membrane; (ER) Endoplasmatic reticulum.

2.2.2 Plasmodesma Formation

PD formation is known to occur in two different ways. We distinguish between primary and secondary PD (Jones et al., 1976). Primary ones form during cytokinesis through formation of ER across the plane of the advancing cell plate. Here, vesicles delivered to the developing division plate, in the vicinity of the ER, fuse and provide, the foundation of the PD (Hepler et al., 1982; Kragler et al., 1998a). In case of primary PD, the cytoplasmic bridge between the cells appears simple as a cylindrical structure. (Figure 4)

In contrast, secondary PD are known to form *de novo* and hence post cytokinetic (Ding and Lucas, 1996). It appears that this process is coupled with a developmental program and / or the position of the cell (Kragler et al., 1998a). Regarding prevailing views, modifications take place on distinct target sites of the cell wall. The modifications occuring within the cell wall, allow thinning in the area of the developing PD. Subsequently ER accumulates in the target region at the thinned cell wall. During this process of cell wall penetration, vesicles deliver membrane and cell wall components which are necessary for assembly of the emerging *de novo* PD (Ding and Lucas, 1996). PD show electron dense, filamentous material, filling the mentioned cavity. Further, it is known that these two types of PD differ in regarding to viral interactions (Figure 4). The Tobacco Mosaic Virus Movement Protein (TMV-MP) seem to interact specifically with secondary PD, giving rise to the assumption that these two types of PD differ regarding their function in situ. (Ding et al., 1992)

Figure 4: Biogenesis of primary and secondary PD

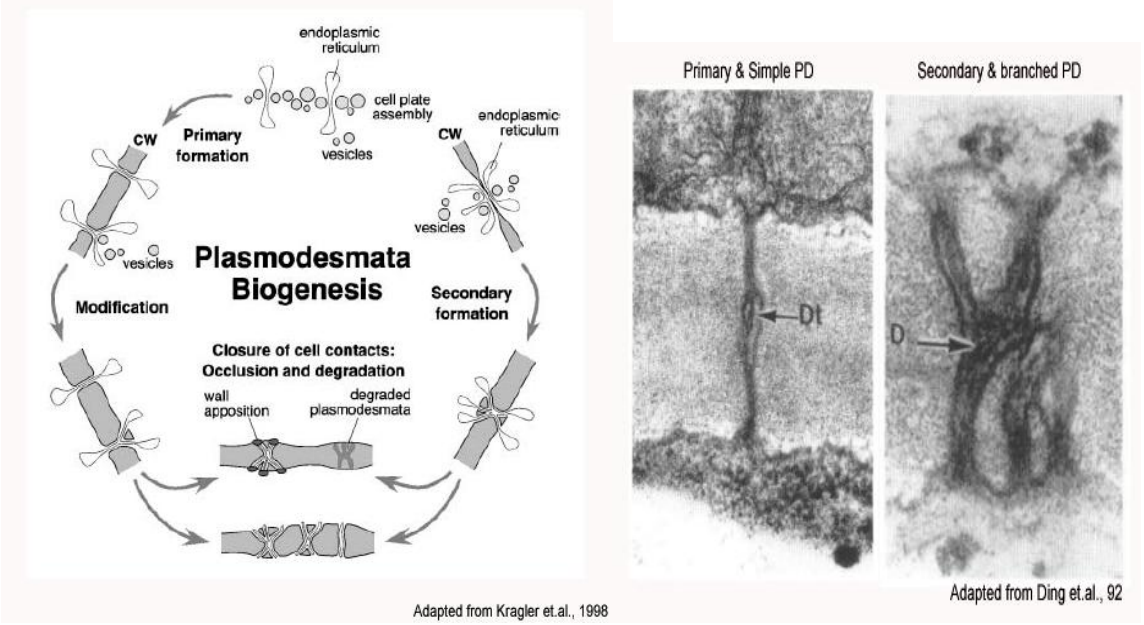

Note: (left) Schema of the biogenesis of secondary and primary PD. (CW) Cell Wall (Adapted from Kragler et al., 1998); (right) Electro micrographic images of the PD in vascular tissue of transgenic Nicotiana tabacum cv Xanthi expressing TMV MP constitutively. Primary PD: Desmotubulus (Dt) is visible in the center of a PD; Secondary PD: The arrowhead marks a electron dense (D) region in the central cavity of a PD which is probably in a dilated state. (Adapted from Ding et al., 1992)

2.2.3 PD associated components and their predicted roles in PD structural dynamics

Whereas the main structural components of PD were mainly identified and examined since the early 60ties, additional PD-associated key players which where suggested to regulate this highly specific and dynamic transport system remained to a large extend unidentified. The interplay of the few identified ones shown to play a role in cell-to-cell movement is unclear.
So far, it is suggested that the dynamic character of PD consists of three different states: OPEN, CLOSED and DILATED (Zambryski and Crawford, 2000).
When PD are open, a gate for small particles like e.g. sugars, hormones, amino acids and minerals is provided (Zambryski and Crawford, 2000). This state is defined through a basal size exclusion limit (SEL) of 0,9 – 1 kDa. It reflects the size of molecules (Stokes radius of 0,75nm) that are permitted to pass passive through the PD in Nicotiana tabaccum (Stokes radius ~2,5nm) (Wolf et al., 1989).
The term “non-targeted” refers to the fact that these molecules do not interact with PD-associated components. Here, transport occurs by gradient-dependened diffusion, in contrast to so called “targeted”, active transported molecules (Crawford and Zambryski, 2000).
Further investigations of SEL dynamics revealed that the limit of the open state highly differs between species, cell types, developmental states or PD types. The SEL can be affected by various factors like changes of the physiological state, age and growth conditions (Oparka et al., 1999; Crawford and Zambryski, 2000, 2001; Kim et al., 2002, Zambryski and Crawford, 2000, Heinlein et al., 2004; Stadler et al., 2005).
Changes of the physiological state, pressure differences, application of the Actin stabilizer phalloidin, plasmolysis, or Ca^{2+} influx seem to reduce, whereas profilin or Actin-disrupting drugs increase the SEL (Ding et al., 1996; Crawford & Zambryski 2000).
Studies of plant development uncovered that the predicted basal SEL of max. 1kDa could be as high as 10 kDa, e.g. for non-targeted molecules (stroke radius of 2,4 - 3,1 nm) during torpedo stage in plant embryogesis (Wolf et al., 1989; Waigmann et al., 1994; Kim et al., 2005).
As reported by Crawford and Zambryski (2001), experimental studies revealed a maximum gradient-depended, non-targeted transport-limit of approximately 50 kDa. This unspecific symplasmic diffusion of proteins (e.g. GFP (27 kDa) or double GFP (54 kDa)) is increased in nascent tissues and green house grown plants in comparison to culture grown ones.

PD are either transient or permanently sealed (closed state) (Oparka et al., 1995; Zambryski and Crawford, 2001).
The function of such symplasmic isolations is obvious in e.g. water conducting immature xylem vessels and tracheids (Lachaud and Maurousset et al., 1996). Here the PD to adjacent parenchyma cells are sealed in the final stages of programmed cell death. Another example is the symplasmic restriction of the leaf-to-apex signaling at the onset of flowering (Gisel et al., 2002). Irrespective the commonly accepted function of PD to regulate transport, through two mechanical principles it remains to be shown whether closing or opening is the mechanism to regulate transport.

One regulatory pathway might be established by F-Actin (White et al., 1994) and the associated motor protein Myosin VIII (Reichelt et al., 1999; Ding et al., 1996; Baluska et al., 2001). These cytoskeletal components are known to be associated with the ER and are found within PD in a helical manner (Overall and Blackman et al., 1996). Ding et al., 1992 argued that the Actin filaments represent the globular proteins associated with ER and PM, whereas Myosin reflects the observed spokes interconnecting them (Figure 3). Actin, as well as the unconventional Myosin VIII, was shown to be regulated by Ca^{2+} levels (Knight and Kendrik-Jones, 1993). Calreticulin, a Ca^{2+} sequestering protein, was found to be ER associated at PD (Baluska et al., 1999). The prevailing hypothesis is, that in case of PD closure upon an increased Ca^{2+} level, unidentified factors interacting with Calreticulin. This leads to contraction of the predicted Actin/Myosin–complex which result in turn, in a constriction of the micro channels (Ding et al., 1996). Contrary actions could be induced by docking of actively transported proteins, which will be discussed below.
A complete seal off of the gateway could furthermore be provided by deposition of Callose within collar-like structures at the plasmodesmatal neck. The Callose causes an occlusion of the gate and loss of the internal desmotubular structure (Turner et al., 1994). Here, it seems that this process is forced by increased levels of plant hormones like Abscisic acid (ABA) (Botha et al., 2000).

A second theory is based on the findings of Overall et al (1996) and Blackman et al (1999). Centrin, a contractile, Ca^{2+}-interacting protein, resides at the neck region of PD. Phosphorylation of Centrin nanofilaments lead to their contraction and as a result, to closure of a the cytoplasmic annulus (Zambryski and Crawford, 2000). Two cell wall associated protein kinases were found to be the current major candidates for Centrin phosphorylation: the Ca^{2+} depended protein kinase (CDPK) by Yahalom et al (1998) and a member of the casein kinase family I – the plasmodesmata associated protein kinase (PAPK) (Lee et al., 2005). It should be noted that the CDPK is regulated by Ca^{2+} levels and suggested to be part of the Calreticulin system. The PAPK appears Ca^{2+} independent but interacts with PD, viral movement proteins and endogenous non-cell autonomous proteins, known to move actively through PD.

In a third predicted mechanism Calreticulin is suggested to induce the increase of Ca^{2+} levels. This leads to deactivation of several kinases like CDPK and dephosphorylation of Centrin, which will cause contraction and a symplasmic seal off. Lower Ca^{2+} levels should lead to protein kinase activation which phosphorylate Centrin, causing a dilatation of the cytoplasmic annulus (Zambryski and Crawford, 2000).

2.2.4 Non-cell autonomous proteins – the cargo of dilated plasmodesmata (A glance on PD´s cargo bay)

Beside the discussed open and closed state, which either allow or restrict non-targeted (passive) cell-to-cell transport, PD are capable to enter a third one: the dilated state.
Non-targeted molecules exceeding the basal SEL are thought to remain cell autonomous. As mentioned before, new studies revealed that the SEL for special proteins sees increased up to 50-60 kDa. It is suggested that this is possible through passive diffusion and hence heavily depended on various factors like tissue, environment, protein concentration and species (Oparka et al., 1999; Crawford and Zambrysky 2001).

On the other side PD also provide a pathway for active and size-independent targeted transport. Several factors are able to interact with components of PD and thereby influencing the SEL in a way, that PD become dilated. As mentioned before, calcium levels and cytoskeleton components are known to be involved in this process. However, targeted protein transport is an active and energy-dependent process. Proteins which are able to use the symplasmic pathway via PD, appear in contrast to non-targeted transported macromolecules of similar size, often in “puncta” at the PD junctions (Itaya et al., 1997; Crawford & Zambryski 2001).

The first proteinaceous candidates that were found to be able to move from cell-to-cell were the movement proteins (MP) of plant viruses such as the tobacco mosaic virus (TMV-MP) which gate PD and mediate viral spread throughout the plant tissue (Wolf et al.,.1989). After infection, the TMV-MP (30kDa) becomes translated in the penetrated plant cell. It was found there associated with his own viral RNA (vRNA) forming a protein-RNA complex (Citovsky et al., 1990, 1992; Heinlein et al., 1998). This so called viral ribonucleoprotein complex (vRNP; Citovsky et al., 1992) and is, like the MP alone, able to increase the SEL (Wolf et al., 1998; Waigmann et al., 1994) and mediates its own transport. To access the symplasmic trafficking pathway, the TMV-MP interacts with several proteins, microtubules, Calreticulin (Chen et al., 2005), PD-associated casein kinases (Lee et al., 2005), cell wall-modifying enzymes, such as pectin methyl esterase (Chen et al., 2000) and furthermore the NON-CELL-AUTONOMOUS PATHWAY PROTEIN1 (NCAPP1; Lee et al., 2003).

Obviously, this targeted transport mechanism did not evolve for the transport of viral MPs and RNPs. Closer investigations of the symplasmic transport of endogenous factors revealed that the homeobox transcription factor KNOTTED1 (KN1) as well as several structural homologous and orthologous factors, appear permitted to move from cell-to-cell. To distinguish these moving factors from cell autonomous ones, they were termed non-cell-autonomous proteins (NCAP) (Haywood et al., 2002). Some of these NCAPs also show affinity to their own mRNA and transport it, similar to the viral MPs, to adjacent cells. (Lucas et al., 1995; Kim et al., 2005; Winter et al., 2007)
Kragler et al (1998b, 2000) showed that the moving TMV-MP and vRNP utilize the same PD components as the NCAPs. It is also suggested that this process of transport occurs in several uncoupled steps, very similar to the TMV-MP, which seems to mimic the NCAPs access procedure (Kragler et al., 1998b).

The model of this multi-step process of targeted transport through PD is based on known data about translocation of molecules into the nucleus (Lee et al., 2000). Parallels between protein movement through the nuclear pore complex (NPC; diameter ~9nm) and the PD suggest that a similar mechanism seems to be utilized in both gateway systems. (Kragler et al., 1998; Lucas et al., 1993) In a first step the TMV-MP, as well as KN1 are known to interact with PD associated components. This docking process results, on the one hand, result in spatial dilatation of the PD diameter – an increase of the SEL, and on the other hand in a modification of the target protein. The hypothesis is underlined by the finding, that the TMV-MP is phosporylated by a cell wall associated protein kinase (Citrovsky et al., 1993). Similar modifications were suggested occur during the NCAP docking process. These modifications could be the initiation of a conformational change of the cargo. Kragler et al (1998b) argued that a combination of protein unfolding and physical increase in micro channel diameter would be essential for KN1 cell-to-cell movement.
In experiments based on microinjection KN1 (~5,5nm), fused to spherical gold particles (2x1,4nm), requires in sum a PD dilatation from the basal SEL of max 2,5 nm up to 8,3 nm. Similar data was gained through microinjection experiments using the TMV-MP as target. Here it was additional shown that cell autonomous Dextrans of a size between 30 and 40 nm, were also able to gain access in trans to the symplasmic pathway, after physical dilation by the TMV-MP (Waigmann et al., 1994). Suggesting a common transport machinery, Lucas et al (1995) verified these findings by showing that KN1 also mediates the cell-to-cell movement of 39 kDa F-dextrans, which requires a dilation of plasmodesmata to approximately 9,3 nm. Also inhibitions of PD transport affected movement of both TMV-MP and KN1 (Kragler et al., 1998).
However, PD were shown to provide a long distance route for NCAP and RNP through the vasculatur (Lucas et al., 2001; Kim et al., 2002; Yoo et al., 2004; Long and Lucas et al., 2006). Here, phloem sap proteins up to 200 kDa (~10,5nm) were found to move targeted from cell-to-cell, whereas co-transport of Dextrans in trans was limited to approximately 22 kDa (cited Kragler et al., 1998). This indicates interactions between target proteins and PD associated receptors, which were assumed to cause conformational changes of the cargo. Also the existence of PD-associated chaperons suggests that unfolding occurs during transport. In a final step, interaction with the internal PD transport machinery, such as the Actin/Myosin complex, should facilitate active transfer through the micro channels.

Much more is known about symplasmic trafficking of viral MP´s than of NCAP´s. For example, studies on the TMV-MP showed, that it could be located only as cargo of secondary, branched PD but not of primary, simple ones (Oparka et. al., 1999; Haywood et al., 2002). Comparisons of the behaviour of viral and endogenous components, will help to solve the remaining riddles about the progress and the regulation of the symplasmic cell-to-cell trafficking via PD in the future.

Figure 5: Model of the symplasmic transport to and trough plasmodesmata

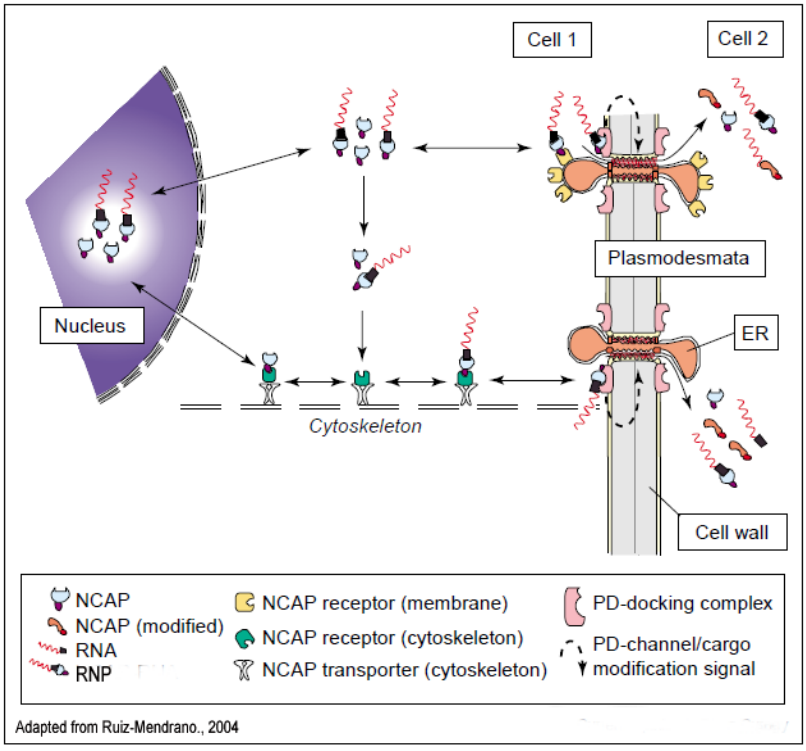

Note: The figure displays the current model of the transport of NCAPs (non cell-autonomous proteins, e.g. Zm KNOTTED1, At STM, TMV-MP) and RNA´s as complexes of both. (RNP; ribonucleoproteins). Here the cargos were transported from the nucleus to the cell wall by either the cytoskeleton or other cell components. Subsequently after docking to the plasmodesmata, proteins as well as PD associated receptors/chaperons are thought to be activated. As a result the cargo becomes unfolded and the SEL of the PD increases to enable passage of the target from cell to cell. (Adapted from Ruiz-Mendrano).

1.3 The cell-cell transport via the apoplast

Apoplasmic transport events reflect a diffusion process in which small extracellular peptides were delivered via vesicles or channels across cell borders. The cargo passes plasma membrane and cell wall through exocytosis or transport complexes such as membrane spanning channels and accumulates in the extra cellular space between cells. From there it subsequently enters a neighbouring cell through the same secretion/internalisation process. In comparison to the symplasmic pathway, the apoplasmic provides an undirected transition of molecules (Figure 6 D), depending on receptors in target cells.
A good example of the apoplasmic communication pathway is the model of a stem cell regulatory feedback loop, which is necessary to assure correct development of any plant.
All upper surface organs of a plant derive from a set of undifferentiated, pluripotent stem cells located at the tip of the shoot. This area is defined as the shoot apical meristem (SAM) and finds his opposite pole in the root apical meristem (RAM). The stem cell pool of the SAM consists of 3 layers as shown in Figure 6 B. In the model plant *Arabidopsis thaliana* a fragile balance between factors such as WUSCHEL (WUS) and CLAVATA (CLV1, CLV2 and CLV3) regulates self renewal and maintains the spatial dimension and identity of undifferentiated stem cells. For sure, other essential factors are involved in this process but they are not of further interest regarding apoplasmic cell-cell transport.

The SAM can be sub-divided into 2 areas. The central zone where stem cell layers L1 – L3 (Figure 6 B) are located, and the peripheral zone (rip meristem below and the flank meristems) where organ formation is initiated. The stem cells within the central zone divide slowly, but increased mitosis can be detected in meristematic rip and flank zones where organ formation occurs (Steeves and Sussex et al., 1998).
The homeodomain transcription factor WUS (Laux et al., 1996) is expressed in the central zone underneath L3. Its presence defines a subset of overlying cells (L1 - L3) as stem cells (Mayer et al., 1998). WUS mutants show defective meristems in early embryo stages including loss of meristem and primordia in the seedling as well as extremely reduced floral organs. Ectopic, root specific expression of WUS revealed, that WUS is responsible for shoot identity (Lenhard et al., 2002; Gallois et al., 2004).
Clark et al. (1993, 1995) revealed that a membrane bound receptor complex in the central meristem is responsible for negative regulation of WUS. This complex is composed of the Leucine-rich repeat (LRR) protein kinase CLV1 (Leyser and Furner et al., 1992) and CLV2 which is an LRR protein lacking kinase activity and stabilizes the complex. CLV1 dependent negative regulation of WUS was revealed through mutations within clv1, which lead to a phenotype which resembles WUS overexpression and show besides increased flower organs, enlarged and differentiation inhibited meristems (Clark et al., 1993).

An additional key player is provided by the small extracellular ligand CLV3 (Clark et al., 1995) which is expressed in L1 of the central zone (Figure 6 D). Mutations within the clv3 gene result in a phenotype similar to CLV1 mutants, which indicates an essential interaction between CLV1 and CLV3 (Clark et al., 1995; Brand et al., 2000).

This small CLV3 peptide is secreted and apoplasmically delivered into L2 and L3. Here the components of the CLV1 and CLV2 complex are expressed (Figure 6 C). After entering these layers, the CLV3 ligand binds the complex. This leads to transcriptional repression of WUS within the central zone layers 2 and 3 (Clark et al., 1995, 1997). Within L1- L3, WUS is assumed to promote CLV1 expression which establishes a negative regulatory feedback loop. This loop allows maintenance of the equilibrium between promotion and inhibition of stem cell renewal and differentiation within the shoot apex (Figure 6 A) (Brand et al., 2000; Doerner et al., 2000; Schoof et al., 2000; Lenhard et al., 2002, Gallois et al., 2004).

A homolog of WUS could be found in WUSCHEL-RELEATED HOMEOBOX5 (WOX5) which seems to act in a similar way to maintain the RAM within the root of plants. This theory is confirmed by the fact that ectopicly expressed WUS, driven by the WOX5 promoter is able to restore the quiescent centre and stem cells in wox5-1 mutants which results in complete rescue of mutant phenotype (Sakar et al., 2007).

Figure 6: Regulation of the stem cell population in the SAM by a regulatory feedback loop

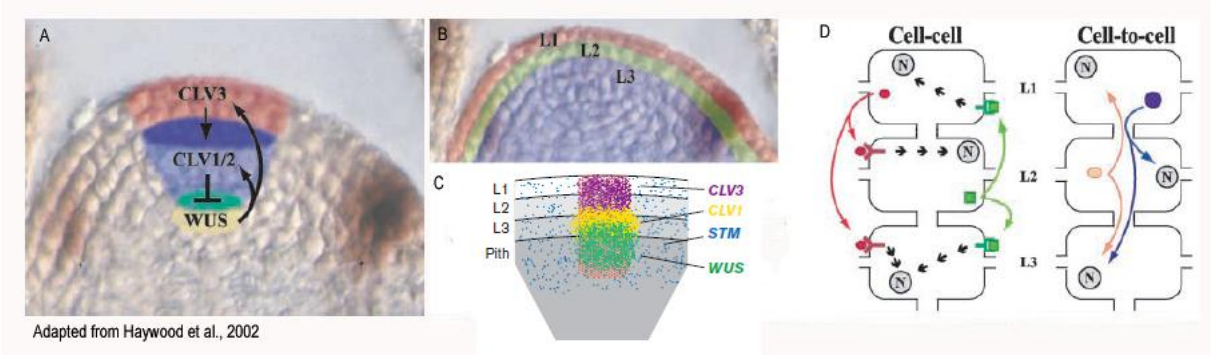

Note: (A) Schemata of the negative regulatory feedback loop which maintains the SAM. CLV3 is transported via the apoplast into the layers below to repress, together with CLV1 and CLV2, WUS expression, whereas WUS promotes CLV3 *expression. (B) L1 represents the ancestor of the epidermal tissue; Internal tissues (mesophyll/ vascular tissue) will derive from L2 and L3); (C) Accumulation of mRNA of CLV1 (yellow) and CLV2 (not shown) is primary restricted to L3. After secretion of the L1-expressed CLV3 (purple) to the L3, the ligand activates the CLV1/CLV2/X complex which leads to repression of WUS expression within layer (L3), establishing a border between the stem cells of the central zone and the organ forming peripheral zone. (D) Schematic comparison of apoplasmic, cell-cell and symplasmic cell-to-cell transport. (L1)Layer1; (L2)Layer2; (L3)Layer3 ;(CLV1-3)CLAVATA 1-3; (WUS)WUSCHEL; (X)Other components; (STM)SHOOTMERISTMLESS.*
(Adapted from Haywood et al., 2002; Doerner et al., 2000)

2. *Transport of homeodomain transcription factors*

2.1 Something about homeodomain (HD) transcription factors

Transcription factors as proteins that are able to bind alone, or associated with others, to promoter sequences, to alter gene expression. In general, genes encoding transcription factors share several conserved sequence segments, which are commonly used to subdivide the appendence to a defined gene families. In plant transcription factors, normally four of these domains can be found: a DNA binding region, an oligomerisation site, a transcription regulation domain and the nuclear localisation signal (NLS) (Liu et al., 1999).

2.1.1 General Structure and Function

A distinct group of transcription factors are encoded by the so called homeobox genes. This family is characterised by a common, 180bp consensus sequence called homeobox which codes for a 60 AA DNA binding region termed homeodomain (HD) (Figure 7). Structural studies revealed that the homeodomain is comprised of 3 α helices which are packed around a hydrophobic core (Gehring et al., 1994).

Figure7: Essential domains of the Zm KN1 protein

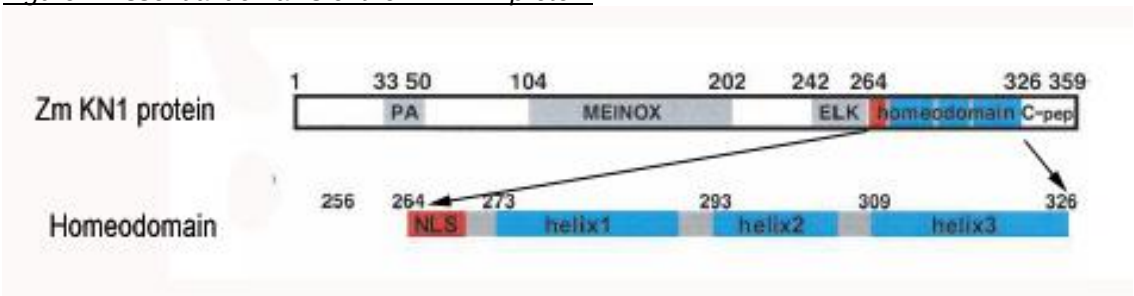

Note: Schemata of the Zm KNOTTED1 protein domains. The augmented area below displays the subdomains of the homeodomain. Peptide antagoniste (PA) (Kragler et al. 2000), MEINOX (Bellaoui et al. 2001), ELK (Kerstetter et al. 1994), homeodomain, and C-terminal region (C-pep). Nuclear localisation signal (NLS). Adapted from Kim et al., 2005

This homeodomain appears to be prerequisite for the DNA binding ability of these transcription factors (Gehring et al., 1994) and due necessary and sufficient for cell-to-cell trafficking via plasmodesmata for a small group of HD-proteins (Kim et al., 2005; Winter et al., 2007).
Within the organism, the homeodomain transcription factors accomplish a developmental regulatory function by controlling spatial and temporal expression patterns of several distinct target genes. These target genes coordinate the correct development of different organs during morphogenesis. In the plant and animal kingdom, these factors seem to be necessary to regulate and maintain differentiation domains and hence the correct development of every new organ (Gehring et al., 2004).

Lewis (1978) identified the homeotic genes in the fruit fly (drosophila melanogaster) as master control genes for segmental development and arrangement. Further investigations by Gehring (1994) revealed that similar genes could be found in plants and that these genes containing also the characteristic homeobox fragment.
So, this conserved homeobox sequence can be found as an essential element in all eukaryotic organisms like sponges, fungi, insecta, vertebrate but also humans and plants (Gehring et al., 1994). Hence, the family of HD genes seems to have evolved very early in the evolution of eukaryotic organisms.
Through sequence comparisons, homeobox genes could be divided into different families, which differ only in few amino acids within the homeodomain. Each member of these subsets of HD proteins share distinct sequence characteristics and can be clearly divided in HD subsets. This classification into subsets also reflects the early evolutionary branches, which can be found in fungi, plants and animals. (Chan et al., 1998; Bürglin et al., 1997)

2.1.2 The TALE Superclass

The HD genes are united in sets called superclasses. One of these is the Three Amino Acid Loop Extension (TALE) superclass.
Within this classification, 4 TALE classes could be identified in animals (MAIS, PBC, TGIF and IRO), 2 in fungi (M-ATYP and the CUP genes) and 2 in the plant kingdom (KNOX and BEL).
Three additional amino acids (AA) are located in the homeobox between helix 1 and 2. This results in the formation of a highly conserved loop. Furthermore several AA conserved in other HD proteins differ in TALE HD proteins. These sequence variations concerning primary helices 1 and 2, but in some cases also helix 3, which is known to be critical for DNA binding. This alternative implementation, which could result in a different target affinity, leads to the suggestion that TALE HD proteins serve related but different purposes to common HD proteins. Moreover, the TALE classes PBX, MAIS and KNOX share a homeodomain version which is enabled for alternative splicing. In this way two proteinogenic versions could be generated from one gene product, which differ completely regarding the N-terminus. Like the additional/unconventional AA within and adjacent the homeobox sequence, alternative splicing could also cause changed protein characteristics regarding gene targeting and HD-depended symplasmic transport. These two features of the TALE HD reflect on the one hand an apparent difference to common HD proteins and on the other a very flexible DNA binding (Bürglin et al., 1997).

2.1.3 The KNOX proteins

2.1.3.1 MEINOX

In this work a special attention is given to the TALE homeodomain class KNOX (KNOTTED1 Homeobox). Despite the early split into the branches of animal and plant kingdom during evolution, an additional sequence motive besite the homeobox could be located in distinct plant HD proteins as well as in animal HD proteins. Comparisons of the MEIS domain (Myeloid Ectrophic Integration Site) with the KNOX domain revealed a likewise conserved consensus termed MEINOX consensus (MEINOX motif). This ~100 bp sequence indicates that the common ancestor of plants and animals showed also a HD protein with a MEINOX motif. The fact that this motif is conserved until the present day reflects its importance for both kingdoms. The suggestion of Bürglin (1997) that this motif plays a role in homodimerisation or heterodimerisation was proven by Bellaoui et al., 2001, Smith et al., 2002, Winter et al., 2007. Protein-protein interaction opens a wide spectrum of transcription regulation. Combinations of different TALE proteins, in addition to alternative splicing, provide a multitude of different transcription factor functions. These compositions appear able to regulate various gene-targets and thus are a very flexible system for developmental regulation and environmental adaptation. Phyllogenetic and biochemical analysis revealed a relatively high degree of homology between the TALE protein classes MAIS and TGIF (animal), CUP (fungi) as well as KNOX and BEL (plants), which gave rise to the suggestion that these classes descended from a common ancestor TALE HD protein. Underlined by the fact that TALE HD proteins underwent much less diversification than common HD proteins, it appears that TALE HD proteins are key factors. This may lead to the predicted, very early evolutionary separation from the ancestral homeobox gene and further to a constant maintenance of the original function over a very long time period (Bürglin et al., 1997).

2.1.3.2 CLASS I

As mentioned before, the KNOX proteins representing one of the two identified TALE HD protein classes in plants. After the first identification of a representative of this class in Zea Mays, homologous KNOX proteins, as well as orthologous ones, were described in rapid succession in various species like *Tomato, Potato, Tobacco* and *Arabidopsis* (Vollbrecht et al., 1991).
Until now, scientists successfully identified 8 members of the KNOX class in Arabidopsis and divided them in two groups based on their nucleotide, respectively amino acid sequence, as well as observed distinct characteristics (Kerstetter et al., 1994). Belonging to the KNOX TALE HD class I are besides At STM (Long et al., 1996), At KNAT1/BP (Lincoln et al., 1994), At KNAT2 (Lincoln et al., 1994) and also the later identified factor At KNAT6 (Dean et al., 2004). These transcription factors were characterised, beside a high degree of internal sequence homology regarding the homeobox/homeodomain, by an obvious high degree of relationship to the eponymous factor KNOTTED 1 (Vollbrecht et al., 1991) in *Maize* (Karstetter et al., 1994)

Interestingly these proteins moreover show, in contrast to class II proteins, cell-to-cell movement which define them as NCAPs. The expression of class I proteins was so far only detected in meristematic tissues. Here, they are imporant regarding formation of meristems and hence lateral organs. It is known that these proteins are downregulated in founder cells, which are recruited to form lateral organs. Furthermore, it seems that these factors also provide essential components of meristem regulation and maintenance in adult plants (Reiser et al., 2000).
Class I loss-of-function mutants show abnormal meristem development, whereas overexpression studies revealed that they effect leaf shape and flower development. Overexpression of KNOX class I results in ectopic meristems on leaf blades, such as knots and lobes (reviewed Reiser et al., 2000; Bellaoui et al., 2001).

2.1.3.3 CLASS II

There are also four members of TALE HD KNOX class II proteins. The roles of the class II proteins remain to be established (Truenrit et al., 2008). The class II proteins differ not only in the conservation of the homeodomain but also in C and N-terminal areas which seem to influence the ability of KNOX proteins to move. Kim (2005b) found out that the homeodomain is responsible for movement through plasmodesmata. Not one of the class II proteins, neither At KNAT3, At KNAT4, At KNAT5 (Serikawa et al., 1996) nor At KNAT7 (Bellaoui et al., 2001) show cell-to-cell movement activity. Another reason for this difference was described by Kragler (2000). His findings revealed a peptide antagonist motif (Figure 7), an N-terminal localized domain within the class I protein Zm KNOTTED, which seems also to be necessary for cell-to-cell movement. So, sequence differences in the N-terminal region of KNOX proteins could also be responsible for the incapability of class II proteins to move from cell to cell.
A second characteristic to distinguish the class II from the class I proteins is displayed by the fact, that class II gene expression could be detected in nearly all tissues, whereas class I expression is restricted to meristematic tissues (Kerstetter et al., 1994).
Both KNOX classes share common features, tor instance their interaction with DNA. *Tobacco* and *Potato* TALE proteins have the capacity to bind regulatory sequences of the Gibberellin (GA) hormone-synthesizing gene GA20-oxidaseI. This was interpreted as an evidence of KNOX protein-mediated negative regulation of GA biosynthesis in the meristem. (Hackbusch et al., 2005)

2.1.4 The BLH proteins

Another class of TALE HD proteins are found in plants are termed as BEL1-Like-Homeodomain proteins (BLH) (Magnani et al., 2008) according to the eponymous factor BEL1 (Reiser et al., 1995). BEL1 (TAIR acc. # At5g41410) represents beside BELLRINGER (BLR (TAIR acc. # At5g02030), also known as PENNYWISE, REPLUMLESS or VAAMANA) the first and best characterized member of this homeodomain protein family. BLH members can be easily distinguished from other HD proteins through an N-terminal located HD with a putative amphipathic α-helix. To avoid misunderstandings regarding nomenclature, the corresponding sequence is termed BELL domain, which together with a second one, the SKY domain, essential for protein interactions.
For example BEL1 is known to be crucial for the production of lateral primordia within developing ovules, the reproductive structures that contain the female gametophyte and develop into seed after fertilization. Recessive mutations result in an inability to initiate the formation of outer integuments which develop into seed coat. (Reiser et al., 1995; Bellaoui et al., 2001)
Beside the ability for homodimerisation, all BLH proteins seem to bind a specific interaction partner of the KNOX class (Hackbusch et al., 2005). Heterodimerisation depends on the MEINOX domain and is necessary for the nuclear import of the proteins. Furthermore, an increased DNA-binding affinity and specificity has been shown (Smith et al., 2002; Bhatt et al., 2004).
This interaction between specific KNOX and BLH proteins is underlined by the fact that the expression patterns overlap within inflorescences and floral apices (Bellaoui et al., 2001).

2.1.5 The OFP proteins

A third group of key players should be introduced at this point. The recently documented OVATE FAMILY PROTEINS (OFP) composed so far of 18 members, which seem to play also an important role with regard to HD function (Hackbusch et al., 2005).
This, in 2002 discovered protein family share a conserved 77 AA C-terminal domain (Liu et al., 2002). Protein interaction studies revealed, that the HD of KNOX and BHL proteins appear capable to interact with this C-terminal domain of At OFPs. For example it was shown that, beside a capacity for homodimerisation, the factor At OFP1 appeared capable to heterodimerize with the BHL protein member BEL1 (Hackbusch et al., 2005).
Early experiments in tomato revealed that mutations in OFP1 cause pear shaped fruit development (Liu et al., 2002). Later performed overexpression assays, with *Nicotiana* and *Arabidopsis* plants show a broad spectrum of developmental variances. Plants expressing OFP1 under the CaMV 35S promoter are stunted, show thickened aerial parts, delayed development and general dwarfism. The leaves on the other hand show a heart shaped and lobed appearance with curved surfaces. Deformed flowers with short, thick filaments and protruded styles resulted in a massive depletion of seed production (Hackbusch et al., 2005). This phenotype can also be found in transgenic KNOX overexpression plants. The recent findings that the KNOX phenotype is partially caused by decreased Gibberellic acid levels, through direct repression of the GA20ox1 gene, goes hand in hand with the observation that

OFP1 overexpression plants exhibit also a decreased expression of exactly this gene by 80%. This indicates the existence of a close functional connection between OFP proteins and TALE HD proteins (Hackbusch et al., 2005).
Subcellular observations of fluorescence tagged At OFP1 and At OFP5 proteins revealed that they can be located in the nucleoli and also cytoplasmically associated with the cytoskeleton.
The strictly nucleus located TALE proteins localized in At OFP1 overexpressing cells also to the cytoplasmic space and colocalized with At OFP1 at microtubules and the cell periphery in punctuate structures.
This indicates that members of the OVATE family regulate microtubule dependened, subcellular localisation of TALE HD proteins (Hackbusch et al., 2005).
Punctate structures formed by OFP-GFP at the microtubules are very similar to those detected with the microtubule-associated protein MPB2C, which is also proven to interact with TALE proteins (Kragler et al., 2003; Winter et al., 2007). Finally should be noted that at least 4 members of the OVATE family were proven to interact with both, KNOX and BHL classes of plant TALE proteins. As mentioned before, the split of BHL and KNOX is predicted to have taken place early in evolution. The fact that some OFPs also show potential to act as a cofactor to the TALE complex in dicotyledonous and monocotyledonous plants, indicates, besides high a conservation of the OFP´s, an ancient functional connection to the development and meristem regulating TALE proteins.

To conclude on the information regarding transgenic phenotypes, interaction studies and subcellular localisation analysis, At OFP1 constitutes presumably an essential pleiotrophic developmental regulator (Hackbusch et al., 2005).

2.2 Class I KNOX proteins like KNOTTED 1 from *Zea mays* and its orthologes STM and KNAT1 in *Arabidopsis thaliana* are able to move from cell to cell.

2.2.1 KN1

Another factor which is able to interact with the Zm KNOTTED1 HD protein is the TMV-MP binding protein 2C (MPB2C) (Winter et al., 2007). Zm KN1 (acc# AAP76321) is a member of the TALE super family (Bürglin et al., 1997) and eponymous for one of the two known subclasses in plants: the class I KNOTTED1-like homeobox (KNOX) family genes.
This 42 kDa protein has a length of 359 amino acids and includes several motifs: the MEINOX, ELK, NLS and the HOMEODOMAIN (HD (Bellaoui et al., 01; Kim et al., 2005c; Karstetter et al., 1994; Vollbrecht et al., 1991) (Figure 7).

Figure 8 : Expression pattern of Zm Knotted1

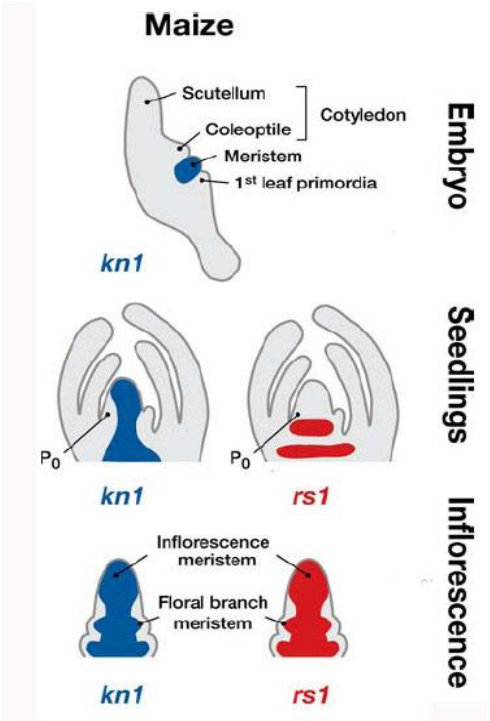

Expression of Zm KN1, like its orthologous At STM in *Arabidopsis thaliana*, takes place in all apical meristems, the vegetative, inflorescence and floral meristems, as well as within the underlying ground meristem. (Kerstetter et al., 1994) Closer investigations disclosed that Zm KN1 and At STM (acc# At1g62360) localize primarily to the nuclei of the cells but also at the nuclear envelope and the ER. Both proteins heterodimerize with other TALE family members, the BELL1 Like proteins (BHL) and bind via their HD, specifically to the DNA to initiate gene expression. (Gehring et al., 1994; Bellaoui et al., 2001; Winter et al., 2007). Smith et al. (2002) recently revealed that such interactions depend on a small KN1 DNA motif (TGACAG(G/C)T) responsible for interactions with e.g. the N terminus of the BHL protein KIP. The resulting complex shows a considerable higher affinity to DNA than the included factors alone. So it is suggested that this complex acts as a transcriptional regulator. These interactions as well as the correct levels of the key players are essential for initiation and maintenance of the SAM by holding them in an undifferentiated and indeterminate state (Jackson et al., 1994; Long et al., 1996) by regulating hormone levels, especially the levels of Gibberellins and Cytokinins (Chen et al., 2004; Jasinsky et al., 2005). Missregulation of the forecited phytohormones results in the same morphological changes of leaves, stem and inflorescence as overexpression of the HD proteins.
However, Zm KN1 is known to interact with PD components, change the SEL and show cell-to-cell movement (Lucas et al., 1995) using the symplasmic pathway. Zm KN1 for instance, was detected in cells of the leaf where no expression occurres (Jackson et al., 1994).

2.2.2 STM

Figure 9: Expression pattern of At STM (blue) and At BP (red)

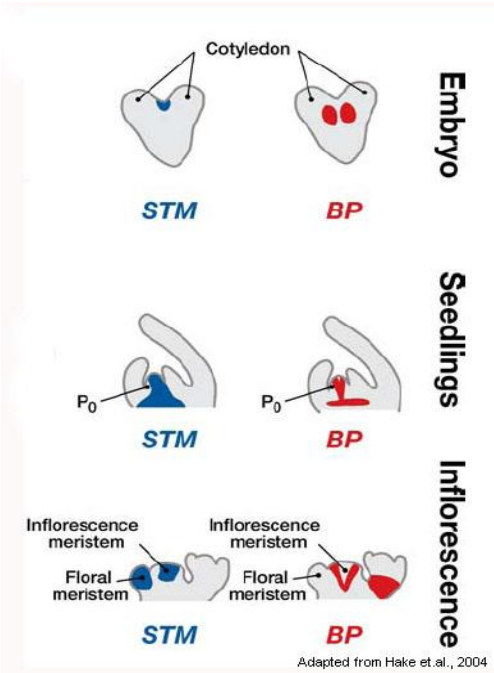

SHOOTMERISTEMLES (STM) is the ortholog of Zm KN1 in *Arabidopsis thaliana* (47% identity) and is also defined as a class I KNOX protein with KNOX-characteristics. STM has a similar embryonic and vegetative expression pattern as KN1 (Figure 8,9) (Hake et al., 2004; Long et al., 1996). Like KNOTTED1, expression of STM takes place in meristems, in the shoot tip of monocotyledon (e.g. *Zea maize*) and dicotyledon plant species. In *Arabidopsis thaliana*, STM is known to interact with several other proteins (Figure 10) and seems to be essential for the formation and maintenance of the shoot apical meristem. During development STM expression is initiated in a single apical cell in late globular stage (Aida et al., 1999, Long and Barton, 1998). Subsequently expression expands and defines the boundaries of the shoot apical meristem. Here, STM is required to hold the meristematic cells in equilibrium between differentiation and an undefined state (Clark et al., 1996) inhibiting differentiation of meristematic cells into organ primordia (Endrizzi et al., 1996), a process driven by the CLAVATA complexes (chapter 2.3, Figure 6D,10). Whereas stm1 mutants fail to initiate the SAM during embryo development, in CLAVATA1 and 2 mutants, which reflect a quite contrary phenotype, an accumulation of undifferentiated cells result in an extraordinary increased SAM. As a consequence, the SAM fails to develop differentiated primordial cells and thus leaves. The antagonistic aspect of STM and the CLAVATA complex was finally proven in phenotypical rescuing of CLAVATA mutants through recessive mutations of *stm* (Clark, et al., 1996).

Another protein family known to interact with STM are the CUP SHAPED COTELYDON (CUC) proteins (Figure 10). The CUC proteins define the boundaries between the SAM and the lateral organs (cotyledons) and are responsible for the bilateral symmetry of dicot plants. During embryo development the CUC gene expression delineates the expression of STM in to the area of the SAM, whereas STM regulates CUC1 and CUC2 expression in later stages of development (Chandler et al., 2008). In contrast to the CLAVATA/STM interplay, the CUC/STM interaction appears to enhance the STM expression. This was supported by closer investigations of *cuc* double mutants where no STM expression could be observed. (Hake et al., 2004)

Figure 10: At STM – a schematic interaction map

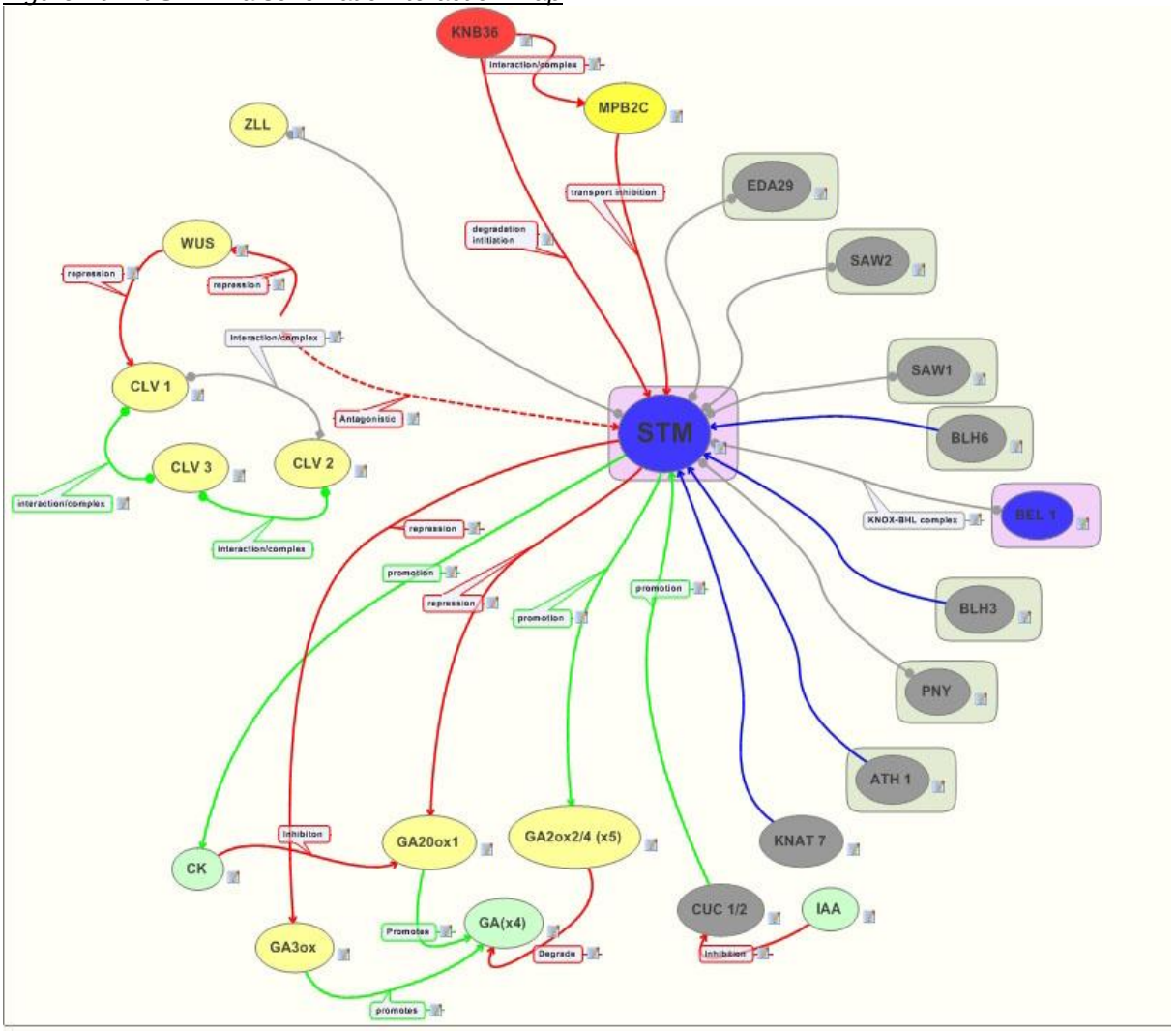

Note: Green connection lines indicate an activation of the factor through At STM, red ones inhibition and grey/blue lines an interaction without further classification. Interaction map was designed with Mindmanager Pro7 (Mindjet)

Furthermore, investigations during the last years revealed the reason why mutations in the *stm* gene alter the morphology of the plant so drastically. STM, which is knownto be regulated by OFP, CLAVATA, CUP and, as discussed later, by KNB36 and MPB2C proteins, appears to be essential in regulation of the phytohormones Gibberellic acid (GA) and Cytokinins (CK).

Regarding CK, which is known to promote cell-division by stimulation of cyclin D, expression, is promoted by STM. GA, on the other hand, is known to be responsible for forced cell-elongation by reorientation of microtubules. Whereas CK seems to be promoted, GA is inhibited by STM in the area of the SAM.

More detailed, STM activates expression of the Isopentenyltransferase (ITP) gene, which is a promoting factor of the Cytokinin biosynthesis (Kulaba et al., 1998; Ori et al., 1999). Cytokinin itself, STM and OFP1 additionally repress the Gibberelin20 Oxidase1 (GA20ox1) gene, which codes for an essential enzyme which acts catalytically during the final steps in GA biosynthesis (Hay et al., 2002; Hay et al., 2004; Hackbusch et al., 2005) (Figure 11).

A similar situation could be seen in case of Gibberellic3 oxidase (GA3ox), which also promotes GA biosynthesis (Hay et al., 2002). For maintaining the balanced state of the SAM, it is essential to avoid GA in this area. It seems that STM is one of the key players in regulation of several GA avoidance mechanisms. Besides repression of the biosynthesis, STM prevents indirectly influx of GA from young leave primordia into the SAM.
More detailed, STM forces Gibberelin2 Oxidase2 & 4 (GA2ox2; GA2ox4) synthesis, which inactivates bioactive GA1-4 and also their precursors within the boundary between SAM and developing primordia (Figure 11) (Jasinsky et al., 2005). In conclusion, KNOX proteins seem to exclude phytohormones which force stem elongation from the SAM and, on the other hand, promote the presence of phytohormones supporting cell division in these tissues. This results in a high density of cells within the shoot apical meristem as well as the maintenance of the undifferentiated state of these cells until they reach the area of developing primordia. Here the contact with GA and other factors promote differentiation and cell elongation, which results in development of primordia and respectively leaves.
Severe *stm* mutants fail to develop an apical meristem and no true leaves are formed (Figure 12 B,C). Weak alleles result in plants with a dwarfed, bushy phenotype which shows besides a late vegetative – inflorescence transition, a reduced number of flowers, which show premature termination and fused flowering organs. In general an altered morphology regarding rosette development, leaf-shape and secondary shoots could be seen (Endrizzi et al., 1996). Overexpression of STM results, similar to KN1 overexpression, in heavy morphological defects whereas the mosty apparent one could be seen in formation of lobed leafs with ectopic meristem formation (knots) (Figure 12 A) (Hake et al., 2004).

Figure 11: Predicted model of phytohormone regulation within the SAM

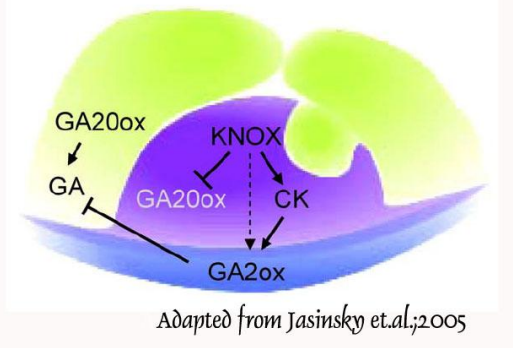

Note: KNOX proteins (e.g. STM) inhibit Gibberellic Acid (GA) biosynthesis through repression of GA-precursor genes and promotion of Cytokinin synthesis.

Figure12: STM phenotypes

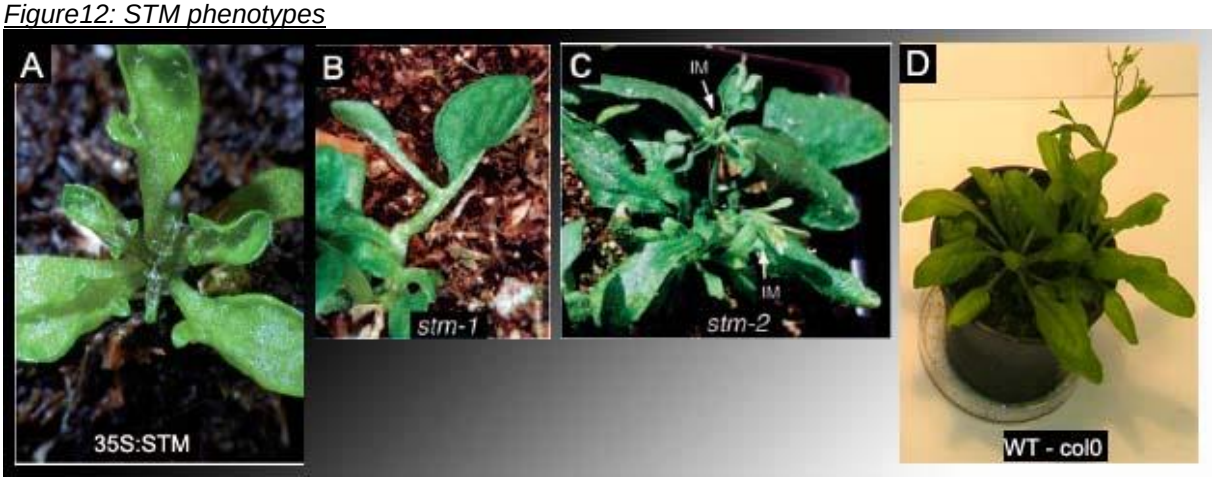

Note: Overexpression of At STM in Arabidopsis thaliana leads to development of ectopic meristems on rosette leaves. The Leaves become lobed, curled and/or wrinkled (A). The loss of function mutant stm-1(B) fail to develop true leaves, stm-2 appear dwarfed and bushy with abnormal florescence development (C).Wildtype col0 plants in different stages. (D). (Adapted from Cole et al., 2006, Clark et al., 1996).

3.3.3 KNAT 1

Knotted like from Arabidopsis thaliana1 (KNAT1) which is also known as Brevipedicellus (BP) is a class 1 homeobox transcription factor (Lincoln et al., 1994). Whereas CLAVATA and STM competitively regulate meristem activity, KNAT1 and STM act in a redundant fashion (Truernit et al., 2006). KNAT1 and STM show 47% identity on the protein level and their mRNAs could both be detected in all meristematic tissues. During plant life cycle KNAT1 expression takes place in all stages, always as a regulator of internode development (Smith & Hake 2003): In early embryo development within cells destined to become hypocotyl, in late heart stage in the cells subtending the SAM and in torpedo stage where strong expression persists in the hypocotyl and at the leaf/meristem boundary (Douglas et al., 2002; Hake et al., 2004). Figure 9 highlights the differences of the expression patterns of mature plants between BP and STM inside the SAM. Whereas STM and KN1 expression primarily occurs in the central zone, BP can be detected in the adjacent periphery and lightly in the rip zone as well as in the underlying sub apical tissue (Lincoln et al., 1994) defining the SAM boundary and the base of leaf primordia (Reiser et al., 2000). Besides it should be mentioned that Smith & Hake predicted an internode region inside the shoot apical tissue defined through the presence of KNAT1.

As noted before KNAT1 regulates internode development. This regulatory function is known to be provided not by KNAT1 alone, but rather as a heterodimeric complex with the BEL1 like homeodomain protein Pennywise (PNY) before subsequent association with DNA takes place (Smith and Hake 2003; Hay et al., 2004). This is supported by several facts. The expression pattern of BP and PNY overlap in meristems and the proteins interact. They act also synergistically (Smith and Hake, 2003).

Mutants of both genes lead to a similar phenotype including dwarfed plants showing reduced internodes (sepal, petal, stamen, silique and pedicle) as well as an altered vascular system (Figure 13). An obvious feature of the KNAT1 mutants is the slant of the pedicles. Additionally it was observed that beside and increased number of paraclades (adventitious shoots), unusual cauline leaf development occurs at the base of the newly formed shoots (Smith and Hake, 2003). Severe mutations result in complete loss of apical dominance.
The KNAT1 overexpression phenotype exhibits similar characteristics as KN1 or STM overexpressing plants. This includes ectopic meristem formation in rosette and cauline leaves, which result in lobed, wrinkled, curled and/or spatulated, serrated leaves depending on the degree of severity. Additionally should be noted that KNAT1, similar to STM, seem to play a mayor role in several regulation processes. KNAT1 represses KNAT6 and KNAT2 (Pautot et al., 2008), SAW1 and SAW2 (Kumar et al., 2007), GA20ox1 and GA3ox1 (Hay et al., 2002).
Summarized, KNAT1 acts as a non-cell autonomous homeodomain transcription factor (Kim et al., 2005b) which complexes with BLH proteins to act in a regulatory manner in shoot apical, florescence and floral meristems. Among other duties, BP interacts specifically with PYN and regulates general internode development as also the maintenance of the SAM in a redundant fashion to STM.

Figure 13: KNAT1/BP phenotypes

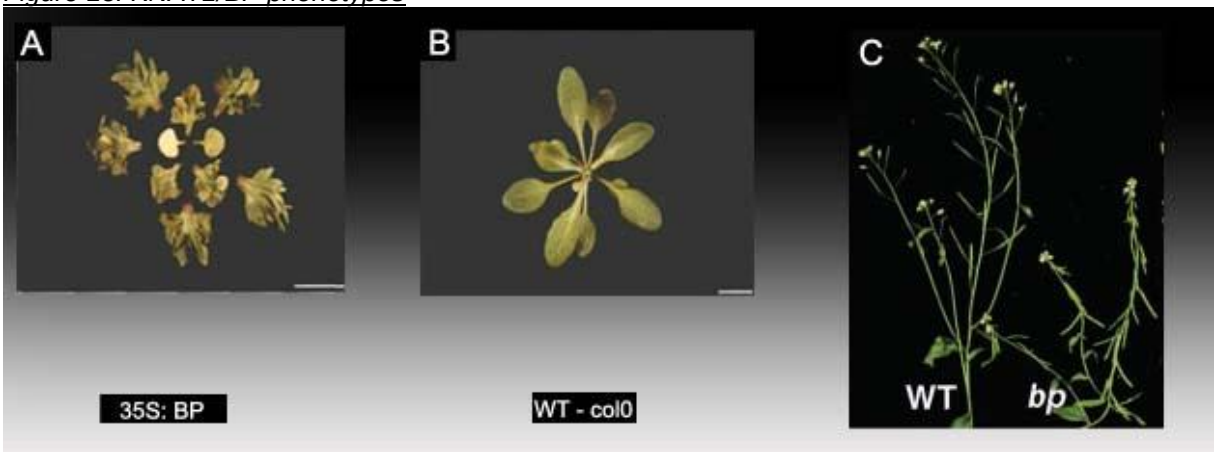

Note: Overexpression of KNAT1/BP in Arabidopsis thaliana leads to lobed, serrated and curled leaves (A). Mutants display a dwarfed phenotype with an increased number of paraclades, reduced internodes and slant pedicles (C-bp). Wildtype col0 (B, C-WT). Adapted from Lincoln et al., 1994 and Hake et al., 2003)

3. *MPB2C, a selective gatekeeper interacts with Class I KNOX proteins and a viral protein*

3.1 A short story about MPB2C

In the course of investigation of the symplasmic cell-to-cell transport of the Tobacco Mosaic Virus Movement Protein (TMV-MP30) via plasmodesmata (PD), Kragler (2003) isolated an interaction partner of MP30 with a length of 327 AA and a weight of approximately 36 kDa. Regarding to its function the novel protein was called Nt MPB2C (viral Movement Protein Binding 2C) (GenBank acc. # AAL955696). This plant endogenous factor was found exclusively associated with the microtubules in a punctate manner. Transient expression assays depict that the protein neither could be found in nuclei nor in association with other cytoplasmic organelles. Nt MPB2C as also its ortholog in *Arabidopsis thaliana* appear in punctate patterns in the cytosole, whereas in onwardly expressing cells and cells with high expression, MPB2C generally forms large aggregates.

The At MPB2C gene (TAIR acc. #At5g08120) exists as a single copy in the genome and is 62% similar the tobacco orthologous. MPB2C could also be found in Rice (GenBank acc. #AU094801), Sorghum (GenBank acc. #BE356348), Soybean (GenBank acc. # BE347146), Tomato (GenBank acc. #AI898765) and Maize (GenBank acc. #BE186113), whereas no releated proteins could be found in non-plant organisms (Kragler et al., 2003).
MPB2C harbours a hydrophobic and a predicted coiled coil domain which allows protein homodimerisation and interaction with several other proteins. Yeast Two-Hybrid interaction assays suggest that it interacts with TMV MP30, Nt MPB2C, Zm KN1, At STM and At KNB36 (figure 15B).
Further, analysis (http://elm.eu.org) of the protein revealed several phosporylation and glycosylation sites, which offer a broad range of distinct modification possibilities.
RNA overlay assays also show that the MPB2C protein binds to RNA, but also has negative effects on RNA binding capacity of its interaction partner KN1.
Microinjection studies suggested that MPB2C is not able to move from cell-to-cell via PD. Regarding tissue specificity, we found that MPB2C is expressed in areas overlapping or adjacent to At STM, At KNB36 and also At KNAT1.
Summarized, expression takes place in all tissues associated with meristems, including the vascular procambium of leaf primordia, cotyledons, stem and root meristem as well as lateral and floral meristems (see this thesis/results). At MPB2C knock out lines fail to be established, because At MPB2C loss-of-function seems to be lethal. One aim of this work was to establish MPB2C TILLING lines, carrying point mutations to reduce function of the native protein.

We assume that MPB2C is a cell autonomous factor which is involved in regulation of HD transcription factors and distinct virus proteins in an inhibitory manner including cell-to-cell transport and protein degradation (Winter et al., 2007).

3.2 MPB2C arrests the Tobacco Mosaic Virus Movement Protein (TMV-MP) at the microtubules

At MPB2C like Nt MPB2C has been observed to interact with the viral movement protein (TMV- MP) from tobacco mosaic virus but not with the cucumber mosaic virus movement protein (CMV-MP). The virus, using its viral MP, is able gain access to the PD, alters the size exclusion limit (SEL) of the PD (Waigmann et al, 1994) to transfers viral RNA-MP complexes (vRNP) into adjacent cells (Kragler et al, 2003). Within the cell, the TMV appears associated with the endoplasmatic reticulum (ER), with the cell wall (PD) in a punctuate manner and also with the microfilaments, where it was suggested to use a myosin-driven transport machinery to reach the PD (Ashby et al, 2006).

However, it seems that the viral spread of the TMV is not depending on the existence of microtubules (Gillespie et al, 2002; Kragler et al, 2003; Curin et al, 2006). This has been shown in experiments including an altered version of the native MP30, the MPR3, which shows no affinity to microtubules. The mutant protein exhibits an increased cell-to-cell movement capacity. The same results were obtained in *in situ* experiments with a disrupted microtubule cytoskeleton. In both cases neither local nor systemic spread of TMV was inhibited (cited, Kragler et al., 2003).
On the other hand, transient expression assays showed that MPB2C interacts with the TMV-MP, which leads to an accumulation of the protein at microtubules and endoplasmatic rediculum and decreases transport to neighbouring cells (Kragler et al., 2003).
The model predicts that MPB2C acts as decisive factor which is crucial for TMV-MP intercellular transport. TMV-MP is known to become polyubiquitinylated and it is suggested that it becomes subsequently submitted into the ubiquitin-depended 26S proteasome pathway. Support for this is found by MG115-depended inhibition of the 26S proteasome, which result in the predicted accumulation of the MP at the ER (Reichelt & Beachy et al., 2000).
Concluding, MPB2C acts as an negative effector of TMV-MP cell-to-cell transport activity and one could also expect that MPB2C represents a component of a degradation pathway, regarding facts like the formation of an MPB2C-MP30 complex and its subsequent detention at the microtubules.

3.3 MPB2C is a negative regulator of KN1 in a way similar to the TMV-MP

As mentioned before, MPB2C was also found as an interaction partner of Zm KNOTTED1 (KN1) and its ortholog At STM. Closer investigations revealed that this interaction depends on a distinct domain of KN1 and STM. Yeast 2-hybrid assays, including MPB2C, KN1 and truncated versions of KN1, showed that this interaction depend striktly on the presence of the homeodomain. MPB2C appeared able to interact with KN1ΔN (KN1 without MEINOX domain) but not with truncated KN1 versions regarding the homeodomain (KN1ΔC, KN1ΔHD). Further applied overlay assays, including a transport inhibited version of KN1 ($KN1^{M6}$), additional show that the protein interaction seems to be dependned on the presence but not on the functionality of the homeodomain. Concluded, we could say that the presence of a homeodomain is essential for the interaction beween MPB2C and specific transcription factors like KN1 and STM (Winter et. al. 2007).

Whereas the MEINOX domain of KNOX class I transcription factors is known to be essential for heterodimerisation with BLH proteins, the homeodomain appears essential for cell-to-cell movement. Now it was shown that this domain is also necessary for an interaction with MPB2C. To figure out wether the transport ability of these proteins is influenced by the binding of MPB2C, microinjections approaches and transient co-expression via particle bombardment were applied.
Gold particles coated with plasmids coding for At MPB2C and Zm KN1 were bombarded in *Arabidopsis* and *Tobacco* leaves to investigate if MPB2C is able to influence the symplasmic transport of KN1 into adjacent cells. In comparison to KN1 alone, transient overexpression in combination with MPB2C leads to an inability to alter the size exclusion limit. Therefore, no symplasmic transport of KN1 via PD could be seen in the presence of transient overexpressed MPB2C (unpublished data).

To verifiy MPB2C as a negative transport regulator of KN1 in planta, we established transgene plants overexpression At MPB2C with a trichome rescue background (see results capter 3)

Figure 14: Active and putative interaction partners of At MPB2C

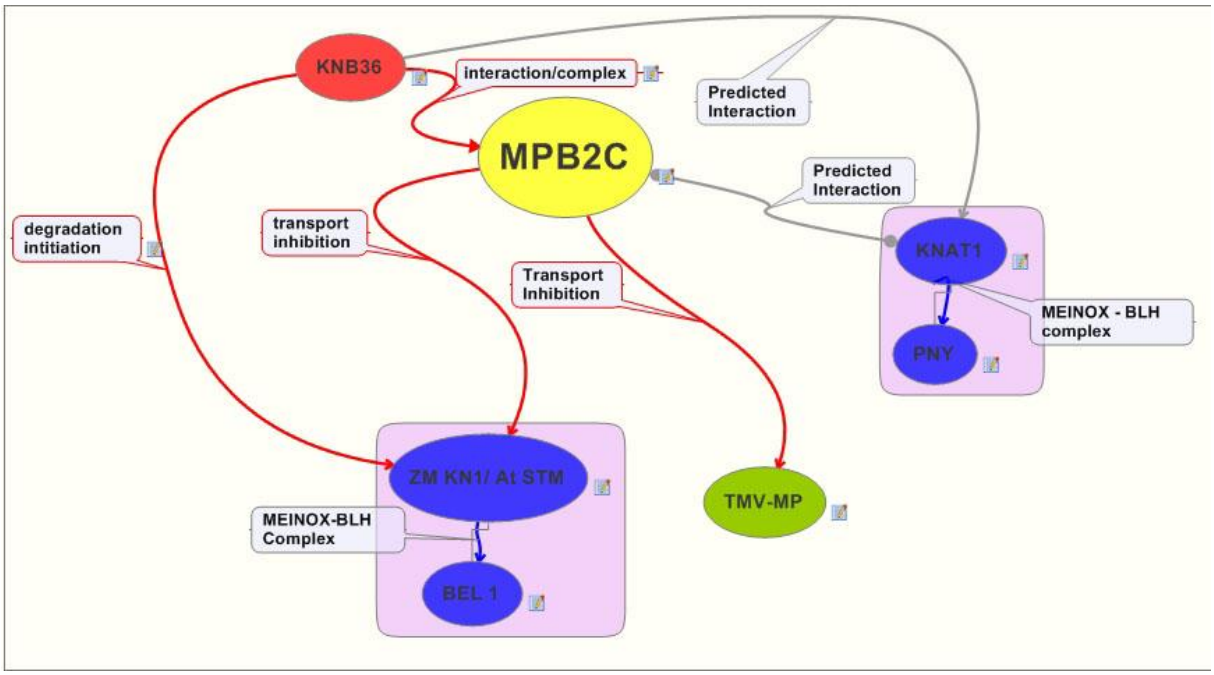

Note: MPB2C interacts with the Tabacco Mosaic Virus Movement Protein (TMV-MP) and class I KNOX factors (Zea mays KNOTTED 1 (Zm KN1); Arabidopsis thaliana SHOOTMERISTEMLESS (At STM). MPB2C is also known to interact with At KNB36 and maybe At KNAT1.

4. ***The novel protein KNB36 which interacts with MPB2C and herbal TALE proteins seem to set the seal on their fate***

4.1 Known facts of KNOTTED1-BINDING PROTEIN 36 (KNB36)

The At KNB36 protein (TAIR acc. # At5g03050) is a novel factor, isolated as an interaction partner of KN1 and later identified as an MPB2C binding protein. Foregoing investigations, using KNB36 from *Nicotiana tabacum* (GenBank acc.# DQ303421) driven by the 35S promoter, in transient expression assays including particle bombardment revealed that KNB36 localizes to the nucleus of the cell and seems to be non-cell autonomous. Nt KNB36 has an orthologe in *Arabidopsis* with an identity of 53,9 %.

Nt and At KNB36 were used as bait in Yeast two-hybrid assays. Several plant homeotic proteins like KN1, STM, LEAFY (LFY; (Sessions et al., 2000; Wu et al., al., 2003)) SHORT ROOT (SHR; (Nakajima et al., 2001; Gallagher et al., 2004)) BEL1, the MADS-box proteins APETALA1 (AP1; (Sessions et al., 2000)), APETALA3 (AP3; (Jack et al., 1992)), NCAPP1 and PP16 from Cucurbita maxima (Lee et al., 2003; Xoconostle-Cazares et al., 1999), were probed for protein interaction with KNB36. As shown in figure 15B, KNB36 forms specific heterodimeres with KN1 and MPB2C, but also with STM and BEL1 which is known to interact with KN1/STM. Because no interaction could be seen with LFY, SHR, AP1, AP3, NCAPP1 and PP16, it was suggested that KNB36 specifically interacts with distinct target proteins. In course of investigations, it was proven that KNB36, like MPB2C is able to form homodimers but also heterodimers also with their ortholog relatives from tobacco (Kragler et al., unpublished data). In silico analysis of the amino acid sequence predicts a coil-coiled region (Figure 15) suggested to mediate protein dimerizations (Hu et al., 2000).

To pinpoint the domains necessary for interaction between KNB36 and KN1/STM, several truncated versions of KN1 were used in yeast two-hybrid interaction assays. This includes KN1ΔN, KN1ΔC and KN1ΔHD (figure 15F). Interaction of Nt KNB36 as well as At KNB36 was proven using KN1 full, KN1ΔC and KN1ΔHD as bait but not with KN1ΔN. So it seems obvious that the successful interaction of KNB36 with KNOX factors like KN1 relies strictly on the MEINOX domain (Kragler et al., data not shown) which is interestingly also known to be essential for KNOX – BLH interactions (Bellaoui et al., 2001). Further in silico investigations of the protein structure revealed a cyclin substrate recognition side, which gave rise to the notion that At KNB36 is a factor involved in the cell cycle machinery. Data from rice Yeast two-hybrid screens has shown that a orthologous of At KNB36 interacts with cyclin B2.2 (GI:147743079) which is acting during the G2/M phase of the mitotic cell cycle (Cooper et al., 2003).

To conclude, KNB36 is localized in the nucleus and interacts specifically with the microtubules associated factor MPB2C as well as with specific TALE proteins like the KNOX protein KN1 and the BLH protein BEL1. In this work we will provide a detailed map of the KNB36 expression pattern throughout plant development and reveal that KNB36 not only colocalizes with TALE proteins but also seems to regulate HD-protein stability by submitting them to the degradation pathway.

Figure 15: Active and putative interaction partners of At KNB36 and At MPB2C

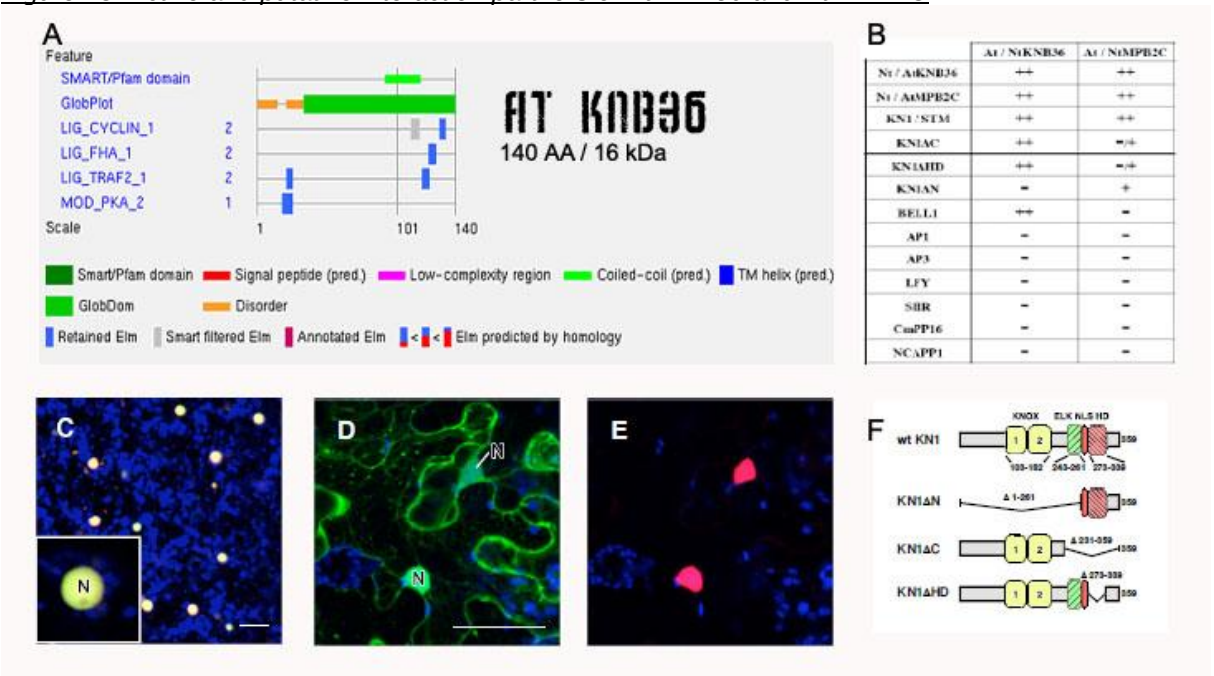

Note: (A) Predicted protein structure of At KNB36 (http://elm.eu.org); LIG_CYCLIN_1 (predicted cyclin interaction side AA130-133); SMART/Pfam domain (predicted coiled coil domain AA91-115 for homodimerisation and heterodimerisation with TALE proteins via KNOX domain); (B) Data from Yeast two-hybrid assay: At KNB36 as a potential interaction partner of Nt/At KNB36, Nt/At MPB2C, KNOTTED1, STM and BEL1. Knock out studies revealed that the interaction of KNB36 and KN1 depends on the KN1 homeodomain (HD). (F) Schemata of the knock out constructs used in the Yeast two-hybrid assay. Confocal images of fluorescent fusion proteins: (C) Transient co-expression of At KNB36-GFP and At KNB36-mRFP1; Transient co-expression of (D) Zm KN1-GFP and (E) At KNB36-mRFP1, 1-3 days after agrobacterium mediated infiltration. (D, E)Colocalisation of Zm KN1 and At KNB36 within the nucleus of infiltrated cells. KN1ΔN (KN1 without MEINOX domain); KN1ΔC (KN1 without ELK, NLS and HD); KN1ΔHD (KN1 without HD)

II. RESULTS

1. *In situ localisation of At KNB36 promoter activity*

First the question in which tissues of the plant At KNB36 expression occurs, was addressed. The goal was to compare the gained insights with the already well documented expression patterns of TALE proteins and other suggested interaction partners of At KNB36. Primarily we focused on tissues suggested to overlap or border the expression zones of the predicted interaction partners such as At STM/Zm KN1, At KNAT1/BP and At MPB2C.
For promoter analysis, transgenic plants were established through agrobacteria mediated transformation of Col0 wild type plants by applying the floral dip method.
The used binary vector (pKGWFS7) contained a EgfpER-GUS construct as a reporter, fused to the regulatory upstream region (from -753bp to -1bp) of the genomic At KNB36 ($Pro_{AT\ KNB36}$:EgfpER-GUS). The resulting expression vector was termed pA4.

The results were derived from 10 independent transgenic lines over a period of 3 generations (T1, T2, T3) which were examined during different developmental stages (3 days after germination (DAG); 16 DAG; 3 month after germination (MAG)). The data presented was consistent in a minimum of 5 independent transgenic lines (exceptions are noted).
Arabidopsis thaliana (ecotype Col0) wild type plants and transgenic lines expressing GUS, driven by the CaMV35S promoter (Pro_{35S}:GUS; line E6.3, E6.5) served as negative and positive control in all experiments.
Details regarding the assembly of the used expression vector (pA4) and the production of the examined transgenic plant lines (A4.1 – A4.13) are described in methods. A semi-quantitative RT-PCR was performed (Figure 16).

Here, RNA of Col0 wild type plants was isolated and cDNA was amplified using the primers
FK177 5`(5`-AATGGAAGAAGACGCAGGGAATGGAGGA- 3´) and
FK178 3`(5`-CCTCATTGCTCAATGCTAGGATTCTGAAT- 3´) for At KNB36 (35 PCR cycles). To standardize the expression levels the primers
FK424 5`(5`-GGAAGGATCTGTACGGTAAC- 3´) and
FK425 3`(5`-TGTGAACGATTCCTGGACCT- 3´) directed against Actin2 (TAIR acc# At3g18780) cDNA were used.

Figure 16: Verification via semi-quantitative RT-PCR

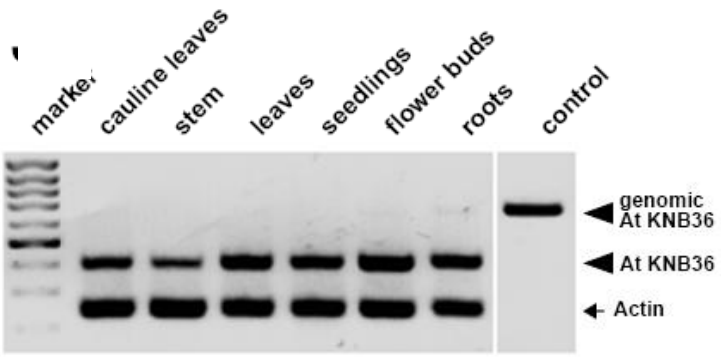

Note: Results of semi-quantitative RT-PCR targeting At KNB36 mRNA in different tissues of A. thaliana. As marked, the upper bands disclose presence of At KNB36 mRNA in roots, flowering buds, seedlings but also in rosette and, albeit weaker, in cauline leaves and stem. All samples were standardized against constitutive expressed Actin (lower lane of bands). At KNB36 genomic DNA (673bp); At KNB36 cDNA (423bp); At Actin (226bp)

1.1 At KNB36 promoter activity in seedlings (3 / 16 DAG)

Whereas no $Pro_{At\ KNB36}$:GUS dependened expression signal is visible in dormant seeds, an specific signal appeared in the corm of the germinating seedling at the root tip and the vascular procambium of the cotyledons. First results gave rise to the assumption that the premature seedling (< 3DAG) shows an unspecific signal in the entire cormus which regresses from the hypocotyl to the distal poles of the plant. Furthermore, in comparison to 3 DAG old seedlings, in 16 DAG old ones the signal in the cotyledon veins seemed to regress in the basal part of the leaf blade and the petiole.
However, high specificity within the immature seedling was revealed through the application of optimized staining procedures (see methods) and showed specific localisation of the signal at the radical, the vascular procambium of cotyledons radicle and the leaf primordia including the area of the SAM (Figure 17,18).

- **SAM & Leafprimordia**

Around the 3rd DAG, GUS signals can be detected within developing leaf primordia (82%) and the connected subapical bifurcation of the (pro-) vascular strand (Figure 17).
In the semi-spherical emerging leaves, At KNB36 seems to be expressed lateral in the area of the meristematic tissue of the 1st order procambium strand. The abaxial part of the procambium, which is presumptive the origin of the GUS signal, is known to differentiate into the phloem (Meyerovitz and Somerville, 2003) which pervades together with the xylem as vascular bundles in the mature leaf. To underline that At KNB36 expression takes primary place in the precursors of the vascular cells, it should be noted that cells of the 1st order procambium strand are first visible after 3DAG.

We detected At KNB36 expression also in the shoot apical meristem (SAM) between the primordial protrusions. The area of the SAM showed also an obvious GUS signal but it should be mentioned that this area is only composed of few cells and the employed techniques have to be improved to verify the weak signal in the SAM.

Figure 17: At KNB36 expression in the leaf primordia of 3 DAG seedlings

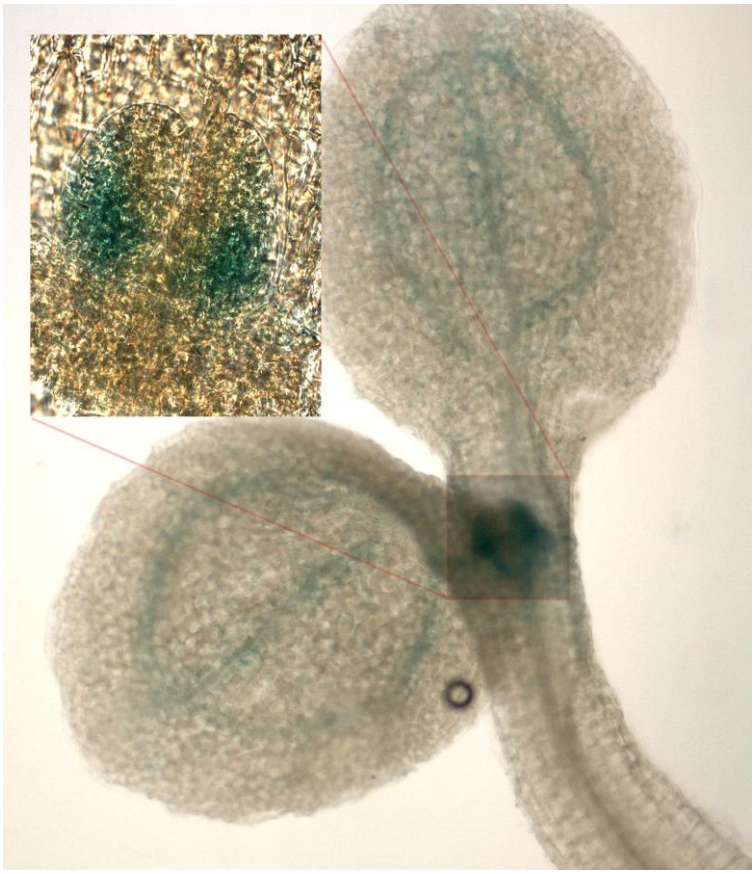

Note: Transgenic T2 line A4.1.2 (box upper left) expressing GUS under At KNB36 promoter. GUS signals in blue mark the leafprimordia, the subapical bifurcation of the (pro-) vascular strand and the (pro-) vascular tissues in the cotelydons of a 3 DAG old seedling.

- **Procamium & Vascular Bundles of Cotyledons and Radicle**

At KNB36 can be seen strongly in the vascular bundles of the cotyledons (64%) (Figure18 A-D).
At the first bifurcation of the lamina (1st order vasculature strand) in the 1st loops of the 2nd order vasculature strand at the distal pole of the cotyledons, a signal is detected (Figure 18 E,F; 20 E). Here the signal reached through the flanking ground meristem (GM) and epidermal cells to the margin of the leaf and appeared diffuse in the tissues surrounding the bifurcation (Classification of vein orders by Hickery et.al.,1973).

In the 16 DAG old rosette leaf At KNB36 expression can be found similar to that in cotyledons which declines to the distal pole of the leaf and also within the differentiated vascular bundles (Figure 18 E,F; 20 A-D) (completion of differentiation into phloem and xylem after 14 DAG (Scarpella et.al.,2004)).
The signal in the vasculature of cotyledons and also rosette leaves regresses until complete maturity of the organs has reached. GUS stains of 16 DAG old plantlets showed only weak remaining signals.
Unlike leaves, in **roots** At KNB36 expression seems to be constant regarding procambium and vascular bundles. Here ongoing strong signals could be detected in 94% within the vasculature of the radicle whereas in comparison only 12 % of the investigated seedlings showed signals in the vascular system of the hypocotyl. Like the strong expression at the distal pole of the cotyledons, conspicuously strong GUS signals appear at the boundary of root and hypocotyl (Figure 22 D). 16 DAG old transgenic plantlets show unchanged strong expression signals in the mature vasculature of the roots.

Figure 18: KNB36 expression in the vascular system and belonging precursor tissues

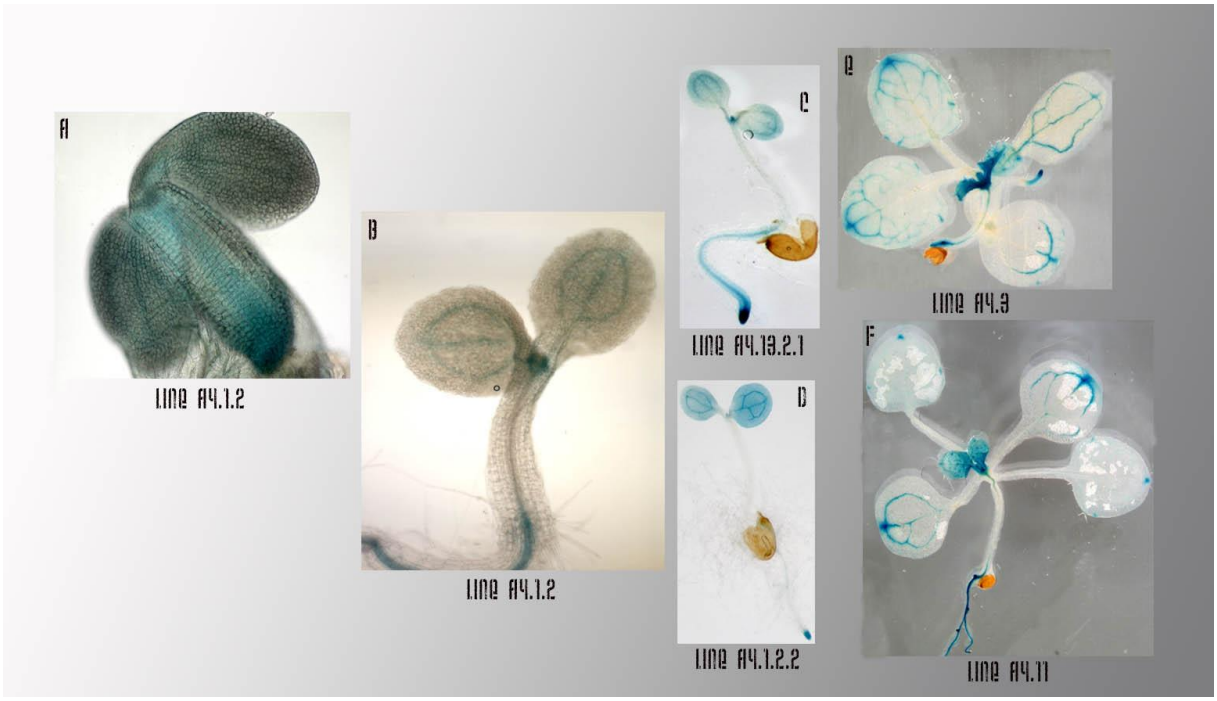

Note: Transgenic T2 & T3 lines showing PROAt KNB36:GUS expression. At KNB36 is expressed in meristematic highly active tissue. In 3 DAG old plants these tissues can be found in the shoot and the root tip as well as in the developing pro-vascular tissue. The blue GUS signal confirms that that At KNB36 is expressed strongly in these tissues (A, B, C, D). Compared to 3 DAG old seedlings, 16 DAG old plants shown the same pattern of activity, including tips and vasculature of primary and secondary roots, the SAM and the developing leaf. Fully differentiated leaves and the hypocotyl displayed no obvious signals. Only at the tip of the vascular bundles low expression could be detected. (E, F)

Expression in the root tip could be found in all examined transgenic lines at all developmental stages (Table 1; Graph 1). Closer investigations of the tip of 3 DAG old seedlings revealed specific expression in distinct areas.
In general, signals appear in the **meristematic zone** and **the elongation zone**, were cell division and expansion promotes the stable grown of the root. No signals could be seen in the zone were cells differentiate. As it can be seen in figure 19, At KNB36 seems to be highly expressed in the **meristematic tissue** which is composed of the 4 central cells and the 4 types of cell initials (Figure 26) (Dolan et al., 1993, Scheres et al., 2002). Furthermore strong GUS signals could be detected in cells flanking the procambium which is the **pericycle**, **endodermis** and **cortex**. Some lines show weak signals in the area of the procambium which will later differentiate into style tissue. No expression occurs in tissues like the lateral and the columella root cap or in the endodermis.

Figure 19: KNB36 expression in the root of Seedlings (3DAG)

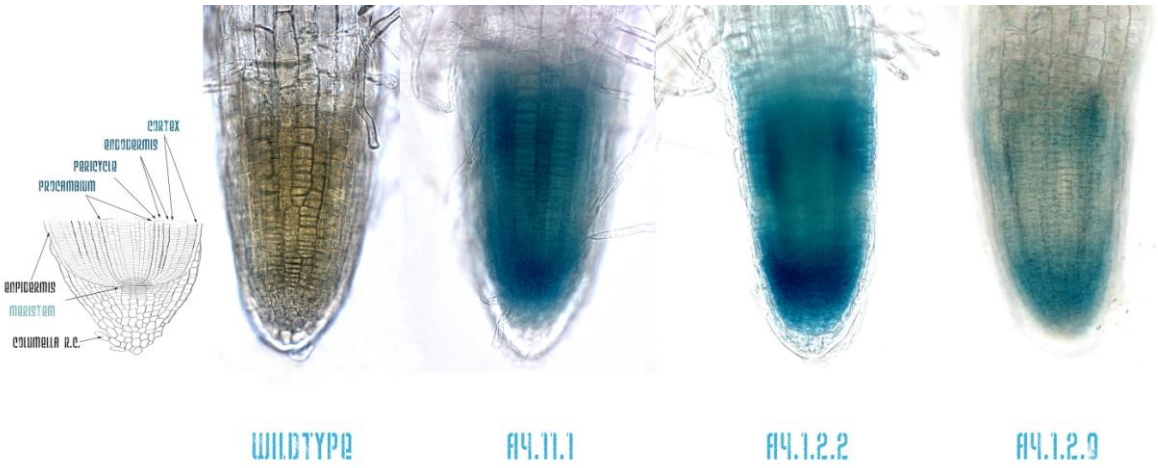

Note: PRO AtKNB36 dependent expression of GUS could be detected in the meristematic and elongation zone. Strong activity could be seen in the meristem itself and in the surrounding cell layers. Hotspots were also the distal area of elongating tissues like pericycle, endodermis and the inner layers of the cortex.

Graph 1: Statistically evaluated expression of At KNB36 in different tissues of the seedling (3DAG)

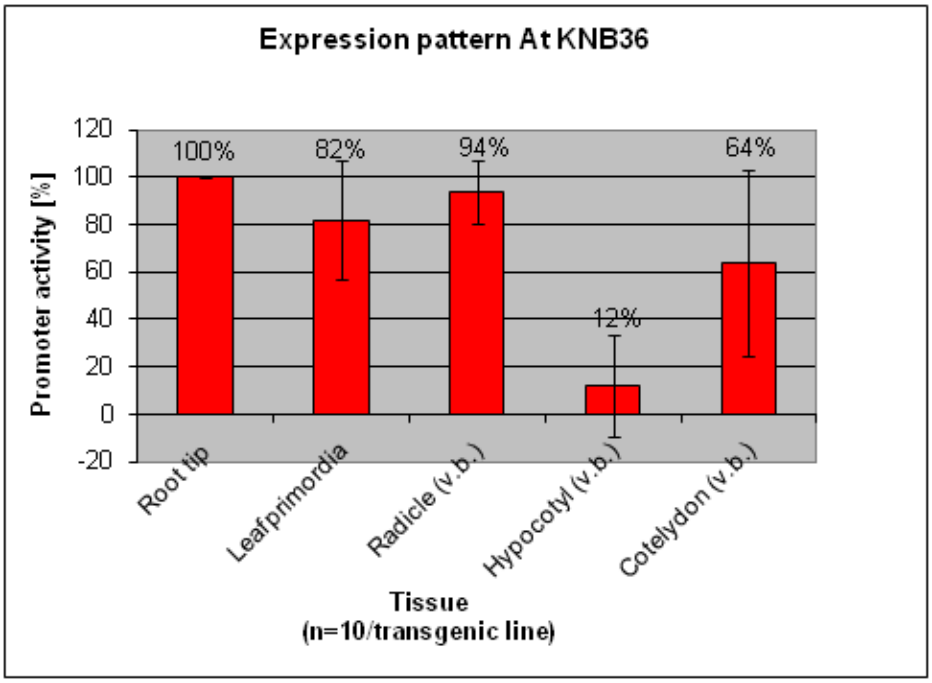

Note: The graph is based of the data of 5 independent transgenic 3 DAG old lines which aredisplayed in table 1. Obvious expression takes place in meristematic tissue of the root tip, leaf primordia and the vascular bundles (v.b.) blocks. Promoter activity could be detected in meristematic tissue. After 3 DAG, the KNB36 promoter is most active at the poles of the plant, at root and shoot tip and the leaf primordia. The Hypocotyl shows low activity in 3 DAG old plants. Also in fully differentiated vascular bundles of cotelydons and jung leaves KNB36 activity is very low. Summarized KNB36 is expressed in/or surrounding tissues with high meristematic activity.

Table 1: Observed expression pattern in 5 independent lines harbouring $Pro_{AT\ KNB36}$:EgfpER-GUS

Line Nr.:	**Generation**	**Roottip** (n=50)	**Leafprimordia** (n=50)	**Vascular procambium / bundles**		
				Radicula (n=50)	**Hypocotyl** (n=50)	**Cotyledons** (n=50)
A4.1.2	T2	10/10	10/10	10/10	5/10	10/10
A4.3.1	T2	10/10	9/10	7/10	0/10	7/10
A4.5.1	T2	10/10	8/10	10/10	0/10	6/10
A4.13.2	T2	10/10	10/10	10/10	1/10	9/10
A4.10.3	T2	10/10	4/10	10/10	0/10	0/10
Σ		50/50 **(100%)**	41/50 **(82%)**	47/50 **(94%)**	6/50 **(12%)**	32/50 **(64%)**

Note: Evaluated expression data of 5 independent transgenic lines which expressing GUS driven by the At KNB36 promoter.

1.2 At KNB36 promoter activity in mature plants

- **SAM & Leaves**

Our data suggests that the KNB36 promoter has a similar expression activity in mature plants as in seedlings with respect to meristems. The At KNB36 promoter seems to be active in the **vegetative meristem** as long as primordia are initiated and within the **leaf primordia**.
GUS stains of various parts of the stem, excluding the floral apical meristem, showed no signals.

Figure 20: At KNB36 expression during leaf development

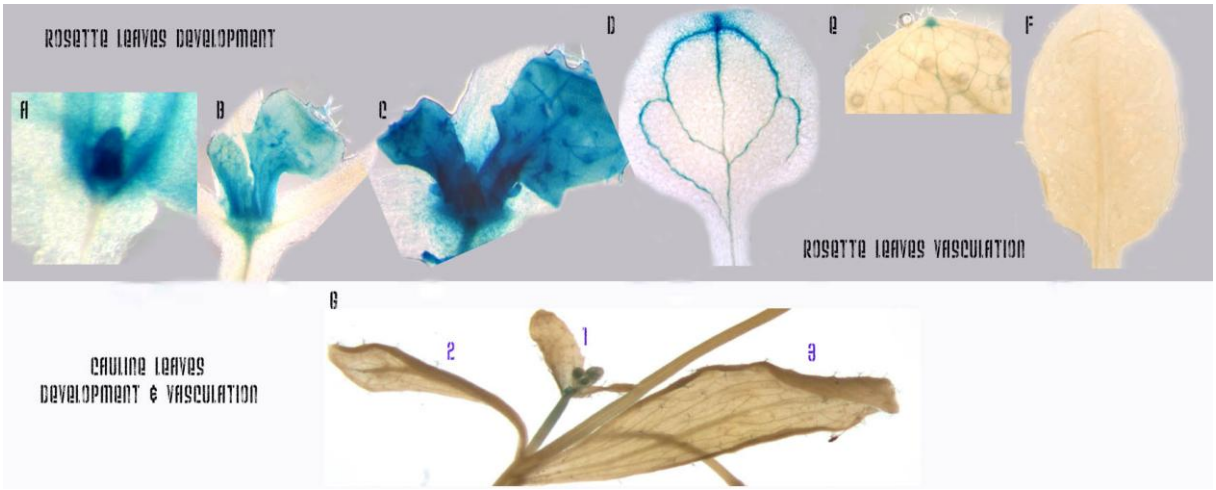

Note: The At KNB36 signal could be found in meristematic active tissue like the SAM (A), the vasculature of the cotyledons (D,E) and the emerging leaves (3DAG and 16DAG)(B,C) but not in differentiated, mature tissues (F,G).

- **Procamium & Vascular bundles of Rosette Leaves**

It was mentioned before, that At KNB36 expression is active in the vascular cells and their precursors in cotyledons and rosetteleaves. As observed in cotyledons the signal vanished slowly in later development stages of rosette leaves. Again at the top-bifurcation of completely differentiated vascular bundles a signal remained over a long period until the signal disappeared completely in the mature leaf (Figure 20 A-F). GUS stains of mature rosette or cauline leaves showed no signal in the petiole (Figure 21A), leaf epidermis, spongy mesophyll, or in the vascular network (Figure 20 G; 24).

- **Lateral Meristems: Axillary buds & Lateral Roots**

We have shown that At KNB36 expression occurs in one type of lateral meristems – the vascular cambium. So we decided to observe the expression in the branches of the inflorescence which can be easy recognized by the cauline leaves (bracts) which are formed at the basal nodes of each branch. Whereas no expression takes place in the cauline leaves or the stem, strong GUS signals were observed within the developing, lateral secondary inflorescences (paraclades, axillary buds) (Figure 21 B,C).
At KNB36 activity could also be detected in the vascular cambium as well as in the differentiated vascular bundles of secondary roots, especially during the reformation of the lateral meristem and in the root tip of the secondary roots (Figure 22 E).
During their initiation from the precursor – the pericycle (pericambium), the primordia of secondary roots showed remarkably strong signals (Figure 22 B)

Figure 21: At KNB36 is expressed in lateral meristems: Axillary buds

Note: As could be seen clearly, the At KNB36 promoter is also highly active in axillary buds. In these tissues which also show high cell division a signal could be detected. In differentiated tissues like leaves or the hypocotyl no At KNB36 was detected in 3MAG old plants.

Figure 22: At KNB36 is expressed in lateral meristems: secondary roots

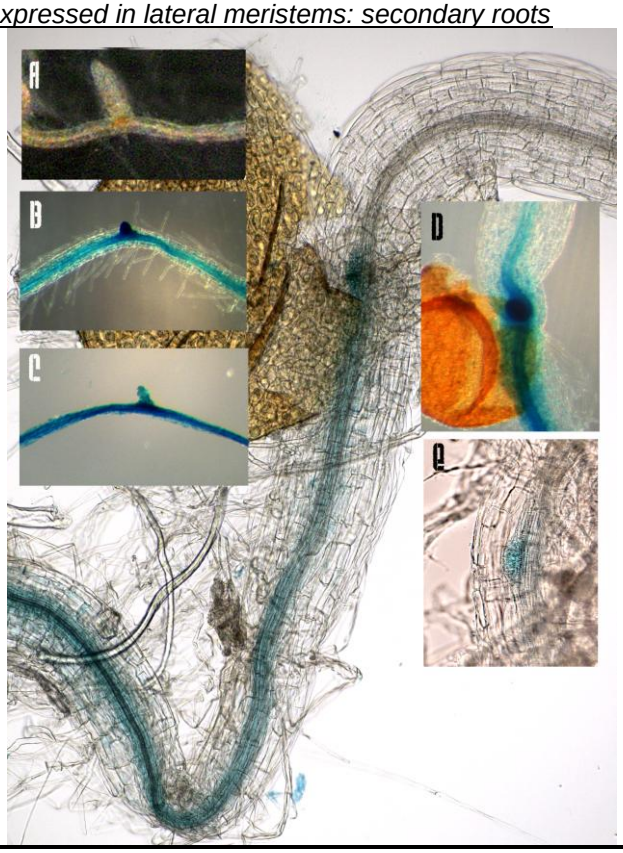

Note: The figure shows root tissue of 3 DAG old plants. Hotspots of At KNB36 expression could be found in the vascular bundles and the tip of secondary roots. Whereas the wild type control (A) show no GUS signal, the positive control (C) show an unspecific signal driven by the 35S promoter. Formation of a lateral meristem (E). Transition from radicula to hypocotyl

1.3 At KNB36 promoter activity in flowering plants

Whereas no signal could be detected in the stem 3 MAG, relativly high levels of the ProAt KNB36 dependened signals appear in tissues of the inflorescence (Figure 24).

- **Carpel**

The KNB36 promoter shows a complex developmental stage dependened activity within the carpel. As presented in figure 24 C, At KNB36 expression occurs in the early carpel and increases during development until carpel and stamen become mature and hence ready for (self-) pollination. Subsequently after fertilisation the signal in the **surrounding carpel tissue** and the **septum** regresses. The regression starts from the centre of the carpel to the distal, respectively the basal regions of the developing siliques (Figure 24 C7-9). The remaining signal at the apical part of the growing siliques is mainly concentrated in the surrounding carpel tissue. At the poles the signal remains in the **abscission layers** at the carpel/silique base (Figure 23A-C) and the **elongated papillary cells** at the stigma (Figure 23B) More unspecific signals could also be seen in this areas in transgenic control lines E6.5 and E6.5.2 (PRO_{35S}:GUS-TAP) but never in Col0 wildtype control lines.

Figure 23: GUS signals in abscission layers and elongated papillary cells of carpel/silique

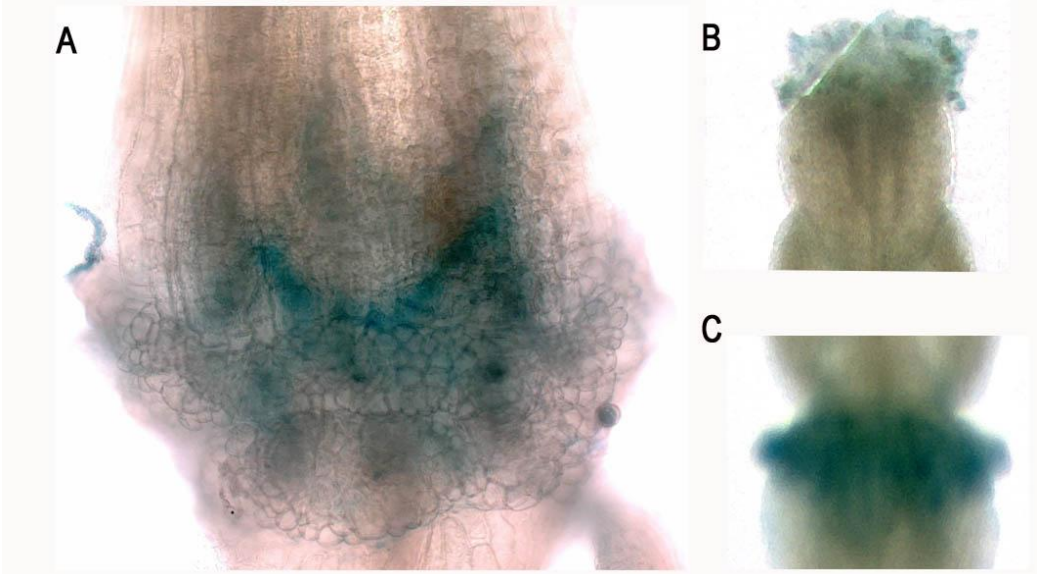

Note: Unclear signal in the abscission zone of the carpel/silique (A,C), the elongated papillary cells of the stigma. It is not clear if this signals remain as artefacts as identified in wt pollen grains. Mentioned signals were found in transgenic lines expression GUS driven by the endogenous At KNB36 promoter as well as in transgenic PRO_{35S}:GUS-TAP overexpressing plants. The signal was never detected in Col0 WT plants.

- **Petal, Sepal & Stamina**

We also detected staining in petals of flowering plants. After reaching a distinct point in flower development, GUS signals indicate At KNB36 expression in several transgenic lines (n=10). However, although no signal could be found in the petal of negative controls or transgenic lines harbouring the later discussed $Pro_{AT\ MPB2C}$:EgfpER-GUS, we did not detect unambiguous defined expression in petals. No signals appeared in the stem, mature siliques or, sepals.
As anticipated a strong signal appeared in the pollen grain (Figure 24C,D) of the mature stamina too, which was suggested as an artefact by Plegt and Bino 1989 and Hu et al.1990, albeit the signal was never detected in Col0 WT controls.

Figure 24: KNB36 expression patterns during flowering

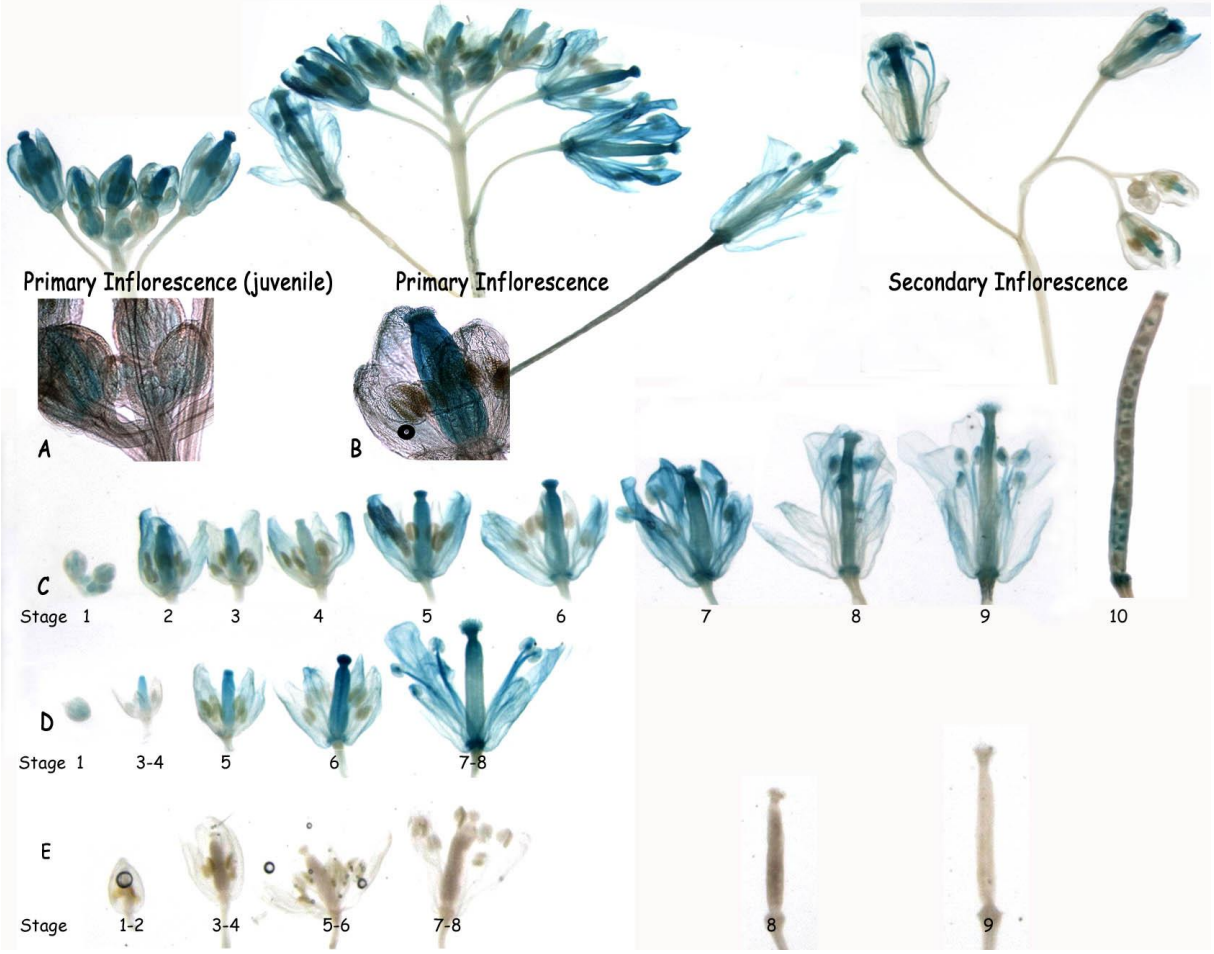

Note: GUS stainings of transgenic Arabidopsis line A4.1.10 (A,D) line A4.3.7 (B,C) and Col0 WT (E). Carpel development and maturity degree is visualized through an arbitrary chosen scale which is sectioned in 10 stages. The major checkpoints shaping the scale are the emerging of the juvenile flowering bud (stage1), the pollination (between stage 6-7) and the mature silique/seeds (stage 10). At KNB36 expression takes place in the whole flower cormus until stage 6. After pollination the expression declines to the distal poles of the carpel/silique and remains strong in the area of the abscission zone and unfertilized ovules.

- **Ovules and Associated Tissues**

After removal of the carpel envelope, GUS signals were also visible in the developing ovules (Figure 25 A). Closer investigations show GUS signals exclusive in well defined areas of the ovules and within septum and replum (Figure 25 B,C).
In early stages strong signals could be detected within the replum, which contains the transmitting tract for the pollen tubes and vascular bundles, and the connection to the ovules, the funiculi. Before fertilization the expression seems to be restricted to the embryo sac and the enveloping inner integument in ovules, the replum and the surrounding carpel tissues. Here no signals appear in the funiculus, the outer integument nor in its origin, the chalaza. As it can be seen in figure 25 D and 24 C-stage10, the At KNB36 promoter remains active in unfertilized ovules which show the greatest distance to the stigma (Figure 25 F) but switches completely off if fertilization was successful (Figure 25 G).
In fertilized and nearly mature siliques, however, it seems that the expression of At KNB36 switches off and declines to the distant poles of the silique, respectively the basal region. In (nearly) mature siliques/seeds no signal could be detected. In the basal region near the abscission layer some unfertilized ovules remained which show GUS. We suggest that in unfertilized ovules, the KNB36 activity dislocates from the interior tissues of the ovule to the funiculus and the chalaza
At KNB36 expression remained relative long at the abscission layers at the base of the siliques and in stigmata.
Furthermore no GUS signal appeared in the fully developed silique, neither in the mature seeds nor in the surrounding envelope.

Figure 25: KNB36 is expressed in ovules and specific tissues of the surrounding carpel tissues

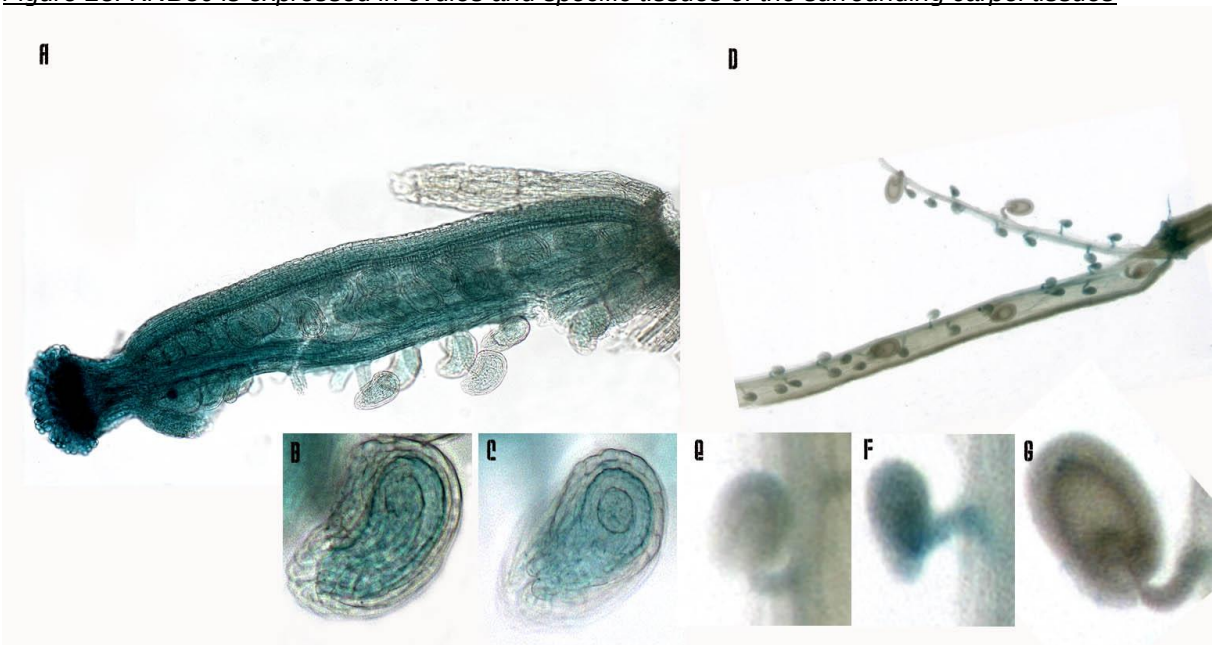

Note: At KNB36 expression during early carpel development: replum, septum, surrounding carpel tissues (A); embryo sac and inner integument of the ovules (B,C); late carpel development and transition to mature silique: weak signals in replum, basal carpel region and unfertilized ovules (D); closeup of unfertilized ovules show signals within tissues of funiculi, and the area of the chalaza.(F,G)

- **Conclusions: tissue specificity of At KNB36**

Summarized, At KNB36 expression is primary localized in meristems and within tissues which show high cell division activity.
Strong expression could be observed in primary meristems like the shoot apical meristem and the root meristem at the distal pole of the plant.
Furthermore it seems that At KNB36 expression is active in all secondary meristems including the axillary buds localized at the nodes of inflorescence branches at the stem and all fascicular meristems **(procambium) in cotyledons**, **primordia**, **leaves**, primary and secondary **roots** and also in the **septum** (replum) of the growing carpel. In roots, expression occurs in precursor tissues surrounding the procambium which differentiate into pericycle, endodermis and cortex cells.
In young leaves the At KNB36 promoter activity, however, seemed to be restricted to developing vascular strands (procambium) and regresses in the fully differentiated phloem and xylem and cannot be found in mature rosette leaves, cauline leaves, the hypocotyl and the stem.
Within the inflorescence, expression could be detected in the floral meristem as well as in the carpel. In early carpel stages, specific expression patterns could be localized in the **replum**, the **embryo sac** and the **inner integument** of ovules, the **surrounding carpel tissue**, the style and receptacle. After pollination the promoter becomes inactive and shows no signal in the embryo and in the other tissues of the dormant seeds until germination is induced. In unfertilized ovules, the promoter is active in the funiculus, chalaza and the proximal area of the outer integument.
The promoter activity in the primary meristems appeared to be constitutive whereas the activity in the flowers and the vascular system seemed to be depended on the developmental stage of the tissue. Excluding the vascular tissues in roots, the signal of the At KNB36 promoter driven GUS regresses until cell division processes stop.

At this point it should be mentioned that the earlier staining (staining procedure 1 and 2; see methods), used for the statistical analysis, lack high resolution. Here, the focus was to determine if there was a signal, in the root tip or in carpel tissue, or not. Stainings were optimized (procedure 3) during the late stages of my diploma work and allowed me to investigate the expression in single tissues inside the radicula and the ovules in the developing silique. This is the reason for the lack of a significant statistical analysis regarding At KNB36 expression in the root meristem, specific precursor cell layers within the roottip or tissues like the replum, the integuments or the embryo sac within ovules.

Figure 26: The Arabidopsis root – organisation and pattern formation

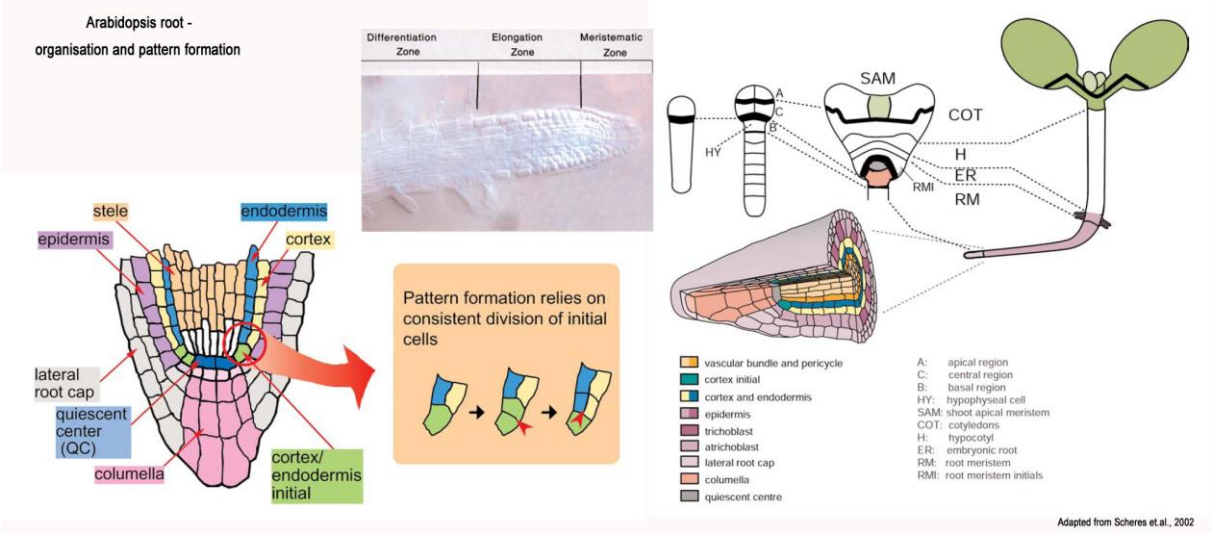

Note: The schemata illustrate the development of the Arabidopsis root. Cells of different root tissues originating within the root meristem and differentiate, according to the positional information, into various tissues which define the fully developed root.

2. *In situ localisation of At MPB2C expression*

To analyze the expression pattern of At MPB2C and correlate its activity to At STM/Zm KN1, KNAT1/BP and At KNB36 expression, transgenic plant lines were established by Niko Winter.

Thus, the regulatory upstream region (from -495bp to -1bp) of the genomic At MPB2C was cloned in the pKGWFS7 binary vector which provides a tissue specific GUS reporter. Subsequently transgenic plant lines were produced with the $Pro_{AT\ MPB2C}$:EgfpER-GUS constructs (Binary vector **1/1** and **2/1**) through transformation of Arabidopsis thaliana (ecotype Col0) via the floral dip method. (Transgenic lines **1/1**.1-7 and **2/1**.1-15). The below-mentioned data are an outcome of several GUS staining approaches with these transgenic lines in different developmental stages (3 DAG/ 3 MAG) and from a minimum of 5 independent lines. The lines were examined over a period of 3 generations (T1, T2, T3) to exclude artefacts which may result from multiple insertions, knockout of other genes by randomized insertion by agrobacteria or influence of the zygosity of the inserted construct.

Similar to the At KNB36 promoter analysis, wild type plants and transgenic Pro_{35S}:GUS lines (pE6) served as negative and positive control in each approach.

Staining protocols were optimized during the period of examination which results in a varying quality of the below-mentioned figures. Unspecific blue staining of tissues constitutes the effect of treatment with Acetone (80%) for longer than 1 hour. As a result cells were heavily damaged and GUS signals were able spread to neighbouring tissues.

RNA transcription of At MPB2C in the predicted tissues was confirmed through production of corresponding cDNA´s via RT-PCR (Figure 27). Specific primers used for reverse transcriptase reaction were FK228 3´(5´-ATAATATGTAAAGGCTAGTGATTG-3´) and for subsequently performed PCR (25 PCR cycles) FK228 in combination with FK227 5´(5´-CACCATGTATGAGCAGCAGCAAC-3´). All reactions were standardized against Actin cDNA (For details see methods)

Figure 27: Verification via semi-quantitative RT-PCR

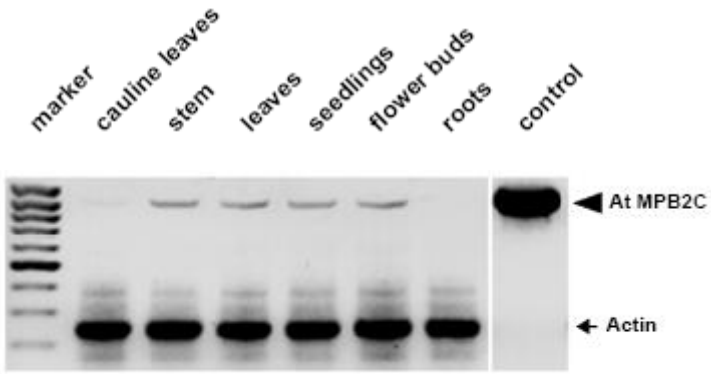

Note: In general At MPB2C is, in comparison to At KNB36, very weakly transcribed. However, weak bands indicate transcription of this gene in stem, leaves, seedlings and flowering buds. Additional a faint band could be seen in cauline leaves, whereas no, or very weak, transcription takes place in root tissues. The reactions were standardized against constitutive expressed Actin. At MPB2C CDS: 981bp

2.1 At MPB2C promoter activity seedlings (3 / 16 DAG)

Examination of dormant seeds of the T1 and T2 generation suggests that the At MPB2C promoter is inactive at this developmental stage of the plant (Figure 36). During the first 3 days after germination expression seemed to be localized to the vascular procambium of the complete cormus except the tip of the radicle (Figure 29B). It should be mentioned that this data originates only from one transgenic line (1/1-1) which provides remarkable strong expression during all generations. However, the expression pattern of At MPB2C in line 1/1-1 seems to be consistent in comparison to the other investigated lines in all developmental stages.

- **SAM & Leaf primordia**

Strong GUS expression was detected in tissues surrounding the shoot apical meristem and the leaf primordia (Figure 28). Similar to the expression of At KNB36, At MPB2C shows high intensity in 97% of investigated emerging leaves. Unfortunately it was not possible to provide GUS stained seedlings with a resolution high enough to identify the signal within the leaf primordia. Clearly visible was, however, activity within the subapical bifurcation of the vascular procambium which connects the two primordial protrusions.

Figure 28: At MPB2C expression in the leaf primordia of seedlings (3DAG)

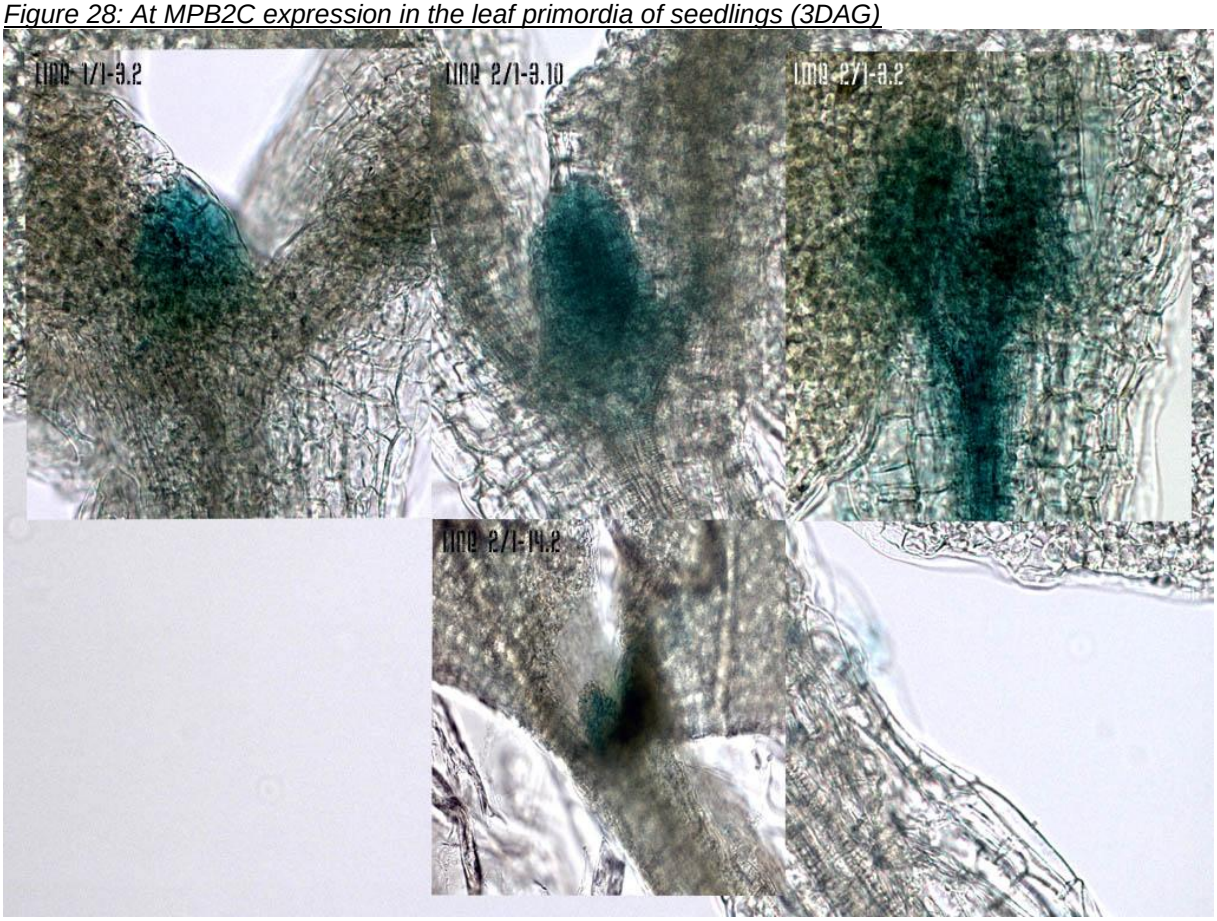

Note: Expression pattern of At MPB2C in 3 DAG old T2 seedlings: primordial protrusions (line #1/1-3.2; line #2/1-14.2); developing leaves (line #2/1-3.109; subapical bifurcation of vascular procambium (line#2/1-3.2)

- **Procamium & Vascular bundles of Cotyledons, Radicle and Hypocotyl**

The observation of the cotyledons of stained 3 DAG old transgenic seedlings revealed At MPB2C expression in the procambium strands of 84% (Graph2) of the investigated plants, which is similar to the expression pattern of At KNB36. (Because 16 DAG old plantlets were not examined, it is not possible to make a statement about the expression in the completely differentiated vascular bundles or the phloem and xylem within the hypocotyl or the roots.) In 3 DAG old seedlings, GUS signals could be seen in the procambium of the hypocotyl (34%) and also in the radicle (50%) (Table2). High variations regarding expression in the vascular procambium appear between the investigated lines. Whereas for example line 1/1-1 and line 2/1-3 show At MPB2C promoter activity within the hypocotyl in nearly all individuals, just one out of ten individuals of line 2/1-2 show activity here. In comparison expression in the vascular procambium can be seen in line 1/1-1 and 2/1-2 but never in line 2/1-3. The statistical dispersion is too large to make a correct statement in this case. Amazing is the fact that most of the independent lines show consistent signals within the vascular system of the cotyledons (84%). Consistent with the promoter-GUS activity in various tissues within these transgenic seedlings, semi-quantitative RT-PCR assays indicate that At MPB2C is, as assumed, produced in seedlings.

Figure 29: At MPB2C expression in procambium and vascular bundles

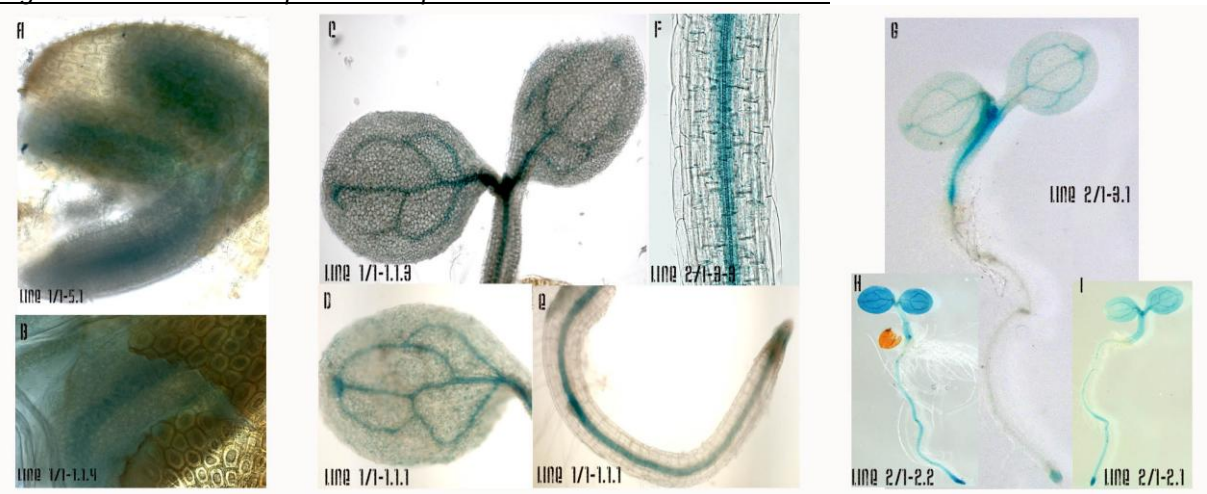

Note: At MPB2C expression pattern in the whole procambium of the vasculature in germinating seedlings (A,B); procambium/vasculation of the cotyledons (C,D,G,H,I); unclear signal in the procambium/vasculation of hypocotyl (F, H,I) and the radicle (E,H,I versus G)

- **Tip of the Radicle**

Optimized GUS stains and closer investigations of the tip of the radicle (3DAG) revealed specific expression within the tissues of this organ. As it can be seen in figure 30, very weak At MPB2C expression appears in the **meristematic** and also in the **elongation zone**, but not in the specialisation zone of the radicle. In the meristematic zone At MPB2C promoter driven GUS expression is detected in the **lateral root cap,** which flanks the root apical meristem and the cell initials. Also in the close proximity to the meristem signals appeared in some few layers of the distal (columella) **root cap**. As outlined in figure 31, expression occurs additionally in **central cell layers**, the procambium and style, above the meristem. We observed expression in this area in the strong expressing line 1/1.1. We could verify this signal in line 2/1-2 and very weak in line 2/1-14. As it can be seen in figure 30, most lines showed signals in few cells of the **epidermis** or **cortex** in proximity to the root meristem. No continual expressed, coherent pattern could be observed in epidermal and cortex cells.

Figure 30: At MPB2C expression in the root of Seedlings (3DAG)

Note: Expression pattern of At MPB2C in the tip of the radicle of 3 DAG old transgenic seedlings. Expression takes place in the elongation zone (area of the endodermis, cortex and procambium/style) and meristematic zone (lateral and columella root cap) but not in tissues of the specialisation area.

Figure31: At MPB2C expression pattern visualized throughout the root

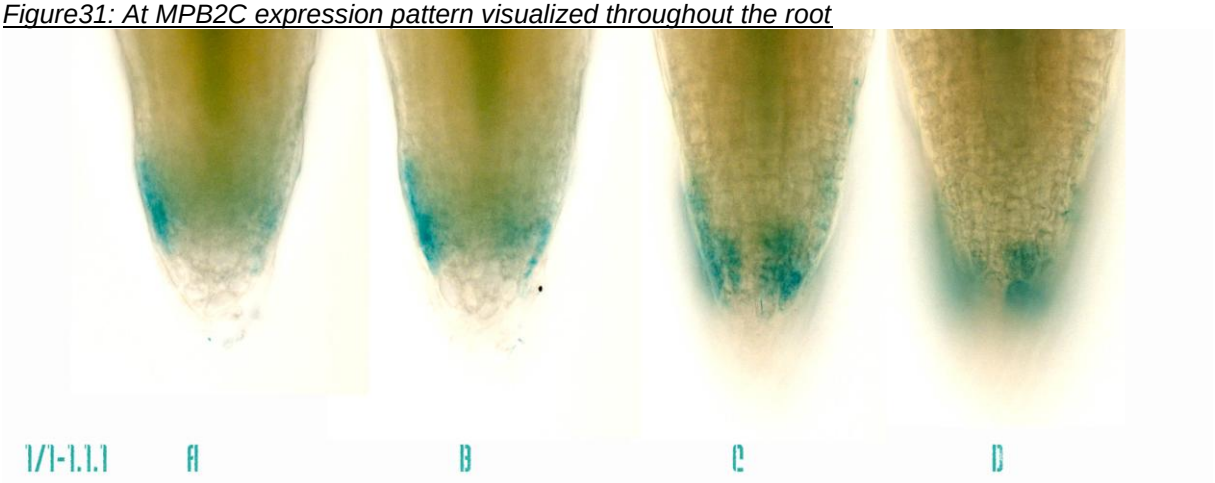

Note: Cross section of the root tip of the transgenic 3 DAG old T3 line 1/1-1.1.1 to illustrate the spatial expression pattern. Expression of At MPB2C is visible in the meristematic zone, the columella and lateral root cap.

Graph 2: Statistically evaluated expression of At MPB2C in different tissues of 4 DAG old seedling

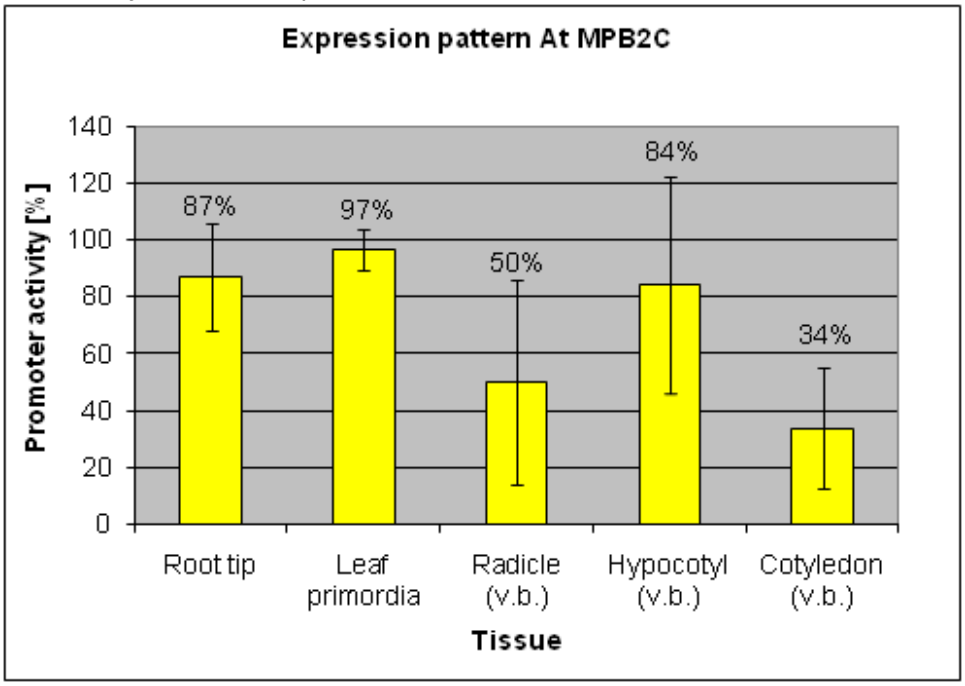

Note: The graph shows the promoter activity of 6 independent transgenic lines, expressing EgfpER-GUS under the endogenous At MPB2C promoter. These lines, as displayed in the table below where analyzed for expression of GUS. Data is not associated with the expression strength of the promoter in different tissues. At MPB2C is clearly active in tissues of the root tip and the leaf primordia. Cell type specificity is shown in table 2 below. The data also suggests that expression takes place in cotyledons and the radicle (vasculature). Tissues of the hypocotyl were found to have no or very low At MPB2C promoter activity.

Table2: Observed expression pattern in 6 independent transgenic lines harbouring $PRO_{At\ MPB2C}$:EgfpER-GUS

Line Nr.:	Generation	Roottip (n=53)	Leafprimordia (n=58)	Vascular Procambium / Bundles		
				Radicula (n=58)	Hypocotyl (n=56)	Cotyledons (n=58)
2/1-1	T1	10/10	8/10	2/10	0/10	10/10
2/1-2	T1	9/9	10/10	10/10	1/10	10/10
2/1-3	T1	5/10	10/10	0/10	9/10	4/10
2/1-14	T1	10/10	10/10	6/10	0/10	9/10
1/1-1.1	T2	7/9	9/9	8/9	6/7	9/9
1/1-3	T1	5/5	9/9	3/9	3/9	7/9
Σ		46/53 **(87%)**	56/58 **(97%)**	29/58 **(50%)**	19/56 **(34%)**	49/58 **(84%)**

Note: Data based on 6 independent transgenic lines expressing GUS under the At MPB2C promoter in 4 days after DAG old seedlings. 10 individuals per line were investigated and compared to each other and the wild type controls. 5 plant lines were investigated in the T1 generation, one in the T2 generation.

2.2 At MPB2C promoter activity in mature plants

- **Procamium & Vascular Bundles of Rosette Leaves**

As mentioned before, rosette or cauline leaves during early developmental stages were not examined.
RT-PCR analysis of RNA derived from wild type rosette leaves showed that RNA of At MPB2C can be found in rosette leaves, suggesting that the promoter is active in these tissues. No or very weak RNA was observed in cauline leaves.
Several GUS stainings of mature (3 MAG) transgenic plants indicate no promoter activity in the vascular bundles of mature rosette or cauline leaves (Figure 32).

Figure 32: No At MPB2C promoter activity in mature rosette leaves

Whereas At MPB2C promoter activity could be detected in the vascular procambium of the hypocotyl in 34% of the examined seedlings (3DAG) (Figure 29) no signal appeared in the vascular bundles of the mature stem in these lines (Figure 34). Semi-quantitative RT-RCR assays indicate that At MPB2C RNA can be found in stem tissues. Here, and also for mature rosette and cauline leaves, more specific methods should be applied to verify these findings. GUS signals always appear at the intersection of GUS stained stems and petioles of mature leaves. Here the signal seems to have migrated in the vascular bundles starting at the intersection and vanishes after 2-5 millimetres (Figure 32). Because this signal appeared only in the area of damaged cells we conclude that the GUS signal is not caused by the At MPB2C promoter activity and may be attributed to the plant stress response system.
No At MPB2C RNA could been detected in wild type roots and so far no GUS stainings were done examining the expression in developing or mature primary roots.

- **Lateral Meristems: Axillary buds & Lateral Roots**

Similar to the expression pattern of At KNB36 strong activity of the At MPB2C promoter could be observed in the branches of the stem, the axillary buds. Closer investigations of the lateral root showed expression in the emerging lateral root primordia at the pericycle in 3-4 DAG old seedlings. The temporal developmental pattern of lateral roots in Arabidopsis, shows formation of lateral meristems, 1-2 days after germination. The emerging lateral root can be visualized approximately 5-7 DAG.

Figure 33: At MPB2C is expressed in the area of lateral meristems: lateral root development

Note: Formation of lateral meristem in a 3-4 DAG old Arabidopsis seedling. GUS signals defining At MPB2C promoter activity in the area of a lateral root formation.

2.3 At MPB2C promoter activity in flowering plants

During the transition from vegetative to flowering stage no changes of At MPB2C expression in the cormus could be observed. No significant GUS signals could be detected in mature stem, cauline or rosette leaves. However, strong promoter activity appeared in new emerging tissues representing the primary and secondary sexual organs of the plant. Of course expression was also detected in new emerging organs which were not connected with the flower apparatus, like lateral roots.

- **Carpel**

Like the At KNB36 promoter, the At MPB2C promoter seems to become highly active in the emerging flower of Arabidopsis. Here we observed a very complex and tissue specific expression pattern which is stage dependent. There is no difference in the chronological and spatial expression pattern between primary and secondary inflorescences. A closer look showed that the promoter activity is weak in the entire young carpel. The activity increases until the carpel becomes fully developed and ready for (self-) pollination. In this phase the signals become more specific and could be localized to the septum (replum & transmitting tract) and to tissues associated with emerging ovules and the surrounding carpel tissue. Until pollination takes place, the

signal decreases. The GUS signal regresses slowly to some specific tissues associated with the ovules (Figure 36). Like in At KNB36 reporter lines, a conspicuous signal can be seen in the abscission zone of the silique as well as in the stigma and the elongated papillary cells.
The At MPB2C expression in septum, ovules, stigma, papillary cells and surrounding carpel tissue, reaches its peak at the pollination stage, whereas the region which defines the abscission zone of the carpel/silique, remains inactive until this stage. As can be seen in figure 35, At MPB2C promoter activity is missing between the stigma and the distal pole of the silique, the abscission zone (Figure 35A-F). No signals can be found in mature siliques or dormant sees (Figure 34/7; Figure 36).

Figure 34: At MPB2C expression pattern during flower development

Note: GUS stained primary and secondary inflorescence of the transgenic line 2.1-3, expressing GUS driven by the At MPB2C Promoter. Carpel/silique development was sectioned in 7 stages. Weak expression of GUS could be seen in early stages (1,2). Strong activity in nearly all organs of the flower excluding the abscission zone (3, 4) Abrupt inactivation of the promoter until pollination (5) and regression of the signal to the abscission layer and ovule associated tissues at the basal pole of the silique (6). No signal could be seen in the mature silique (7). The fictive represented scale sets the point of pollination approximately at stage 3

Figure 35: GUS signals in abscission layers and elongated papillary cells of carpel/silique

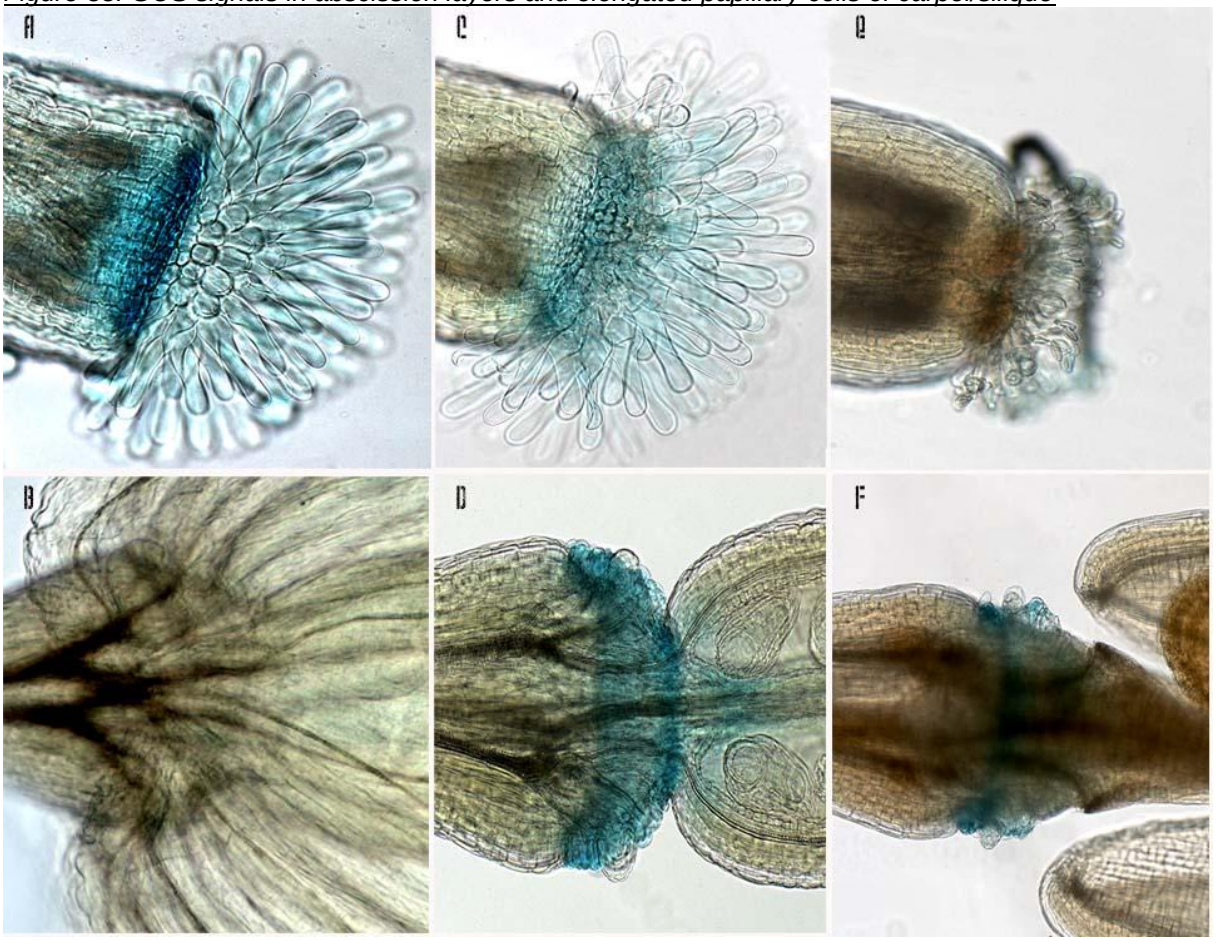

Note: GUS signals indicates strong and specific At MPB2C promoter activity within stigma and papillary cells (A) but not in the area of the abscission zone (B). At MPB2C expression decreases in stigma and papillary cells during maturation of the silique (C), but switches on in the area of the abscission zone. (D). In mature siliques only a faint GUS signal remains in the area of the abscission zone. (F)

- **Petal, Sepal and Stamina**

As illustrated in figure 34, no GUS stain was detected in other flowering organs than the carpel associated tissues. Several GUS stains verify that the At MPB2C promoter is inactive during all stages of flowering within petal and sepal tissues. Regarding stamina we observe an activity pattern which also seems to be connected with the ongoing maturation of the silique/seeds. In early stages of flower development no GUS signals could be detected in any stamina tissue. After carpels become mature and ready for pollination, MPB2C promoter activity was observed in pollen grains, but not in anthers or filaments. The GUS signal in pollen remains until the transition from carpel to silique is completed. As mentioned before during characterisation of the KNB36 expression pattern, the signals within pollen grains were designated as artefacts. (Figure 34) However, the same pollen derived signals could be seen in Pro_{35S}:GUS control lines but never in Arabidopsis wild type lines.
Summarized the At MPB2C promoter activity is limited to the carpel associated tissues of the flower and appears to be inactive in anthers, sepals and petals.

- **Ovules and Associated Tissues**

Closer investigations of the developing carpel reveal that the At MPB2C promoter is active in specific tissues of the developing ovules (Figure 36). Here activity could be observed in the funiculus, the chalaza and faint at the proximal part of the outer integument which is originating from the chalaza. No At MPB2C expression seems to take place in the interior tissues like the ovule itself including the embryosac, the inner integuments and the distal areas of the outer integument. After the carpel becomes mature and successfully pollinated, the signal vanished. Similar to the temporal and spatial expression pattern of At KNB36, MPB2C expression regresses from the distant to the basal pole (Figure 34, stage 5-6). Here, some basal ovules remain unfertilized and show ongoing promoter activity until fertilisation takes place or the silique finally dries out. We suggest that in this case the expression is limited to the funiculus. At this point it should be mentioned that, regarding ovules, At MPB2C expression takes place were no At KNB36 expression could be observed and vice versa.

Figure 36 :Expression of At MPB2C in ovules and the funiculus

Note: Developing carpel from Arabidopsis thaliana expressing GUS driven by the At MPB2C promoter. Signals could be seen in funiculus, chalaza and the proximal area of the outer integument but not in the interior of ovules or inner integuments. Below: comparison of a developing ovule and a mature seed.

- **Conclusions: tissue specificity of At MPB2C**

Summarized we can say that At MPB2C expression is primary localized around meristems and sometimes within tissues which show high cell division activity.
Strong expression could be observed **in the area of primary meristems** like the shoot apical meristem and the root meristem at the distal pole of the plant.
Furthermore it seems that the At MPB2C promoter is active in the area of secondary meristems including all fascicular meristems **(procambium) in cotyledons**, **primordia**, **leaves**, primary **roots** and also in the **septum** (replum) of the growing carpel. In roots, expression is localized to the meristematic zone, in the area of the **lateral and columella root cap** but not in the epidermis or the quiescent centre itself. Weaker expression takes also place in the root elongation zone in the area of the **endodermis**, the **cortex** and the **procambium** but not in the specialisation zone were cells are nearly fully differentiated.
In young leaves the At MPB2C promoter activity, however, seemed to be restricted to **developing vascular strands** (procambium) and regresses in the fully differentiated phloem. Whereas low levels of MPB2C could be detected in the procambium of hypocotyl and radicula, no signals appear in the mature hypocotyl, cauline or rosette leaves. When the plant switches from vegetative to sexual phase, expression could be detected in the **floral meristem**, and in later stages within the **carpel** but not in sepals or petals. In early stages of carpel development, specific expression patterns could be localized to the **Septum (Replum/transmitting tract), surrounding carpel tissue** and strong in **stigma** and associated **papillary cells**. During the maturation process of the ovaries, MPB2C is expressed specifically in the exterior regions of the ovules including the **funiculus,** the **chalaza** and the proximal region of the **outer integument**, but cannot be seen in the tissues of the embryosac or the inner integuments. After pollination the promoter becomes inactive and no signals can be detected in fertilized ovules/embryos, the carpel tissue or the stigma. Weak GUS signals remain in the basal region of the silique (abscission zone) and within the funiculi of unfertilized ovules.

Figure 37: Tissues of flowering organs and ovules in Arabidopsis thaliana:

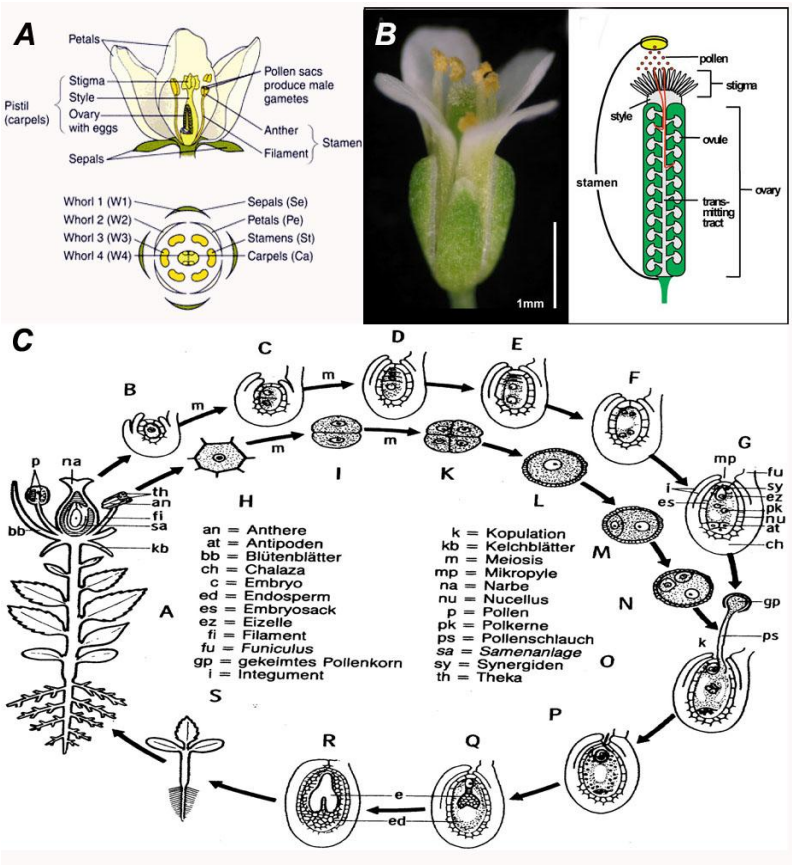

Note: (A) Schemata of the Arabidopsis thaliana flower. (B) Image of an Arabidopsis thaliana wild type flower and a schemata of the localisation and function of organs necessary for sexual reproduction. (C) Angiosperm lifecycle including detailed schemata of development and maturation steps regarding sexual organs / sexual reproduction.

3. Production of stable transgenic plants overexpressing At MPB2C in GLABRA1-rescue lines and Col0 background

3.1 Trichome Rescue: an In Planta transport assay for Arabidopsis thaliana

To examine whether At MPB2C interacts with class I KNOX proteins and is able to influence the symplasmic transport of Zm KNOTTED (KN1) in Arabidopsis thaliana, an in planta transport assay was used.
For understanding of the function of the in planta assay developed by Kim et al. (2005b) it is necessary to know some facts about the key element – the GLABROUS1 (GL1) protein. In wild type plants GL1 is expressed amongst others in epidermal precursors where it is able to initiate trichome development (Larkin et al., 1993; Oppenheimer et al., 1991). If this member of the MYB transcription factor family is functional deficient like in gl1 mutants, these plants fail to develop trichomes. To test if the GL1 protein is able to traffic through the symplasmic pathway via PD, GL1 rescue plants were produced expressing GL1, driven by the promoter of the Rubisco small subunit (PRO_{RbcS}), specifically in the underlying mesophyll cells. As can be seen in the schematic figure 38, GL1 is not able to move from the mesophyll into the epidermal cell layer. As a result these plants also lack trichomes like the original gl1 mutant. In the next step they modified the construct driven by the RbcS promoter through a C-terminal fusion with an N-terminal truncated KN1 construct (KN1HD) containing only the NLS and homeodomain of this gene. Additional, this GL1-KN1-HD contains an N-terminal fused GFP for verification purposes. After insertion of this PRO_{RbcS}:GFP-GL1-KN1HD construct to gl1 mutants, trichome development could be rescued. Here the number of developed trichomes correlates with the efficiency of GFP-GL1-KN1HD transport from underlying tissues into the epidermis. (Kim et al., 2005b)

Figure38: Schema of the trafficking assay

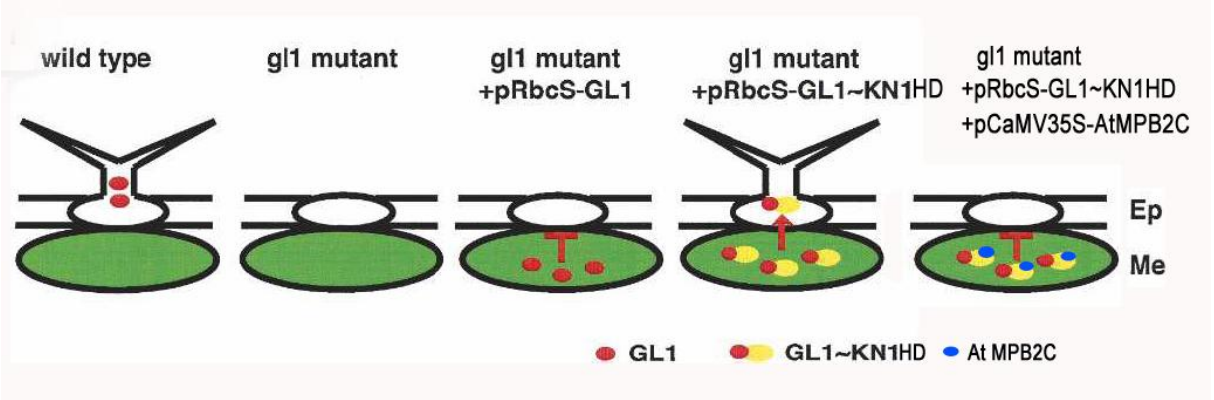

Note: In the wild type GL1 is able to initiate trichome development in an epidermal precursor. No trichome development could be observed in gl1 knock out mutants and gl1 mutants expressing GL1 in mesophyll cells driven by the RbcS promoter which validates the fact that GL1 acts cell autonomously. However, trichomes could be seen in gl1 mutants expressing GL1-KN1HD in the mesophyll what shows that the KN1 homeodomain is responsible for transport of GL1 from the mesophyll into epidermal cells were trichome development is initiated. Again no trichomes appeared gl1/ ProRbcS:GFP-GL1-KN1HD rescue plants which additional express At MPB2C under the CaMV35S promoter indicating that MPB2C is able to prevent the KN1HD mediated trafficking of GL1. Ep (Epidermis cells); Me (Mesophyll cells). Schema from Kim et al., 2005b; modified.

3.2 Production of various transgenic plants harbouring PRO35S:AtMPB2C

To investigate the question if At MPB2C affects the transport of Zm KN1 in the same way as it does that of TMV-MP, several kinds of transgenic Arabidopsis thaliana plants were established. This includes lines overexpressing At MPB2C-GFP (H4, H6) and At MPB2C-TAP (I3, I9) in a trichome rescue background harbouring the PRO_{RbcS}:GFP-GL1-KN1HD construct. To exclude that overexpression of At MPB2C effects trichome development, Col0 control lines were transformed with the same constructs.

3.3 Verification of the ectopic expressed At MPB2C and the desired background

Transgenic lines harbouring PRO_{35S}:At MPB2C-GFP or PRO_{35S}:At MPB2C-TAP were verified on DNA, RNA and protein levels. For verification on a DNA level, genomic DNA was extracted from transgenic lines and successful amplified via PCR with specific primers FK227 / FK398 (against MPB2C and TAP) and FK156 / FK228 (against the 35S promoter and MPB2C), including wild type DNA as negative and the diluted vector itself as positive control (done by Mag. Nicola Winter).
Verifications on the RNA level were carried out in an RT-PCR approach. Here total RNA was isolated from transgenic Arabidopsis rosette leaves and transcribed into cDNA (FK228). A subsequent PCR including the primer sets noted above, was performed.
Verified plant lines of H4, H6, I3 and I9 were investigated by confocal microscopy (CLSM) as canbe seen in figure 40. Unfortunately it turned out that no GFP signal could be seen in any transgenic plant line harbouring PRO_{35S}:At MPB2C-GFP. Because there appeared also no signal within the cytosol of symplasmically isolated guard cells we suggest that this effect cannot be attributed to systemic silencing of MPB2C as consequence of overexpression. To figure out if the problem was associated with mutations in the construct itself, transient expression assays, including particle bombardment and infiltration with agrobacteria were applied. Here strong expression of At MPB2C could be observed in several independent approaches (Figure 39). It was not possible to make stability arrays of the GFP fusion construct in transgenic plants during my diploma thesis. According to data from Mag. Nico Winter reduction of trichome number was equal in transgenic lines overexpressing MPB2C-TAP and MPB2C-GFP suggesting the MPB2C-GFP construct acts quite as predicted.
Summarized, we assembled successfully 9 independent lines harbouring At MPB2C-GFP in Col0 background and 7 in trichome rescue background. Additionally 36 independent lines, expressing ectopic At MPB2C-TAP in Col0 and 14 in trichome rescue background were verified. Two independent lines of each combination were verified on DNA, RNA and protein level.

Figure39: At MPB2C-mGFP5 appears aggregated within the cytoplasm

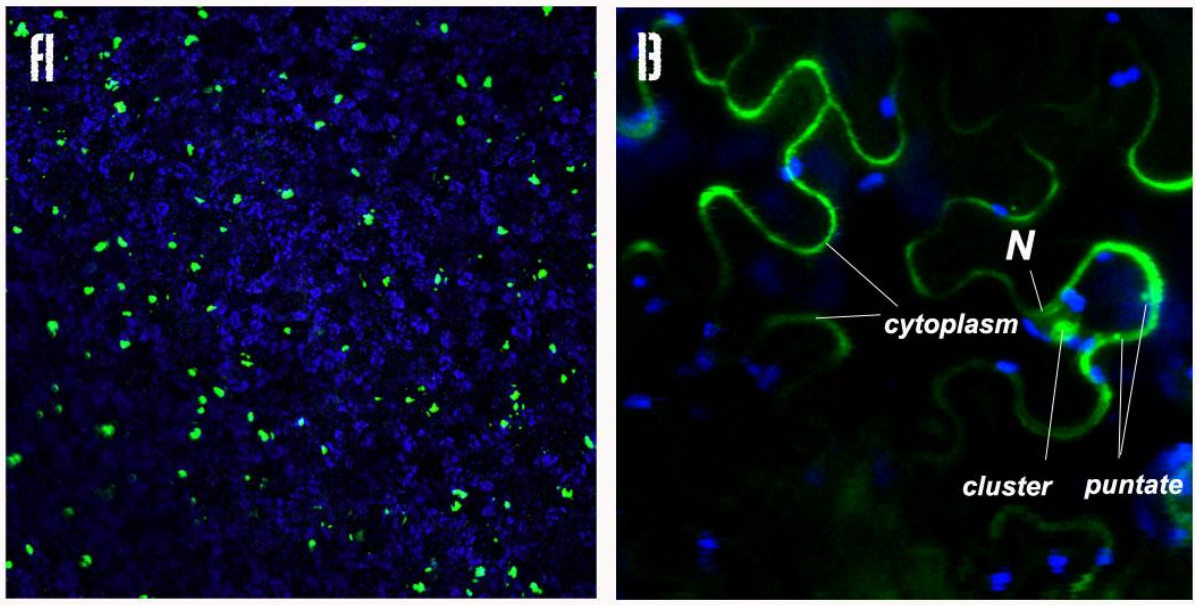

Note: Transient agrobacteria mediated infiltrations show that At MPB2C-mGFP5 appears cytoplasmic but cannot be seen in the nuclei of cells. The expressed protein was only found in the cytoplasm between the vacuole and the cell wall where it is defining the cell shape. It cannot be seen in the nucleus (N) but in clusters in spatial proximity of the nuclear envelope. As it can be seen in (B), MPB2C appears not only in clusters but also in small aggregates, so called punctate structures. At MPB2C was only detected in transient expression assays, confirming the functionality of the construct, but never in transgenic plants. (The association with the microtubules is not shown). Magnification: (A) 10x; (B) close up from a 40x image.

3.4 At MPB2C limits the movement of Zm KNOTTED1 in Arabidopsis

As mentioned in capter introduction, it is already known that Nt/At MPB2C interacts with Zm KNOTTED1 through the specific binding of MPB2C to the KN1 homeodomain (KN1HD). Moreover MPB2C interacts with the movement protein of the Tobacco Mosaic Virus (TMV-MP) and limits the TMV-MP movement from cell to cell. We show that overexpression of At MPB2C-TAP in gl1/GFP-GL1-KN1HD trichome rescue plants (TR) results in a loss of the GFP-GL1-KN1HD signal in epidermal nuclei, but not in subepidermal tissues (Figure 40B). This validates the findings gained from Yeast two-hybrid assays that At MPB2C interacts specifically with the homeodomain of KN1. Furthermore it proves that At MPB2C inhibits the trafficking of the GFP-GL1-KN1HD rescue construct. In line with the absence of signals in epidermal nuclei, an extreme reduction of trichome development was observed in these transgenic lines. In this way the trichome rescue assay proves in two different modalities the MPB2C – KN1HD interaction and the inhibition of the KNOTTED1 movement capability similar to the TMV-MP.
The close analysis of these effects in ensuing generations, their verification as well as the statistical investigation regarding nuclei signals and the varying number of trichomes in these transgenic lines have been continuative taken over by Mag. Nikola Winter (N.Winter diploma thesis; Winter et al., 2007).

Figure40: Overexpression of At MPB2C limits the movement of the GFP-GL1-KN1HD trichome rescue construct and results in a lack of trichomes in transgenic plants.

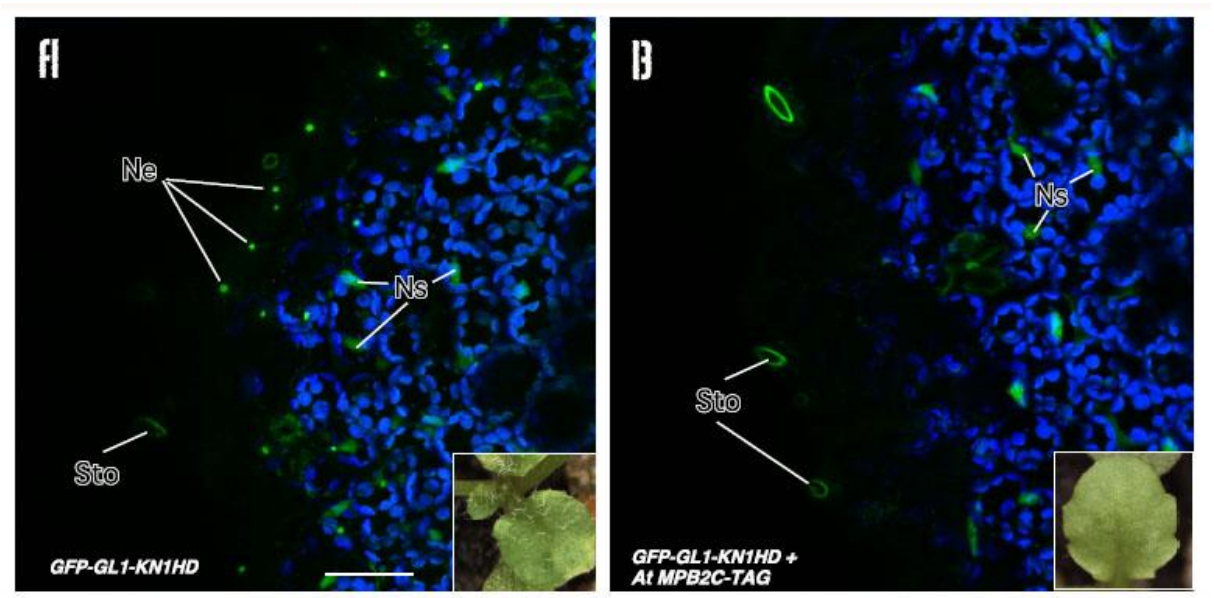

Note: Whereas GFP-GL1-KN1HD signals could be seen in nuclei of epidermal tissues in trichome rescue lines (A), only subepidermal nuclei signals remain in trichome rescue lines overexpressing At MPB2C-TAP (B). In comparison to the trichome rescue lines, no or few trichomes emerge in these plants (compare small boxes in lower right corners). Sto (Stomata); Ne (Nucleus epidermal); Ns (Nucleus subepidermal); Bar:80µm

4. Subcellular distribution of At KNB36-mRFP1/mGFP5 fusion proteins

4.1 At KNB36-mRFP1/mGFP5 appear exclusively in the nuclei of stable transgenic plants

The KNotted1 Binding protein 36 (KNB36) was, as mentioned before, identified in the laboratory as a potential interaction partner of MPB2C. Yeast two-hybrid assays, microinjections and other transient expression assays focused on KNB36 from Nicotiana tabacum. To investigate the interaction potential of KNB36 regarding homeodomain proteins and to verify the findings, new constructs based on the Arabidopsis thaliana KNB36 were cloned. To learn where the At KNB36 protein is localized in vivo, transgenic plants overexpressing tagged versions of KNB36 were established. In two parallel approaches, the genomic ORF of At KNB36 was C-terminal tagged with mGFP5 (constructs pB9 / pB2) using the Gateway™ system. Also the At KNB36 cds was fused to red fluorescent protein 1 (mRFP1) via an alanine linker by classical cloning (construct pJ7.2). Particle bombardment of young Arabidopsis leaves and subsequent analysis of the transient expressing tissues via confocal microscopy serves as the method of choice to verify the functionality of the designed constructs.
Subsequently Arabidopsis thaliana plants were transformed with *Agrobacterium tumefaciens* harbouring the pJ7.2 (PRO_{35S}:AtKNB36_cds – 10xALA – mRFP1) or pB9/pB2 (PRO_{35S}:AtKNB36_genomic_ORF-mGFP5) construct. We transformed successful Arabidopsis with different backgrounds including Col0 and the trichome rescue background (GL1; PRO_{RbcS}:GFP-GL1-KN1HD).
The resulting T1 generation was selected on appropriate antibiotics and positive transformants identified on genomic level via PCR. (FK156/FK259: background verification and FK156/FK178: KNB36 verification) A final verification of the T1 generation was done by confocal microscopy (CLSM). Unfortunately plants with the GL1 background were resistant to Hygromycin. Because Hygromycin is also the selective marker of the pJ7.2 plasmid, the resulting resistance conflict made it impossible to establish the pJ7.2 construct in plants with the GL1 rescue background.

Transient expression in particle bombarded *Arabidopsis* leaves reveal that At KNB36-mGFP5, as well as At KNB36-mRFP1 appears exclusive in the nuclei of transformed cells. These findings were subsequently verified through data received from confocal microscopy of transgenic cauline and rosette leaf samples overexpressing At KNB36 in Col0 background. Here, 3 out of 5 independent transgenic lines, which were positively selected with appropriate antibiotics and confirmed via PCR on DNA level, were self pollinated and observed through 3 generations. Transgenic lines B2.2, B2.4 and B2.6, which are heterozygotic for At KNB36-mGFP5 in T1 generation split correctly according to Mendel´s laws in theT2 generation. The subcellular localisation of the GFP signal was, as suggested by transient expression data, remaining in the nucleus of epidermal and subepidermal (mesophyll) cells. Five T2 individuals of each transgenic line were confirmed as described above and verified through CLSM in two different developmental stages. As can be seen figure 42 some individuals, indicating obvious strong signals in epidermal and subepidermal nuclei, showed 17 days later only GFP signals in the nuclei of the guard cells of the epidermal embedded stomata. Because these cells are known to be symplasmically isolated, the absence of the GFP signal in pavement and mesophyll nuclei indicates systemic silencing of At KNB36-GFP in developmentally advanced plants.

The same effects where noticed in plants overexpression At KNB36-mRFP1. Here also 4 out of 44 independent transgenic lines where chosen for further investigations. Lines J7.3, J7.5, J7.17 and J7.28 showed also a clearly signal in the nuclei of epidermal and subepidermal cells including the nuclei of guard cells. Again, several individuals of two transgenic lines (J7.3, J.5) showed systemic silencing At KNB36 in advanced developmental stages of the T2 generation.
The same strategy was applied to develop transgenic plants harbouring p35S:KNB36-mGFP5 in the gl1/GFP-GL1-KN1HD trichome rescue background. Here we focused on 5 out of 34 independent lines which were positively selected. Lines B9.4, B9.6, B9.7, B9.11 and B9.24 are trichome deficient (Figure 43; Graph 5) and show, consistent with transgenic lines in Col0 background, strong GFP signals within the nuclei of epidermal and subepidermal tissues. As visible in figure 42B and 43B, GFP could also be detected in symplasmically isolated guard cells. As mentioned before the GFP-KN1HD is driven by the RbcS promoter which is only active within the chloroplasts of green tissues. Epidermal guard cells of *Arabidopsis* are known to harbour only a few chloroplasts, therefore the RbcS promoter is marginally active in epidermal tissues and GFP-GL1-KN1HD can only be expressed at low levels here.

Figure41: At KNB36 is located exclusively in the nucleus of cell

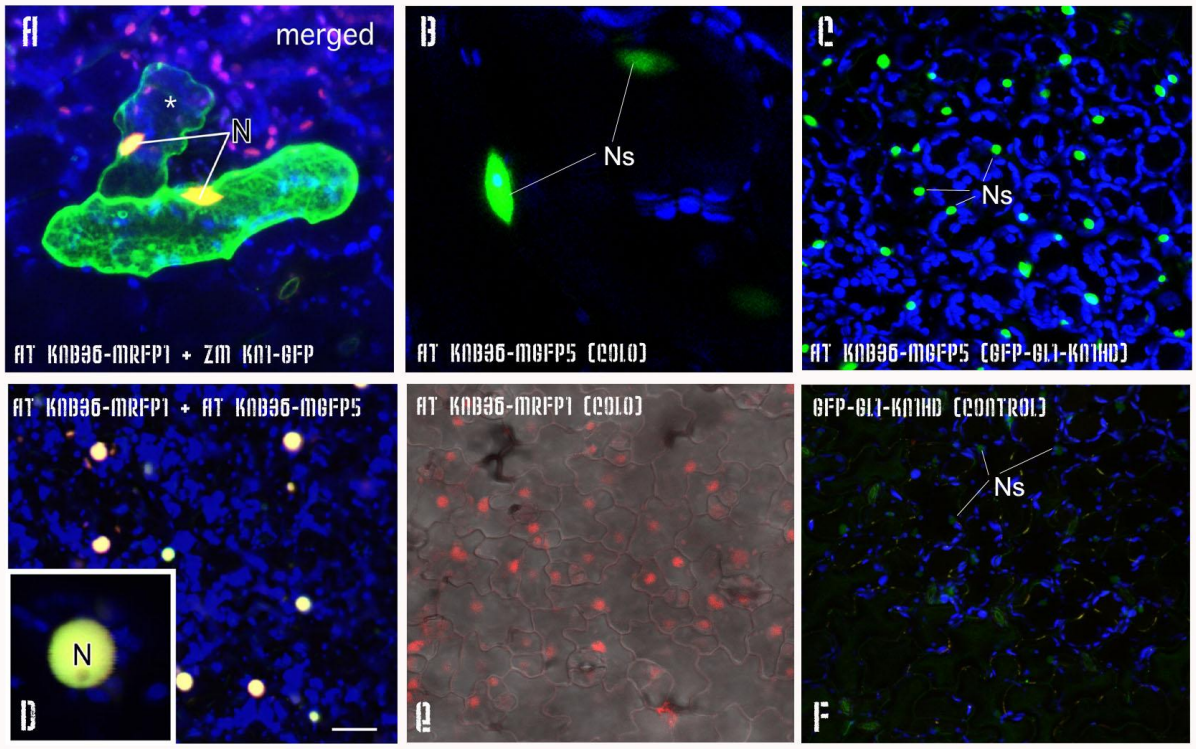

Note: Transient expression, 2-3 days after particle Co-bombardment: At KNB36-mRFP1+At Zm KN1-GFP (A) and At KNB36-mRFP1+At KNB36-mGFP5 (D). KNB36 is exclusive located in the nucleus of the cell. Note that KNB36 and KN1 co-localize within the nucleus (A); Stable expression in transgenic Arabidopsis thaliana: At-KNB36-mGFP5 in Col0 line B2.6.1 (B) and trichome rescue line B9.6.2. (C) At KNB36-mRFP1 in Col0 line J7 (E). Control: GFP-GL1-KN1HD trichome rescue line (F). Note that the GFP signal is obvious weaker than in case of At KNB36-GFP (C). Abbreviations: (N) Nucleus; (Ns) Nucleus subepidermal. Magnification differs in most figures; (C,F : 40x); (E) Image is merged with transmitting light image

Figure42: Systemic silencing of At KNB36-mGFP1 and At KNB36-mRFP1 in Col0

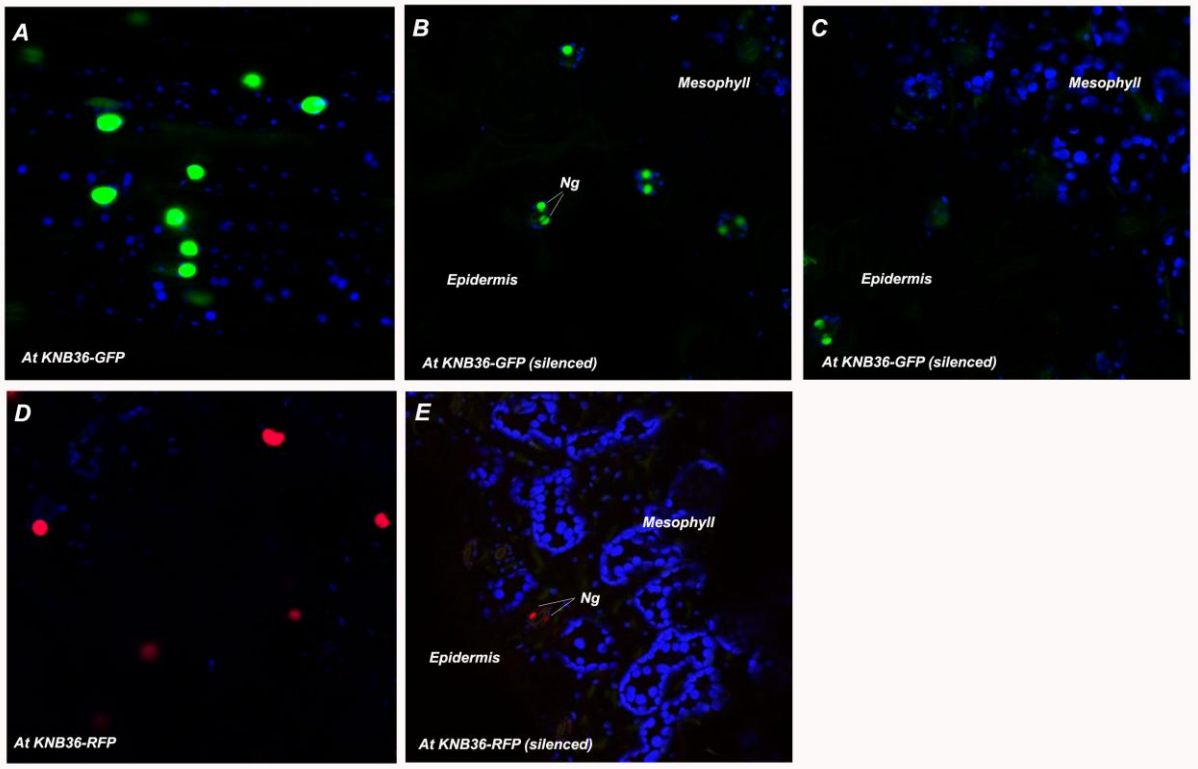

Note: Ectopic expression of At KNB36-mGFP5 (A, B, C) and At KNB36-mRFP1 (D) in transgenic Arabidopsis thaliana Col0 plants. Systemic silencing was registered in several independent lines. No mGFP5 signal could be detected in (B) epidermal or (C) subepidermal tissues of At KNB36-silencing plants. The only exceptions are the nuclei of the stomata guard cells which are symplasmically isolated. The same situation was found in plants overexpressing At KNB36-mRFP1 (E). Again only isolated guard cells show expression of the fluorescently tagged protein. (Ng) Nucleus guard cell; Magnification 40x

Thus, GFP signals in the epidermis of trichome rescue control plants were attributed to proteins which moved across the mesophyll – pavement cell boarder. Here, no GFP could be seen in guard cells of the stomata. Thus, the signals in figure 44B derive from the At KNB36-eGFP5 construct and not from the GFP-KN1HD construct which shows no signal in the nuclei of the guard cells.

Summarized, we were able to clone two different fusions of At KNB36, with mRFP1 and mGFP5, which were successfully tested in transient expression assays. Furthermore we established transgenic lines to verify the findings regarding the subcellular localisation of At KNB36 in two different backgrounds – Col0 and gl1/ GFP-GL1-KN1HD. The At KNB36 fusion protein was found exclusively in the nuclei of epidermal and subepidermal tissues of transgenic plants. Additionally we could show that the ectopic At KNB36 was silenced in several individuals of different independent lines during later stages of development.

Figure43: No GFP-GL1-KN1HD signals could be seen in At KNB36 overexpressing plants:

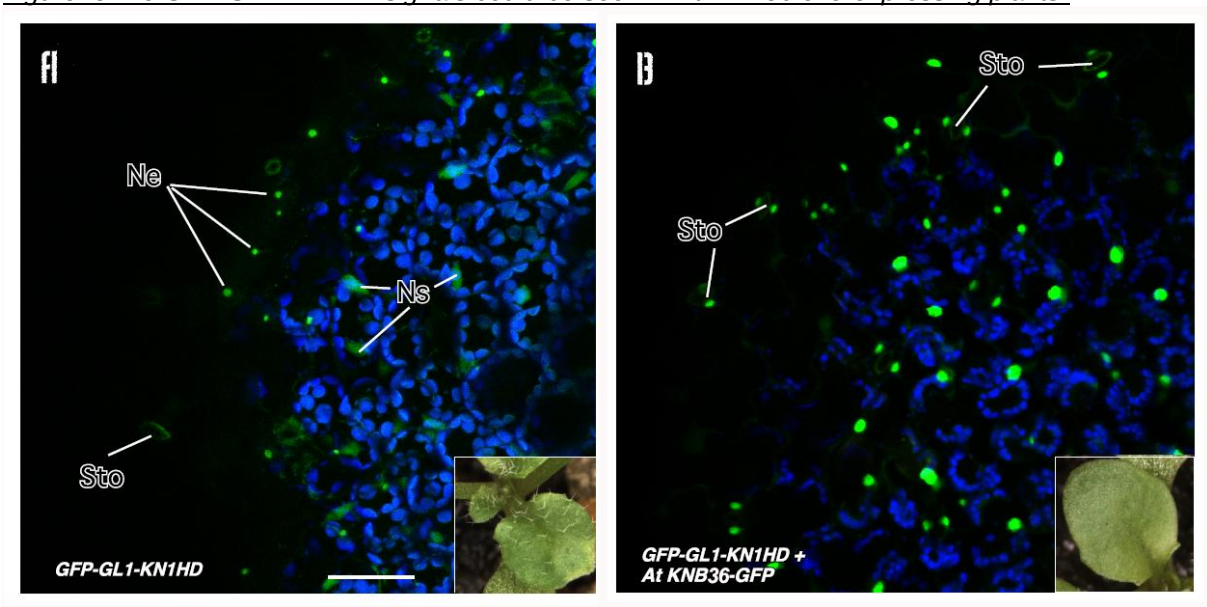

Note: In gl1 control plants harbouring the Pro_{RbcS}:GFP-GL1-KN1HD trichome rescue construct GFP expression could be seen in epidermal and subepidermal (mesophyll) tissues but not in symplasmic isolated guardcells. Transgenic plants with the same genetic background, which additional overexpress At KNB36-GFP, show in addition to epidermal and subepidermal nuclei signals, GFP in the nuclei of guardcells. Sto (Stomata); Ne (epidermal nuclei); Ns (subepidermal nuclei); Bar:80µm

4.2 Overexpression in transgenic GLABRA1-rescue lines results in the loss of trichome development

After successful verification of transgenic B9 lines harbouring Pro_{35S}:At KNB36-mGFP5 in the gl1/ GFP-GL1-KN1HD trichome rescue background, 5 of 34 lines left after antibiotic selection were chosen to examine differences regarding trichome number. Transgenic lines B9.4, B9.6, B9.7, B9.11 and B9.24 showed obviously reduced trichome numbers on the 1st and 2nd true leaf, compared to trichome rescue control lines. The T1 generation was self pollinated and statistically investigated in the T2 generation. Because plants segregated, microscopy was applied again to identify 15 individuals of the 5 target lines expressing At KNB36-mGFP5. Subsequently all trichomes were counted on the 1st and 2nd true leaves of each individual as well as 15 individuals of the trichome rescue control line.
After statistical evaluation, average values and associated standard deviations were calculated. As displayed in graph 5, a drastic reduction of trichome number from an average of 20 to 3 was observed. This indicates that At KNB36-GFP inhibits the GFP-GL1-KN1HD construct. As mentioned before, investigation of the GFP signals were done twice. Putting these findings together with data received from trichome statistics, elevated levels of At KNB36, as observed within lines B9.6 and B9.24, lead to an extreme trichome reduction and in some individuals to a complete loss. Moreover, silencing occurred in several individuals of these lines which correlates with trichome numbers. Lines B9.4 and B9.11 showed besides a strong signal in subepidermal nuclei, only epidermal signals in symplasmically isolated guard cells of the stomata. The silencing of At KNB36-GFP should result in elevated levels of the trichome rescue construct and therefore an increased number of trichomes, which could be observed (Graph 5). We know that At KNB36 is capable of specific interaction with the KNOX domain of Zm KN1, but not with the homeodomain. At MPB2C is able to interact with At KNB36, but also with the KN1 homeodomain. Given that the trichome rescue construct contains only the homeodomain of KN1, we suggest that KNB36, MPB2C and KN1 interact as a trimeric complex. Here MPB2C seems to be a linker between KNB36 and the KN1 homeodomain.
We could find trichome-less individuals could be found in every investigated transgenic line overexpressing At KNB36-GFP (Figure 44). Compared to trichome rescue control lines all individuals of At KNB36-GFP overexpressing plants showed an extremely reduced number of trichomes and a loss of epidermal GFP-KN1HD signals (Figure 43). Influencing silencing signals were observed but fit the model, in which the number of trichomes should increase if KNB36 becomes silenced. The data suggests that an overexpression of At KNB36 results in inhibition/degradation of KN1.

Figure44: Comparison of the trichome appearance between At KNB36-GFP ovrexpression lines and GL1-KN1HD rescue control

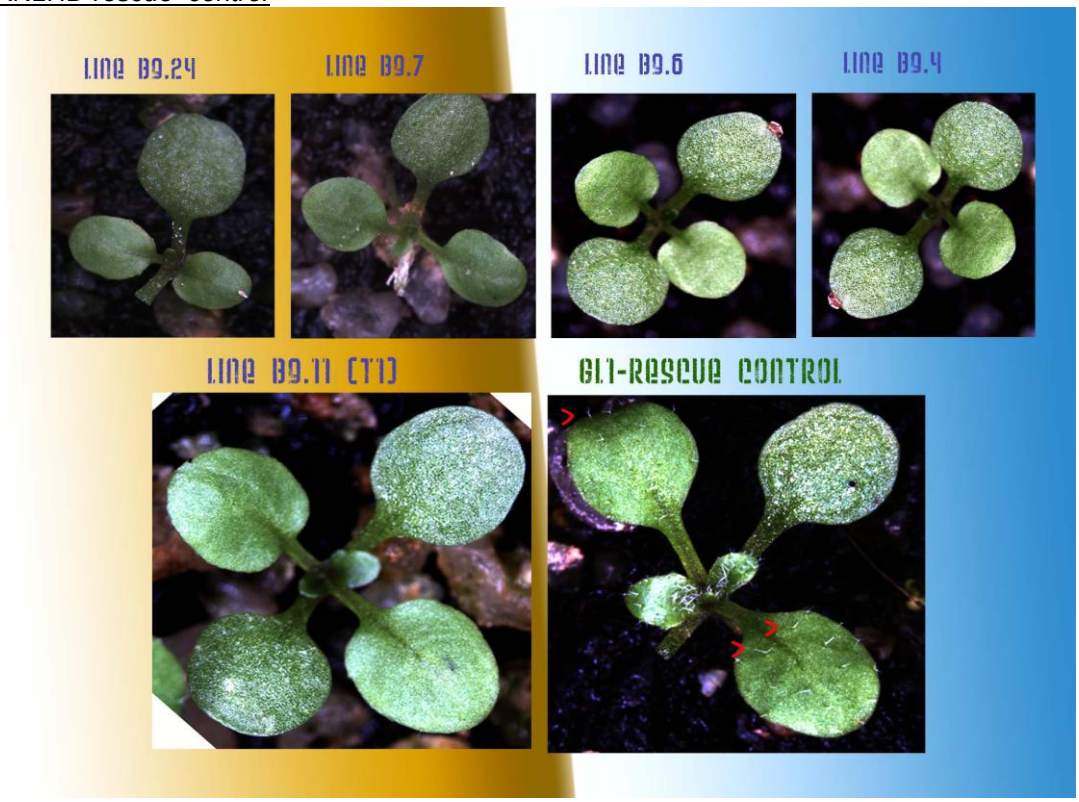

Note: 5 independent transgenic B9 lines overexpressing At KNB36-GFP in Arabidopsis thaliana with gl1/GFP-GL1-KN1HD trichome rescue background. Trichomes could be seen on the first true leaves (red arrows) of untransformed GL1-rescue control, but not in transgenic B9 lines.

Graph5: Decreased numer of trichomes in At KNB36-mGFP5 overexpression lines

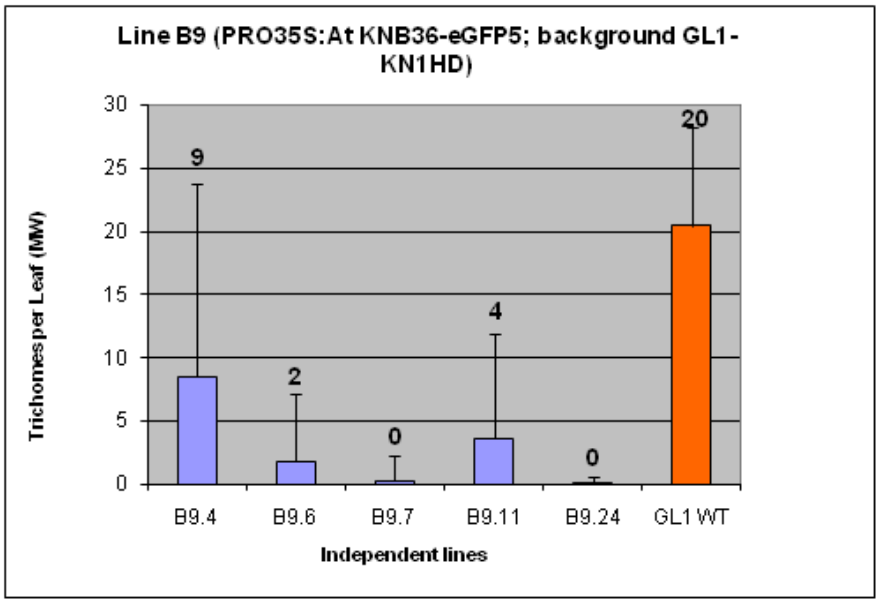

Note: Trichome numbers of the first and second leaf of 15 individuals of 5 transgenic lines (T2) overexpressing At KNB36. Numbers display the average of trichomes per line (standard deviations in brackets: B9.4: 9(15); B9.6:2(5); B7:0(2); B9.11:(8); B9.24:0(0); GL1 WT control: 20(8)

4.3 An unintended designed transgenic line in trichome rescue background seems to be a At KNB36 silencing line.

It should be mentioned that, like with At MPB2C, an At KNB36-TAP tag construct (pD7) was cloned. The number of trichomes appear increased in transgenic lines harbouring the Pro_{35S}: At KNB36-TAP construct in the trichome rescue background (Graph 6). RT-PCRs were applied on RNA extracted and united from 5 individuals. Here, in all 5 investigated lines At KNB36-TAP mRNA, in Col0 background, could be successfully detected. We also investigated KNB36 in the gl1/GFP-GL1-KN1HD background. Again 5 lines (Graph 6) where investigated, but all appeared to be negative on the mRNA level. It was possible to verify the presence of the TAP tag via PCRs with specific primers (FK156 against 35S promoter and FK398 against the TAP tag), which were performed on extracted genomic DNA. Sequencing of the amplified products revealed the C-terminal part of the 35S promoter sequence, the suggested AttB1 recombination site and the N-terminal sequence of the At KNB36 promoter. Putting this together the plants harbouring a construct composed of the native At KNB36 promoter fused with TAP and driven by the 35S promoter (Figure 45). Thus the produced transgenic lines are most likely promoter silencing lines.
Investigation of rosette and cauline leaves with the confocal microscope revealed that the signal of the GFP-GL1-KN1HD construct is very high expressed in single cells and cell cluster and in the nuclei of mesophyll tissues. The extremely high expressed protein was not only located in nuclei but also associated with the endoplasmatic rediculum. These observations were made in four lines (D7.1, D7.2, D7.4 and D7.5). The completely trichome-less line D7.6 showed no fluorescence signal during microscopy (Figure 46).
To investigate these transgenic lines, the trichome phenotype and the subcellular pattern, further a greater number of independent lines has to be analyzed. We suggest that the fusion of the promoter region may induce silencing which leads to complete silencing of the ectopic as well as the endogenous At KNB36. This could explain the cluster formation and the stronger expression of the rescue construct. Grafting experiments using a D7 line as base and the scion of an At KNB36-RFP overexpressing line would be the application of choice to investigate the effects of this construct. Subsequently mRNA levels of At KNB36 should be measured and compared against those of wild type control plants using techniques like RT-PCR and northern blotting. If this theory is correct, At KNB36 is significant involved in the degradation process of TALE proteins like Zm1 and maybe also of At STM or At KNAT1.

Figure 45: Predicted model of the transgene in KNB36 D7 lines

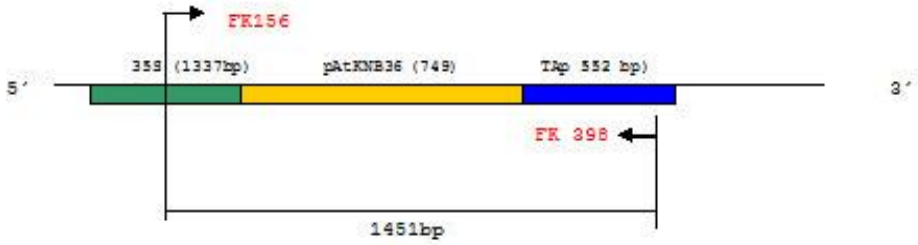

Note: This represents a schematic model of the suggested transgene in D7 lines. Displayed is the sequenced pcr product amplified with primers FK156 and FK398.

Figure46: Subcellular localisation of the GFP-GL1-KN1HD signal in D7 lines.

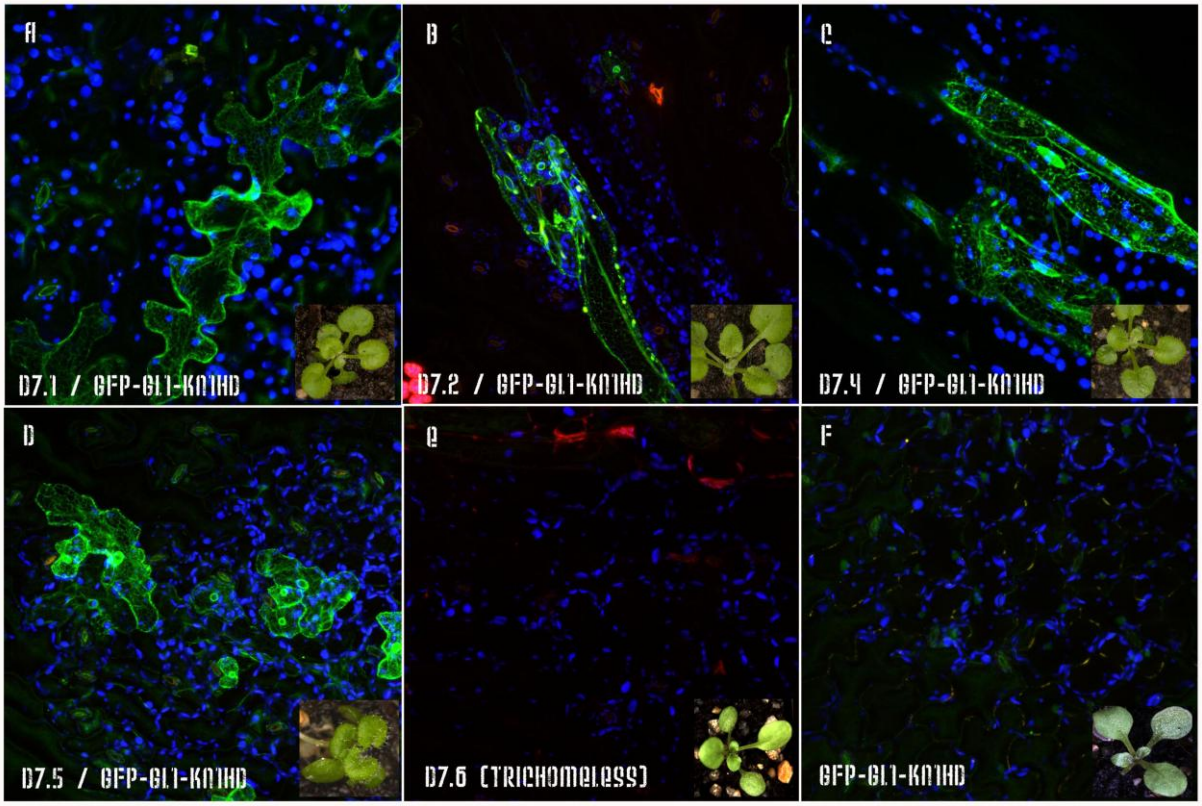

Note: Strong expression of GFP-GL1-KN1HD in transgenic plants harbouring the D7 construct in trichome rescue background (A-D) in comparison to the trichome rescue control line (F). The signal appears cytoplasmic, maybe associated with the ER, but also in the nuclei of epidermal and subepidermal cells of rosette leaves. GFP could be seen in single cells and also clustered (note that the GFP-GL1-KN1HD construct is non-cell autonomous). Also an increased number of trichomes could be seen in D7 lines (A-D, small picture) but not in line D7.6 which was completely trichome-less and showed no fluorescent signals (E). (Generation T1; Magnification: 40x)

Graph6: Increased trichome rescue in transgenic D7 lines

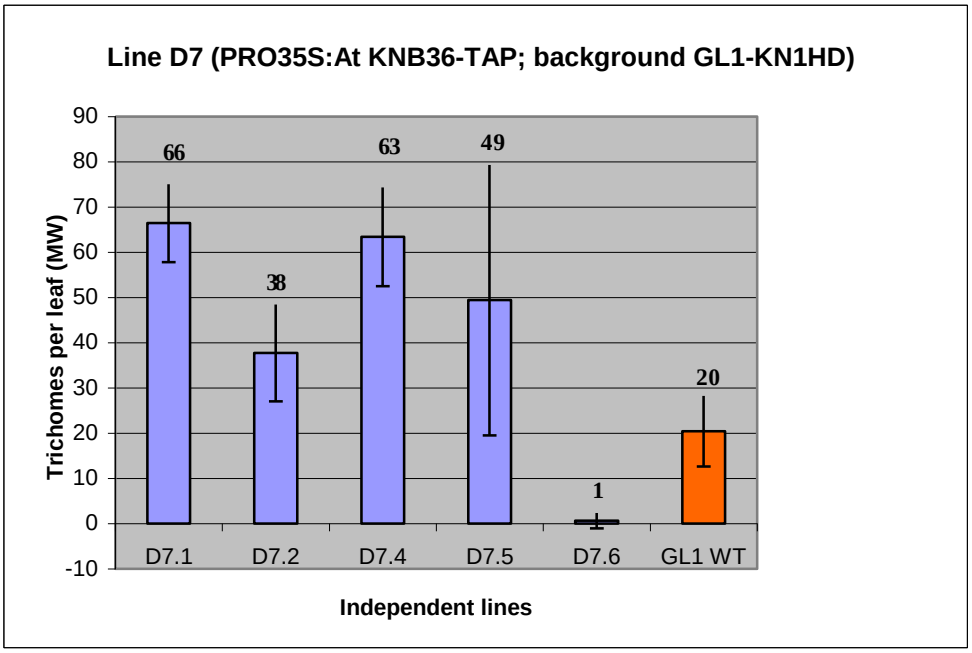

Note : Number of trichomes of the first and second true leaf of transgenic Arabidopsis plants with trichome rescue background. The trichome number of 15 individuals of 5 independent transgenic lines (T2) harbouring the pD7 construct was analyzed. Error bars denote the standard deviation of the arithmetic mean. In comparison to the trichome rescue control (GL1 WT), trichome levels are elevated in case of lines D7.1, D7.2, D7.4 and D7.5, but total loss of trichomes could be observed in line D7.6.

Graph7: Transgenic D7 control lines with col0 background show no significant trichome phenotype

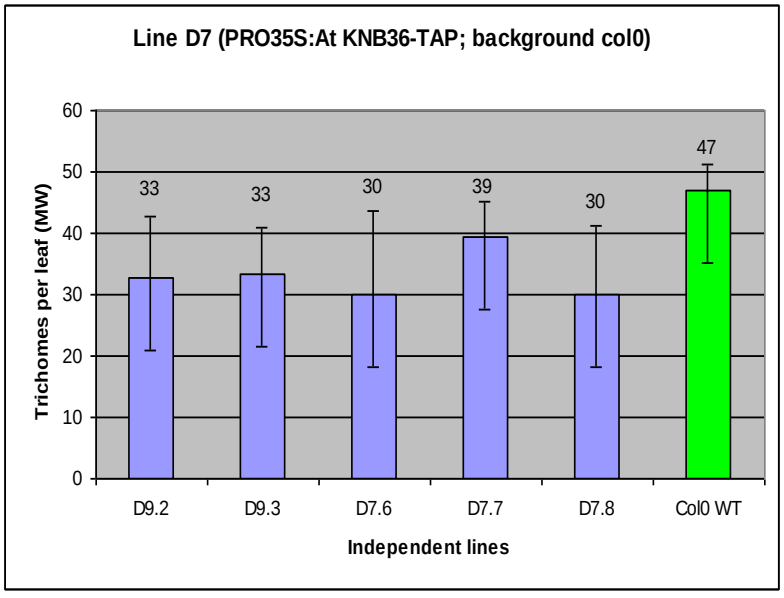

Note Number of trichomes of the first and second leaf of transgenic Arabidopsis plants with Col0 background. Similar conditions and statistical investigation were used for plants with trichome rescue background (graph 6). RT-PCR of D7 and D9 lines has proven the presence of At KNB36-TAP mRNA in rosette leaves. All transgenic lines show a lightly decreased trichome number in comparison to the wild type (Col0 WT). But standard deviation shows that this is statistically not releant.

5. ***At MPB2C TILLING lines show a general dwarfism and adventitious shoots***

5.1 What is TILLING and what are the advantages of this strategy?

Targeting-**I**nduced **L**ocal **L**esions **IN** **G**enomes (TILLING), is a reverse-genetic strategy for the discovery and mapping of induced mutations. TILLING is suitable to investigate any organism. To discover nucleotide changes within a particular gene, PCR was performed with gene-specific primers that were end-labelled with fluorescent molecules. After PCR, samples were denatured and annealed to form heteroduplexes between polymorphic DNA strands. Mismatched base pairs in these heteroduplexes were cleaved by digestion with a single-strand specific nuclease. The resulting products were size-fractionated using denaturing polyacrylamide gel electrophoresis and visualized by fluorescence detection. The migration of cleaved products indicates the approximate location of the nucleotide polymorphisms. Throughput was increased by sample pooling, multi-well liquid handling and automated gel band mapping. Once genomic DNA samples were obtained, pooled and arrayed, thousands of samples could be screened daily.
In conclusion TILLING provides a fast, easy and cheap method to disrupt target genes and examine effects of an imperfectly acting protein. This will be the method of choice if a complete knockout of the target gene leads to lethality what seems to be the case for At MPB2C (Till et al., 03a; Till et al., 03b ; Henikoff et al.,04 ; Comai et. al.. 05).

5.2 Chemical mutagenesis via EMS applied on At MPB2C

The EMS mutagenesis of M1 seeds should cause a point mutation within the At MPB2C gene at the bp 236 (ABRC Stock Nr. CS94728) and bp 428 (ABRC Stock Nr. CS91285) according to the corresponding CDS sequence (TAIR acc. # At5g08120). During replication, the polymerase frequently places a thymin instead of a cytosin (Figure 47) opposite the 0-6-ethylguanin, which was altered through alkylation caused by the EMS. As a result, the C:G base pair changes during subsequent replications in a A:T base pair.
This nucleotide substitution leads an Aspartic acid instead of a Glycin (GGT→GAT) in case of line CS94728 and an Arginine instead of a Lysine (AGA→AAA) in line CS91285.
M3 seeds of verified M2 plants were ordered directly from the TILLING service center.

Figure47: ABRC Stock Nr. CS94728: Mutation at AA79 (G→D /Glycin→Asparatic acid)

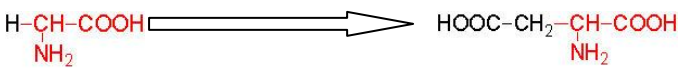

Note: Mutation disrupts predicted Protein Kinase PKA1 (AA77-83); Protein Kinase phosporylation site PKA2 (AA77-83); Phosphorylation recognition side GSK3 (AA77-84) Relevant amino acid sequence:AA76- RRGSMIYT-AA85

ABRC Stock Nr. CS91285 : Mutation at AA143 (R→K/Arginine→Lysine)

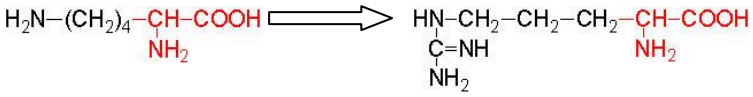

Note: Mutation disrupts predicted coiled coil region (AA126-189)
Relevant amino acid sequence: AA125-NAKALAGAEKEEMSRLREQVNDLQTKLSEKEEVLKSMEMSKNQVNEIQEKLEATNRLVAEKDM–AA190

Figure48: Predicted domains of the AT MPB2C protein

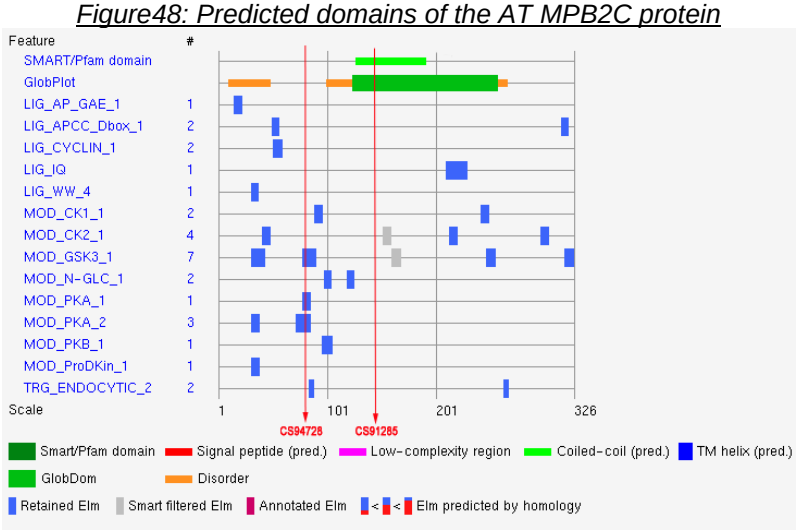

Note: Domains predicted via EML database. Approximate position of TILLING mutations indicated by red arrows. (http://elm.eu.org/)

5.3 Verification of heterozygous and homozygous individuals

To identify the phenotype caused by mutation within the MPB2C gene several characteristics were measured over a period of three generations (M3-M5). Starting with the M3 generation, DNA was extracted from individuals showing a common phenotype. Subsequently PCRs were applied (FK 293/FK295) and the amplified products sequenced. Analysis of the peak size referring to the altered base (Chromas lite 2.0) gave information about the presence as also the zygosity of the investigated M3 individuals. Additionally the germination rate and also the size of M3 individuals were measured and compared to the wild type controls. After identification, seeds resulting from self pollination events were sawed to gain a M4 generation of the target phenotypes. Here mainly the correlation of genomic and phenotypic segregation was examined. Genomic verification regarding the distribution of homo and heterozygosity of the M4 individuals was done with diagnostic digests of PCR products of the MPB2C region which include the target area, as described in more detail in chapter methods. The individuals which show correct mendelian segregation on the phenotypic and genomic level were suggested as plants which display the target phenotype.

The altered morphology should be caused by the inserted point mutation in the At MPB2C gene and serve for an intensive analysis. To gain homozygotic lines carrying the point mutation seeds of selfed M4 target plants were dibbled. The established M5 generation was again verified on the genomic level and used for final statistical analysis. These approaches were done for TILLING line CS94728 and CS91285. Morphological changes in line CS94728 were more severe and in accordance with the predicted impact of the At MPB2C disruption.

5.4 Appearance and frequency of unintentionally background mutations

EMS mutagenesis causes random point mutations everywhere in the genome of the target organism. These background mutations allegorize a problem because it is not easy to know if a damaged At MPB2C gene or a background mutation leads to an obvious phenotype. It was assumed that in previous experiments the knock out of the MPB2C gene leads to lethality (Kragler et al., unpublished data). Mutations in genes expected to impact a phenotypic trait controlled by many genes, such as plant size or leaf shape maybe subjected to epistatic interactions.
This is the reason why we tried to get rid of these additional, unintentional point mutations through a backcross with the Col0 wild type. This was done in 2 approaches. First through pollination of wild type stigma with mature pollen of TILLING lines, which were confirmed as homozygotic for the wanted point mutation and second in reverse through pollination of TILLING stigma with Co0 wild type pollen.
Mutations in genes that effect a phenotype that is controlled by few genes are unlikely to produce phenotypes bastardly by background mutations. Crossing will here not be a prerequisite for analysis. As described above M1 plants will grow from EMS treated seeds. After selfing, M2 individuals will be propagated via single seed descent. After verification of the M2 and an additional round of selfing, each mutation will appear in a ratio of one wild type to two heterozygotes and one homozygote in the M3 plants. One-fourth of the M3 plants of each line should be homozygous regarding the mutation of interest. The seeds can be simply planted and genotyped and if there are enough individuals it should be easy to look for a perfect correlation between genotype and a recessive phenotype.
Based on mutation densities that the providers, ATP (Arabidopsis TILLING Project), had measured in TILLING Arabidopsis and considering overall recombination rates, they estimated that the probability of a closely linked lesion to be mistaken for one in the target gene is only approximately 0.0005. (Henikoff et al., 2004)

5.5 Curly – a phenotypic candidate caused by improper functioning At MPB2C?

- **General dwarfism**

All plants found in TILLING line CS94728, which have a verified mutation showed a generally dwarfism.
The Curly phenotype, which was first intended in the M4 generation, showed the extreme form of dwarfism (Figure 49A, C). Moreover there following differences to Col0 wild type (WT) plants were observed:
The whole Curly plant body, which is primary defined through the rosette, composed of the rosette leaves and later the stem, is dwarfed. Size measurements of 2 month

old M3 plants (n=23) in comparison to wild type controls, grown under the same conditions (n=10) were done. This revealed that homozygotic individuals (n=6) attained an average maximum stem size of 78 mm (28% of WT stem size), and heterozygous individuals (n=17) an average maximum stem size of 100 mm (36 % of WT stem size). The average maximum stem size of the WT control plants of 280 mm (=100%) was ascertained under these grown conditions.
The rosette leaves showed similarity to KN1 overexpression plants (Figure 50), but the rosette leafs of the Curly phenotype lack the knots (Figure 49B) that could be seen in PRO_{35S}:KN1 plants (Figure 50B). There was also no development of ectopic meristems.
Eye-catching at the Curly phenotype is, however, the eponymous upward facing margins of rosette (Figure 50A) and cauline leaves (Figure 49D), and extremely reduced numbers. This is a morphological attribute which can also be seen in KN1 and STM overexpression plants (Figure 12A).
These phenotypes give rise to the assumption that a defective MPB2C leads to higher levels of endogenous STM or KNAT1 which represent the homologous proteins in Arabidopsis thaliana.
We could show that MPB2C is a negative regulator of KN1/STM cell-to-cell transport through plasmodesmata. So it would fit the predicted model that an alternated MPB2C protein is not longer able to regulate the transport of STM. This inability to interact with STM could also represent a missing link to KNB36 which is suggested to regulate protein levels of KN1. Together this would cause a phenotype which appears similar to a KN1/STM or KNAT1 over expression phenotype.

Figure49 : Comparison of homozygous TILLING mutant (Curly) leaves (M4) and wild type plant

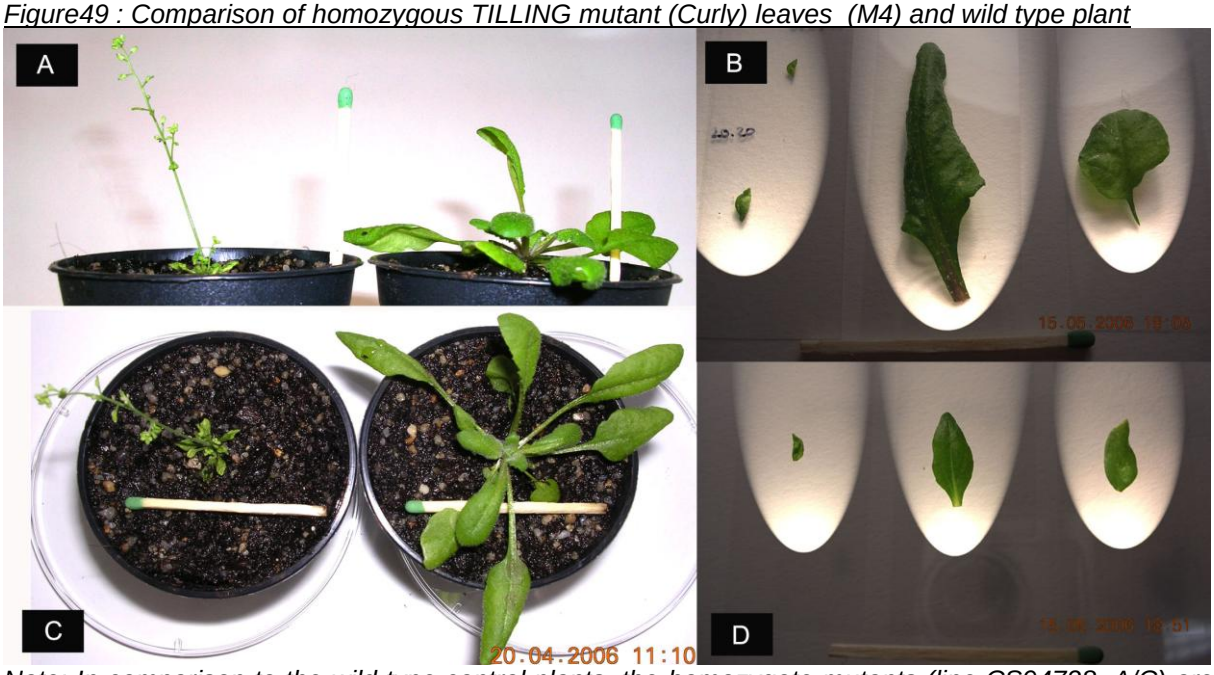

Note: In comparison to the wild type control plants, the homozygote mutants (line CS94728, A/C) are extremely dwarfed and show very early flowering. In A and B could be seen a size difference in comparison to the wild type (Col0) (A/B right), grown in similar environment under same conditions. In later stages the plants develop adventitious shoots which gives the plant a Bushy appearance. The dwarfism is reflected in the complete plant cormus, including rosette leavs (B), cauline leaves (D), stem, florescence and siliques. B/D: Delineation of a Curly leave (left) in comparison to the Col0 control leaf (middle) and a leaf derive from a TILLING line showing a Bushy phenotype (right).

Figure50: Comparison of homozygous TILLING mutant (Curly) and a KN1-overxpression mutant

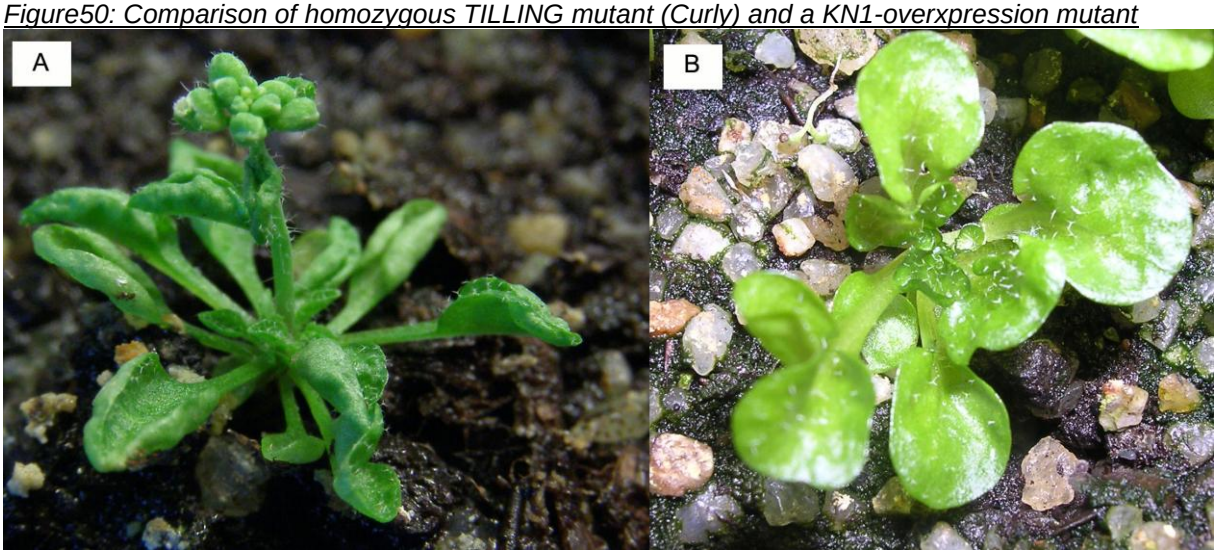

Note: Curly phenotype (A) in comparison to a KN1 overexpression line (B). Both plants are dwarfed and show abnormal development of the rosette leaves. In case of the Curly plant the edges of the rosette leaves face upwards, whereas the KN1 plant showed the classical knots and only a light deformation in a curled way.

- **A touch of Bushy**

The stem of Curly plants develops early and is much smaller than in control plants (Figure 49A,C). After an incipiently regular development of the primary stem, the plant develop several adventitious shoots in later stages (Figure 51), which are as least as high as the primary shoot. The primary shoot and also the adventitious shoots show several floral branches with different length as can be seen in KNAT1 overexpression plants (Frugis et al., 2001). These features shared by both, the Curly and the Bushy phenotype, indicating that the Curly phenotype is homozygotic and more severe form, whereas the Bushy phenotype might resulting from a heterozygotic mutation in the MPB2C gene.
A difference to the later described “Bushy” phenotype is, however, the rare presence of cauline leaves which can only be found in the lower part of the stem (Figure 51). These are extremely dwarfed too (Figure 49D). In plants showing the Bushy phenotype the development of cauline leaves is higher-than-average regarding number and size (Figure 52C).
Furthermore the stem is often not formed straight like in wild type plants, but rather in a zigzag way, most notably in the upper part.

- **Abnormal inflorescence development**

The development of the florescence also seems to be influenced in the investigated mutants.
First of all the primary shoot emerges earlier than in wild type (WT) plants which is in line with a very early flowering response. In the beginning, the morphology of the flowers seem to be normal and well structured but in later stages of flowering the spatial arrangement of blossoms and siliques differly severe from the WT. Neither a radial pattern formation is visible, nor a structure or continuity of internode length (Figure 51).

Moreover it is interesting that the first flowers are impaired in seed production. The plant is able to develop functionally seeds successfully, only in the upper part.
In most flowers the pistil penetrates the bud before pollination can take place. Closer investigation of the flower showed that self pollination seems to be rearly possible. When the growing pistil reaches the pollen, the pollen seems to be still immature and not able to pollinate the pistil in most cases.Unfortunately many pollen contaminations happened and we were not able to verify stable homozygotic plants. The question how cross-pollination took place remains still unsolved.

Figure51 : Comparison of TILLING mutant (Curly) fluorescence and silique and wild type plant

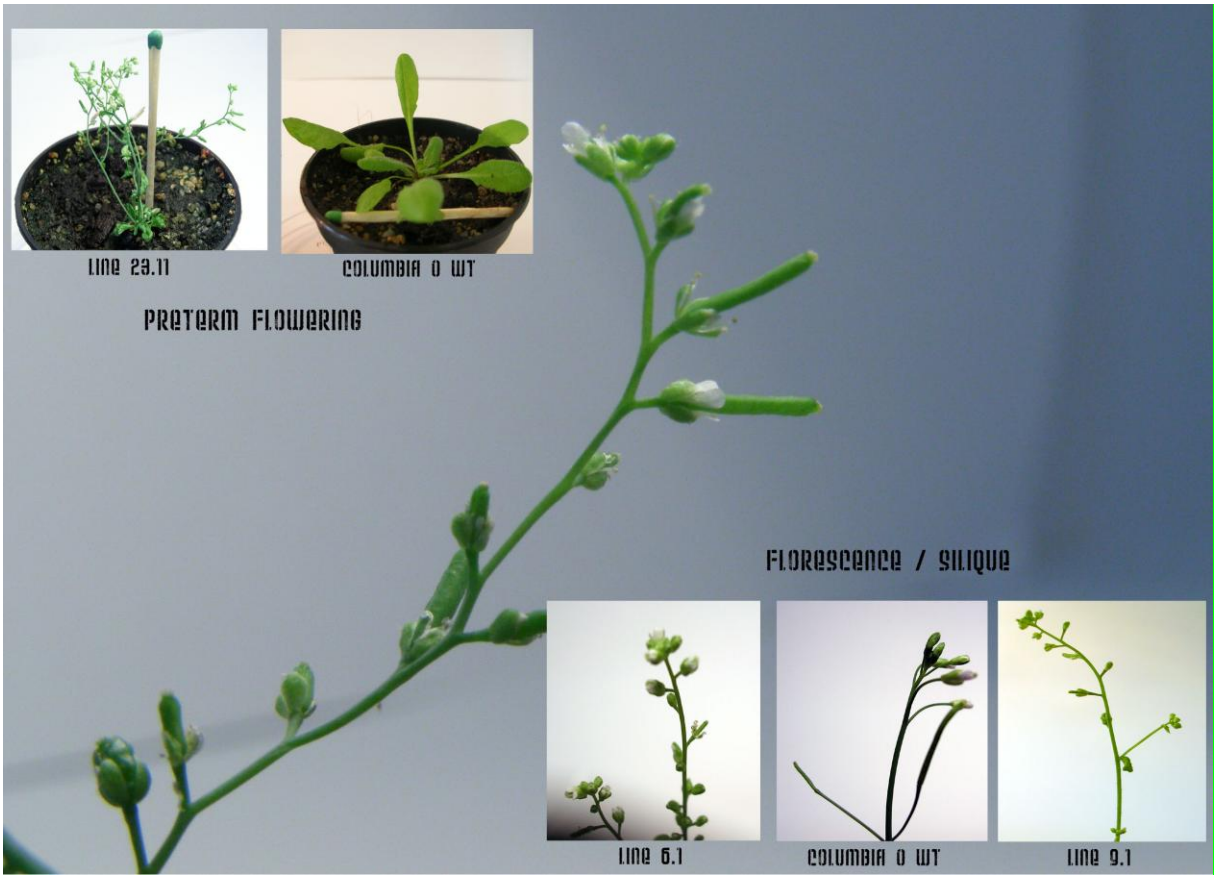

Note: Figure displays 40 DAG old mutant plants (termed Curly) in comparison to the wild type control. The mutants (M4) were verified as homozygote regarding the point mutation within the MPB2C gene. The obvious preterm flowering mutant develops a dwarfed stem which is characterised through a lack of radial patterning and node symmetry. The flower itself appeared abnormal and the development of thick and short siliques seems often be delayed in the basal part of the shoot.

5.6 The Bushy phenotype – a heterozygote version of Curly?

The phenotype which was termed Bushy is generally characterized through a slight dwarfism. The number of rosette leaves is above-average and petioles are short or cannot be identified. In some cases the rosette leaves are bigger than in WT plants and, like the cauline leaves, show a rotund leaf shape. Moreover the leaves appear nearly petiole-less and adnate.
A second severe characteristic of the phenotype is the development of several adventitious shoots which appear simultaneous after the shoot apical meristem enters the reproductive growth phase. The adventitious shoots are often longer than the primary shoot. The shoots are dwarfed and develop in most cases a high number of functional siliques. The distances between the siliques are reduced in comparison to the WT internodes.
The number of cauline leaves is higher-than-average in Bushy plants. Here we should consider that the high number can result from the numerous adventitious shoots.
In addition the M5 generation showed that the Bushy plants show a delayed flowering. Here the question emerges if there is a real connection to the very early flowering Curly phenotype.
In most cases the cauline leafs of the heterozygous individuals were larger than in the WT, whereas the homozygous plants developed more adventitious shoots and very small cauline leaves.

Figure52 : Comparison of heterozygote TILLING mutant (Bushy) and wild type plant

Note: Example of heterozygous verified mutants (A,C) and a wild type control plant (B). Mutant line #15.n.2 (A)(40DAG) shows a rosette with an increased number of rosette leaves which are round with downward facing leaf margins and extremely reduced petioles. Mutant line #20.21 (C) (88DAG) displays an Bushy phenotype with several adventitious shoots, a lack of silique radial patterning and reduced internodes as well as a dwarfed shoot in comparison to the wild type (88DAG)(B). Note: (A) shows the M5 generation whereas (C) displays the phenotype in M4.

First of all it must be noted that the results gained from broad analysis of 3 generations of the TILLING mutant line CS94728 are ambiguous. As it could shown in figure 53, the distribution of the phenotype follows not exactly the mendelian distribution what could be caused by unintended cross pollination.
Furthermore, the distribution of the zygosity does not fit completely the distribution of the investigated phenotypes. So far it is not confirmed that the disruption of MPB2C leads to general dwarfism including leafs, stem and siliques. In addition to the investigations of TILLING line CS94782, which harbours a point mutation within a predicted protein kinase phosphorylation site, a second line was investigated. This mutant line, CS91285, carries a disruption of the MPB2C gene within the predicted coiled coil region suggested to be necessary for protein-protein interactions. Plants of this mutant line were also investigated until the M5 generation but show only medium dwarfism. Here, less M3 individuals were identified to harbour the mutation. Only 4 M3 individuals were verified as homozygotic. These homozygous plants showed a size reduction of 47 % compared to the shoots of wild type plants. During my investigations no other alterations of the morphology, could be seen within 3 generations. Thus this line was not presented in detail in this work.
To conclude, it seems that a disruption within At MPB2C remains to be confirmed because the phenotypes could not be correlated 100% with the genotype.

Figure53: Correlation of phenotypes and zygosity of the At MPB2C pointmutation

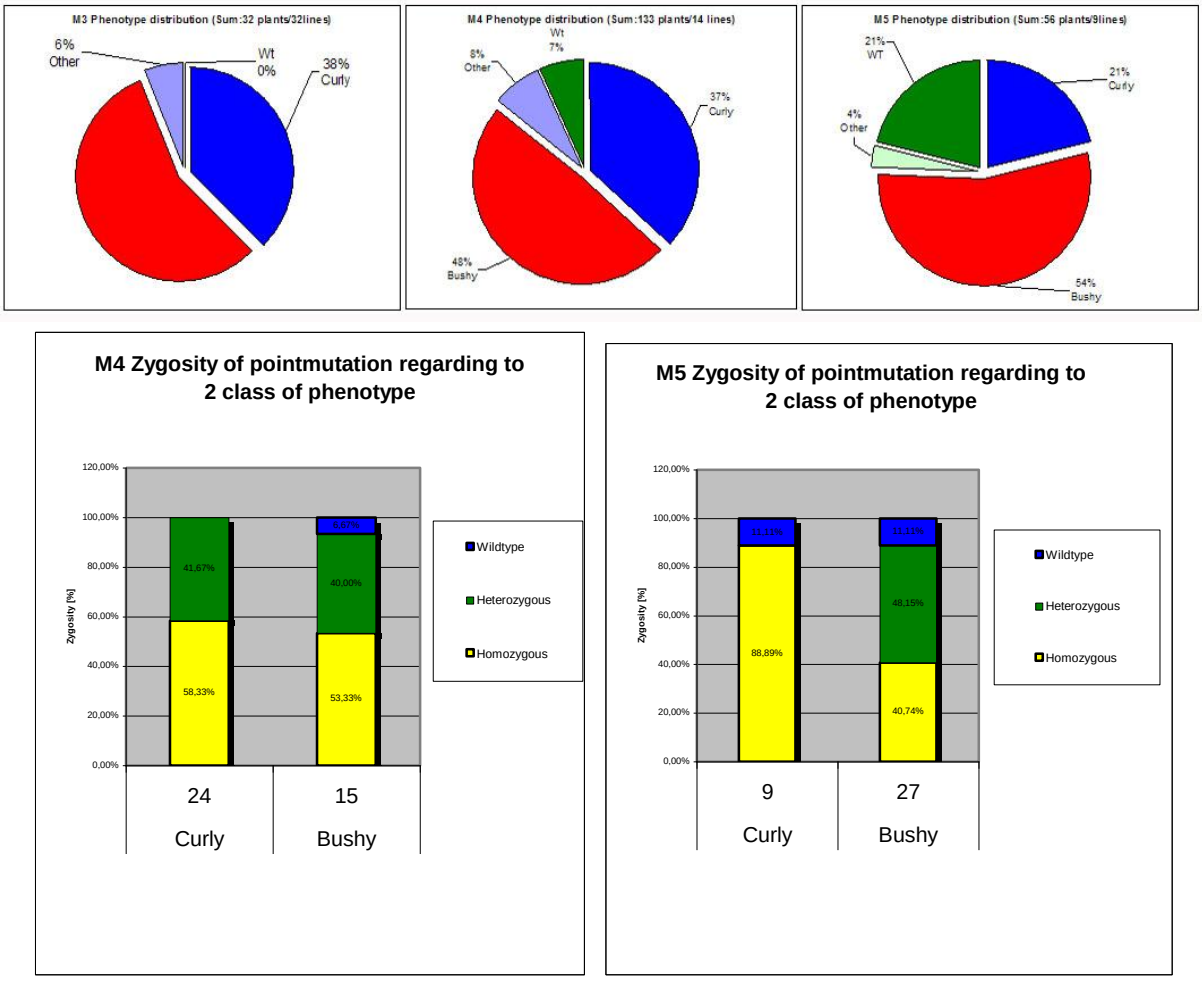

Note: Upper diagram series displays the distribution of the phenotype within 3 generation (M3-M5). Lower left graph displays the distribution of the zygosity found in 14 independent M4 lines (n=39 individuals) regarding 2 classes of phenotype (Curly / Bushy). Lower right graph displays the distribution of the zygosity found in 9 independent M5 lines (n=38 individuals) regarding 2 classes of phenotype (Curly / Bushy).

III. DISCUSSION AND FUTURE ASPECTS

1. *At KNB36 expression patterns correlate with those of TALE homeodomain transcription factors.*

Through various promoter-coupled GUS staining studies on transgenic plants, we could show that the KNB36 promoter is mainly active in tissues which show a high cell division rate and in meristems. It seems that the factor is needed in primary and secondary shoot and root meristems. Completely independent of the plant developmental stage, the protein could be detected within dividing tissues, including the forming vascular system during the fist days after germination as well as in the later stages when the next generation was generated. Here we could show that the KNB36 promoter is active in distinct areas of the developing embryo including the embryo sac and the inner integuments. As mentioned in chapter 3.2.1/2 the expression of distinct KNOX homeodomain transcription factors like At STM and At KNAT1/BP takes also place within meristems, respectively the shoot apical meristem. Also BLH members of the TALE superclass are coexpressed with At KNB36. As mentioned in chapter 3.1.4, At BEL1 represents a TALE protein crucial for the correct development of ovules. GUS stains of these tissues in transgenic *Arabidopsis* show that At KNB36 gene expression is also active in these tissues. Data from yeast 2-hybrid interaction assays suggest that At KNB36 is also an interaction partner of At BEL-like HD proteins. Here we could show that the expression pattern of these proteins overlapp, what supports the notion that At KNB36 is not only an interaction partner of KNOX family members, but also of BLH ones.
By the analysis of fluorescence-tagged At KNB36 transgenic plants it was proven that the protein localizes to the nucleus. Such a localization pattern is also observed for Zm KN1, At STM, At KNAT1/BP and At BEL1. The correlation of tissue specificity and subcellular localisation of At KNB36 supports the data gained from yeast 2-hybrid interaction assays (Figure 15B).
In conclusion we showed that At KNB36 colocalizes with members of both kinds of TALE family proteins, tissue specific within meristems but also on subcellular level within the nucleus. To find out in which specific kind of meristematic cells within shoot and root meristem KNB36 is active, immunolocalization assays remain to be done.

2. ***At KNB36 seems to regulate KN1 protein levels and interacts with At STM, At MPB2C and At KNAT1/BP***

Zea mays KNOTTED1 and its orthologous from Arabidopsis, STM and KNAT1, are expressed in the shoot apex and nearly all meristematic active tissues. Analysis of the At KNB36 promoter reveals that the expression pattern of KNB36 appears to be very similar to these of KNOX proteins.
Coexpression of Zm KN1/At STM and At KNB36 through agrobacteria mediated infiltration and particle bombardment displays that the KNOX factors and KNB36 colocalize within the nucleus of cells. This was confirmed by findings gained from analysis of transgenic overexpression plants. The next step was to examine the role of KNB36 within cells.

Further experiments performed by Mag. Nikola Winter in the Kragler lab with agro-mediated co-infiltrations utilizing the same constructs reveal that the presence of KN1 within the nucleus is increased form 80% to 100%, whereas the cytosolic inclusion bodies are decreased from 25,4% to 1% in comparison to controls expressing KN1 alone. Furthermore, cytosolic accumulation of KN1 in association with the ER and at the nuclear envelope could not be seen in cells transiently coexpressing KNB36.
There are at least two different possible scenarios: On the one hand KN1 which enters the cell, as well as cytosolic KN1, interact with cytosolic KNB36 and this dimerization triggers the nuclear import. Or, on the other hand, cytosolic KN1 interacts with KNB36 and is subsequently submitted to a protein degradation pathway. Support for the latter notion is found with MPB2C. The HD interacting factor seems to play a key role in KNB36 and KNOX protein function. MPB2C was never detected within the cell nucleus and the low coexpression of KNB36 in MPB2C coinfiltration assays suggests that KNB36 might be capable to trigger, with the support of MPB2C, degradation of HD factors. While KN1 seems to be arrested in the nucleus by KNB36, the cytosolic fraction of KN1 is located at the microtubules and subsequently degraded. The change in KN1/STM subcellular presence and distribution after interaction with KNB36 supports the notion that KNB36 triggers either nuclear import or degradation of KN1/STM, or both.

Because the nuclear import system and the plasmodesmatal transport system share common features, it was obvious to investigate whether KNB36 overexpression also affects the cell-to-cell transport ability of KN1/STM.
Therefore we examined single cells overexpressing KN1/STM tagged with GFP/RFP, where additionally KNB36 was also overexpressed. This was done by particle bombardment assays, using gold particles coated with KNB36-RFP and / or Zm KN1-GFP expressing plasmids.
The results indicated that KNB36 has no effect on the transport ability of the KNOX protein. As shown in figure 41, the homeodomain transcription factor KN1 could be located in neighbouring cells with the same frequency as in control experiments.

To find further support for the formation of a dimeric complex of KNOX proteins such as KN1/STM and KNB36, we produced transgenic plants overexpressing KNB36-GFP in gl1/GFP-GL1-KN1HD trichome rescue lines. These lines were nearly trichomeless. Normally, these gl1 deficient lines show a high number of trichomes, which are formed because of the movement capability of the KN1 homeodomain

fused to GFP-GL1. Yeast two-hybrid assays reveal that the homeodomain is responsible for KN1-MPB2C interaction, whereas KNB36 seems to be unable to interact with this domain. So the loss of trichomes in these plants seems to depend on the presence of MPB2C in newly forming leaves. MPB2C interacts with the homeodomain of the trichome rescue construct and KNB36 interacts with MPB2C. These observations support on the one hand the in vivo interaction of MPB2C and KNB36, and provides the other hand, the first hint to the presence of a trimeric complex of KNB36, MPB2C and the homeodomain transcription factor KN1.

Furthermore, some of these KNB36-GFP overexpression lines showed KNB36 systemic silencing. As expected these plants formed a high number of trichomes. These lines show KNB36-GFP signals mainly in the nuclei of the symplasmically isolated guard cells. We suggest that the subepidermal signal is derived from the GFP-GL1-KN1HD construct, whereas the signal detected with in the nuclei of the guard cells could only be KNB36-GFP: silencing of KNB36-GFP could not include the symplasmically isolated guard cells and the expression of the rescue construct in this kind of cells is extremely low and could not be seen in controls. Through the silencing of KNB36-GFP, levels of the subepidermal rescue construct seem to be elevated, which indicates that KNB36 is responsible for the degradation of the rescue construct. Because itself KNB36 cannot bind to the HD of the rescue construct, we suggest that MPB2C acts as a linker between KNB36 and KN1.
Additionally we produced a number of transgenic plant lines harbouring a construct which expresses, driven by the 35S promoter, an aberrant mRNA consisting of the KNB36 promoter and the coding sequence of KNB36. ($pro_{CaMV\ 35S}$: pro_{KNB36}-TAP). These transgenic plants show no overexpression of the KNB36 protein and silence endogenous KNB36 completely by promoter-promoter silencing. These plants form no trichomes and look like gl1 control plants. If KNB36 is completely silenced during the plant development, and the notion is correct that KNB36 is involved in the degradation of KNOX proteins, there should be higher GFP-GL1-KN1HD fluorescent signal in these transgenic lines compared to the control lines solely expressing GFP-GL1-KN1HD. Thus, one would expect that these lines show a more efficient trichome rescue phenotype. This was exactly what we observed. It should be noted that this could also be an effect of GFP-silencing. It is known that ectopic expression of proteins can lead to silencing. However, in these lines the silencing of KNB36 remains to be verified by western blot analysis or northern-blot analysis with KNB36 specific probes.
Summarized we found evidence that KNB36 is able to interact with MPB2C and also with KN1/STM. Because KNB36 interacts specifically with the MEINOX domain of homeodomain transcription factors, MPB2C with the homeodomain, we assume that MPB2C acts as a linker between a specific subset of homeodomain proteins and KNB36. This would result in a trimeric complex between MPB2C, KNB36 and the homeodomain proteins, which may trigger the degradation of the complex. Because MPB2C is an exclusively cytosolic acting factor, the complex formation and the predicted degradation is assumed to happen within the cytoplasm. MPB2C alters the subcellular distribution of its interaction partners by allocating them to microtubules. Similar to MPB2C, KNB36 also seems to alter the subcellular distribution of homeodomain proteins by increasing their presence in the nucleus. However, KNB36 does not affect the ability of HD proteins to move from cell to cell.

3. ***Is the phenotype appearing in transgenic plants with ectopic expression of KNB36 caused by alternating cyclin or hormone levels?***

Preliminary results suggest that plants overexpressing At KNB36 under control of the CaMV 35S promoter are, in contrast to At MPB2C overexpression plants, enlarged (data not shown). The same effect was observed in different transgenic lines overexpressing At KNB36 – TAP, At KNB36 – mGFP5 and also At KNB36 – mRFP1 in comparison to Col0 control lines. Beside this phenotype, some plants were fasciated. However, this this was seen in only two cases of KNB36-mRFP1 plants (e.g. J7.5).
Regarding the enlargement of KNB36 gain of function lines, two possible explanations may be found.

The first explanation includes the aforesaid effect of phytohormones, imbalanced through changed levels of KNOX proteins. It was shown that the MEINOX domain is required in KNOX proteins to heterodimerize with their distinct BHL partners (e.g. STM-BEL1; KNAT1-SAW1, SAW2, PYN) which results in nuclear import. (Hackbush et al., 2005, Smith et al., 2002). Similar, KNB36 interacts with KNOX proteins such as KN1/STM and KNAT1 via their MEINOX domain. Furthermore, a forced nuclear import of KN1 could also be seen in transient co-expression assays including KNB36. As discussed before, we believe that KNOX factors were submitted into the degradation pathway as a complex composed of MPB2C and KNB36 within the cytoplasm. In the KNB36 overexpression scenario it looks like this regulation step is almost prevented through an elevated nuclear import of the KNOX protein. In the nucleus where no MPB2C is present, elevated levels of KN1/STM increases the probability of interaction with TALE partners like the BHL protein BEL1, which is also able to interact with KNB36 but not with MPB2C (Figure15). After heterodimerisation of KNOX and BHL factors it was proven that this complex displays a greater affinity to their target genes. It is also known that KNOX factors like STM and KNAT1 regulate phytohormone levels in a very precise way: up-regulation of CK and down-regulation of GA. Higher levels of CK lead to an increased size and down-regulation of GA amplifies the effect. Additionally KNAT1 is known to control the internode development and therefore the size of the stem. Summarized, it is suggested that an elevated level of KNB36 leads to an increase of KNOX nuclear import which could result in change of phytohormone levels in a way that plants are enlarged.

The second explanation is based on the increase of the cell size caused by endoreduplication events. Endoreduplication is a process defined through duplication of the genome without cell division. As a result of the increased DNA amount, the cell is known to become enlarged.
Yeast two-hybrid assays by Cooper et al., 2003 reveal an unknown proteinogenic interaction partner of rice cyclin CycB2;2 (A2YH60; GI: 147743079). The sequence of this novel protein (AY224538.1; GI: 29367592) was blasted via NCBI against an *Arabidopsis* protein database. The hit with the highest sequence similarity points to At KNB36 (AT5G03050) and identifies the rice cyclin-binding protein AY224538.1 as an orthologous of AT KNB36 in *Oryza sativa*. Alignment results reveal that the cyclin ortholog in *Arabidopsis* is a protein of the CYCB2 family. Unfortunately no explicit orthologous of the rice cyclin itself could be found in *Arabidopsis thaliana* because of the high sequence similarity of the B2 cyclin family. However, the rice B-type cyclin B2;2 (cycB2;2) is known to be expressed during G2/M phase transition of mitosis and

disappears at the beginning of the anaphase. Lee J. et al., (2003) shows that overexpression of this nucleus acting cyclin leads to accelerated root grown without significant increase of the cell size. It is assumed that cycB2;2 promotes cell division within the meristem. Furthermore, cycB2;2 is expressed in the intercalary meristem and the elongation zone of the internodes as well as in adventitious roots. This cyclin is expected to be involved in rapid internodial growth of rice under submergence and in this way crucial for the size of the plant. The loss of the transition of G2 to M phase will inititate an additional round of DNA synthesis without previous cell division and therefore causes endoreduplicaton. We also know that the down-regulation/loss of cycB2;2 could cause the skip of the G2/M phase transition during mitosis. Thus, it is possible that a specific rice cyclin known to control an essential check point during mitosis, is an interaction partner of Os KNB36. Nt/At KNB36 is suggested to submit interaction partners to a degradation pathway. Thus, we assume that At KNB36, which harbours a predicted cyclin binding domain, regulates a distinct cyclin, which might be cycB2.2.

Summarized, KNB36 could interact with cycB2;2 and trigger, similar to the MPB2C/KNOX complex, its degradation. The reduction/loss of this cyclin cause the skipping of the G2/M phase during mitosis which could result in endoreduplication events. This could lead to an enlarged plant. If this hypothesis turns out to be true, KNB36 would be the first known factor interacting with homeodomain transcription factors and also cell cycle components.
Further experiments have to be done to confirm this hypothesis.

Supplemental Figure 1: Alignment of the protein sequence of Os KNB36 and At KNB36:

```
GENE ID: 831689 AT5G03050 | hypothetical protein [Arabidopsis thaliana]

 Score = 90.1 bits (222),  Expect = 7e-19, Method: Compositional matrix adjust.
 Identities = 42/81 (51%), Positives = 59/81 (72%), Gaps = 0/81 (0%)

Query  55   AASAETEEHVQRILLAIDAFTRQVSEMLEAGRALFKNLAADFEDRLCSIHKERVERWEEE  114
             AS E E  + +IL  I++FT+ VS +LE G+ + K L+ +FE+RL  IHKE VE+W++E
Sbjct  49   VASDEMELSIAQILDKIESFTQTVSNLLETGKTMLKELSNEFEERLIMIHKEHVEKWQDE  108

Query  115  IRELRARDAANEQARSLLHNA  135
            I+ELR  DA+NE+  SLLHNA
Sbjct  109  IKELRLLDASNEETTSLLHNA
```

4. *MPB2C as an interaction partner of STM and KNAT1*

KNOX proteins are known to regulate phytohormone levels in the shoot apical meristem. Gibberelin levels, for example, induce/regulate stem elongation, flowering and leaf expansion. Cytokinins, which are found in tissues with high protein biosythesis are known to be responsible for development of scions, adventitious shoots and force DNA replication/cell division. The previous belief is that Cytokinins antagonize Gibberelins (Jasinski et al., 2005).
STM is expressed in apical, vegetative, axillary, fluorescence and floral meristems (Long et al., 1996) similar to KNAT1, which is expressed in the periphery and the rip zone of the SAM as well as in the flower and the fluorescence stem (Lincoln et al.,

1994). At MPB2C promoter-coupled GUS stains revealed that MPB2C is expressed at the boarder of these meristems, partly overlapping with STM/KNAT1 expression patterns.
As reported by Frugis et al, 2001, overexpression of the HD transcription factor KNAT1/BP leads to significantly higher Cytokinin levels within Lettuce sativa shoot apices and leaves. Cytokinins are known to be antagonists of Auxins, which establish the apical dominance. KNAT1/BP overexpression phenotypes show besides alteration of the leaf development, preterm flowering response and generally dwarfism, also development of adventitious shoots and floral branches with different length. The phenotype might be caused by KNOX protein induced accumulation of Cytokinins in the shoot apex. Following the proposed model, KNOX proteins activate the biosynthesis of Cytokinins and repress GA biosynthesis through repression of the GA20 Oxidase1. Additionally, higher levels of Cytokinin activate the GA2 oxidase2, which leads to GA inactivation in the periphery of the SAM. Thus, the balance of GA and Cytokinins in specific tissues is one major factor to define if the cells remain meristematically, or start to differentiate. If this balance is regulated by non cell-autonomous transcription factors, including the KNOX proteins, the operating range of these regulators has to be restricted. Due to data gained from promoter analysis, we suggest that this function could be provided by MPB2C supported by KNB36.
Yeast two-hybrid as well as protein overlay assays identified MPB2C as an interaction partner of the KNOX proteins KN1 and STM. KNAT1/BP displays, beside a redundant function to STM, a greater sequence similarity to KN1 as STM itself and is therefore predicted to be an interaction partner of MPB2C. The KN1/STM-MPB2C interaction was verified by agrobacteria mediated infiltrations: signals were detected, emitted from coexpressed split-YFP constructs of STM and MPB2C. Further approaches including truncated versions of STM revealed that the STM-MPB2C interaction is specific dependent on the presence of the STM homeodomain. This is in line with information gained from the KN1-MPB2C interaction tested in yeast two-hybrid assays. As mentioned before, the homeodomain of KN1/STM is crucial for the ability to move from cell-to-cell through plasmodesmata. To obtain an answer to the question whether MPB2C is capable to regulate HD protein movement, transgenic plants were developed, overexpressing MPB2C in the background of trichome rescue plants. The functional element of this mutant plant line is the homeodomain of KN1, which enables the movement of the GFP-GL1 construct from subepidermal tissue to the epidermis. As a result of the KN1HD mediated movement of the rescue construct, the plant is able to develop trichomes. Overexpression of MPB2C in these plant lines result in a complete loss of trichomes. This indicates on the one hand that MPB2C interacts specifically with the KN1HD *in planta*, and on the other hand that MPB2C seems to be able to block the cell-to-cell movement of the KN1HD which is fused to the trichome rescue construct. Closer investigations on the subcellular level additional revealed, that GFP-GL1-KN1HD is visible in the subepidermal tissues, but not within epidermal cells. This underlines the fact that MPB2C is able to block the symplasmic movement of the construct without reducing its cellular levels (Winter et al., 2007).
Concluded, the trichome rescue experiment reflects the situation in the wild type plant. Here MPB2C, which is known to be expressed around/overlapping meristems, interacts with the homeodomain of KNOX proteins like KN1, STM and maybe KNAT1/BP. After this interaction, the KNOX proteins are no longer able to move via plasmodesmata into adjacent cells. This implicates that the KNOX factors are somewhat restricted to move/act within meristems, but cannot move into adjacent tissues were MPB2C is abundant. So MPB2C seems to limit the extent of movement

of HD factors in the meristematic region and by this means helps to define the meristematic boarder. As a consequence of the absence of these KNOX factors outside the meristem, the balance of the phytohormones changes for the benefit of Gibberelic acid, which leads to cell differentiation and therefore the formation of plant organs.
The loss of this equilibrium between Cytokinins and GA is suggested to result in complete inability of organ formation. This is supported by the fact that MPB2C knockout plants might be lethal (Kragler et al., data not shown). A reason why overexpression of MPB2C in transgenic plants does not display any morphological changes could be explained by an extreme ephemerally of this protein. This is underlined by the observation that MPB2C-GFP signals were never be detetced within transgenic plants and that the protein is very unstable in cell lysats. So we suggest that overexpression of MPB2C has no effect on plant morphology because its degradation rate is high enough to compensate effects of overexpression.

5. ***A similar phenotype appearing in At STM and At KNAT1 mutants can be found in At MPB2C TILLING lines***

As mentioned before, a knockout of the MPB2C gene seems to result in complete lethality. To avoid the lethality of a complete knockout, we studied plants carrying a mutation in distinct predicted domains of MPB2C. The aim was to find mutants which show effects due to reduced MPB2C function but are still able to survive.
We found that in TILLING lines harbouring a mutated MPB2C several independent plants showed a phenotype similar to KNOX protein overexpression. This includes dwarfism, early flower response, development of Curly, wrinkled leaves and also the development of adventitious shoots. This is in line with the assumption that MPB2C interacts also with the homeobox transcription factor KNAT1/BP. Furthermore STM, which is known to interact with MPB2C, is a homolog of KNAT1/BP with an identity of 47% (89% in the HD) (Long et al., 1996).
It is suggested that in MPB2C TILLING lines the Cytokinin levels are above-average and the GA20ox1 levels, as well as the resulting GA levels are significantly lower than in wild type plants. GA20ox1 is essential in GA biosynthesis, especially for GA9, 20 and 17. Manipulations in *potato, rice, tobacco* and *Arabidopsis* showed that reduction of GA20ox1 results in lower GA levels and therefore reduced stem elongation, delayed flowering, reduced petiole length and dwarfism (Carrera et al., 2000, Itoh et al., 2002). Except the changes in flowering reduction, these characteristics could be observed in the described Curly TILLING mutants. GA2ox2/4 overexpression, which leads to complete inactivation of GA, results in severe dwarfism in *Arabidopsis* (Schamburg et al., 2003) and small dark green leaves in *rice* (Sakamoto et al., 01). Both characteristics can be found in the Bushy phenotype in MPB2C TILLING lines. In contrast to the Curly phenotype we observed in Bushy plants delayed flowering linking it to reduced levels of GA.
If MPB2C is no longer able to regulate the cell-to-cell movement of KNOX factors, this may causes transport from the meristem into the adjacent leaf primordia. This could result in higher CK levels and lower GA levels which might be responsible for the TILLING phenotypes. In this case there should be no measurable change in the protein levels but rather a change in the action radius.
Other regulators of At STM can be found in the Ovate protein family. It is suggested that OFP1 regulates TALE HD proteins at the posttranslational level. As STM itself,

OFP1 is proven to downregulate the *GA20 Oxidase1* gene which is crucial in GA biosynthesis. Expression of OFP1 under control of the CaMV 35S promoter leads to a decrease in GA20ox1 levels of up to 80% compared to wild type levels and exhibits dominant pleiotrophic phenotypes. Coexpression of OFP and KNAT1/BP leads to relocalization of KNAT1/BP from the nucleus to the cytoplasmic space where it colocalizes with OFP1 in punctate structures along the cytoskeleton and in the periphery of the cytoplasmic space. Similar structures could be seen during transient overexpression of MPB2C. Hackbush et al. predicted the presence of cofactors which link the TALE protein to the cytoskeleton (Hackbush et al., 2005).
OFP1 overexpression plants displayed amongst other characteristics a dwarfed body with curled and wrinkled leaves like KNOX overexpression plants and MPB2C Tilling lines. Hackbush et al. assumed that the ovate family proteins are specific transport regulation factors of KNOX proteins within the cell as well as transport from cell to cell. In this work we could show that MPB2C is a negative regulator of KN1/STM movement. We suggest that MPB2C could be the missing link between ovate family proteins, TALE proteins and the cytoskeleton, as predicted by Hackbush et al.
The phenotypes seen in TILLING mutants might be caused by the fact that MPB2C is no longer capable to interact with KNOX factors and block their efflux into the differentiating tissues. Maybe it is caused by the incapability to interact with OFP1 at the microtubules, which would cause an above average level of OFP1 and therefore also reduced GA levels. Further experiments are required to find out whether a down-regulation of GA is caused by an interaction of MPB2C with KNOX or OVATE family proteins.

6. ***Appearance of the Curly phenotype does not correlate with the presence of the point mutation***

As mentioned before, the statistical analysis of TILLING lines regarding correlation of the genotypic and phenotypic distribution appeared to be inconsistent.

Heterozygous TILLING plants of the M3 generation were expected to segregate as 25% homozygous, 50% heterozygous and 25% wild type plants. The phenotype and the genotype distribution have to correlate strictly.
If the mutation is dominant, 75% of the plants should show severe or weak characteristics of the predicted phenotype, if recessive, 25% should show a phenotype.
The diagram (Figure 53; M3) indicates a distribution of the phenotype of 38% Curly, 56% Bushy and 6% others. At the beginning we suspected that plants showing the Curly phenotype were homozygous plants and Bushy phenotype were heterozygous. Examination of the genotype showed 40% Curly mutants as homozygotes instead of 25% or 75%, whereas 15% of the Bushy mutants were genotyped as homozygous. Additional 2 plants which show the Curly phenotype were genotyped as wt plants. This inconsistency could be attributed to contaminations in the PCR. Thus, we self-pollinated several homozygous and heterozygous verified, plants to investigate the distribution of genotype and phenotype in the M4 generation. To minimize the possibility of PCR contamination a restriction based verification method was established (see Methods).

Of the M4 progeny, one of the 4 propagated homozygous lines showed a heterozygous genotype (1 individual). This means that the verification in the M3 as a homozygous parental plant was wrong. Another line, which was verified as homozygous in M3, showed 2 plants which exhibited a wild type phenotype. Bar of this fact, whether 100% of the individual M4 plants with a Curly appearance, nor with Bushy appearance could be verified as homozygous. Although the plants were selected according to their phenotypic appearance and verified on DNA level, it was not possible to establish more than one line displaying the parental phenotype in the next generation. We assume that, as a consequence of growing 50 -100 plants on limited space, the plants were accidentally cross-pollinated by wild type plants. This might be the case in three lines (#15 and line #18 and #24). In all three heterozygous Bushy lines, no Curly phenotype ever appeared during the M3 and M4 generation. In the M5 generation suddenly 60% Curly appearance in the progeny of line #15 emerged whereas line #18 and #24 showed 0% Curly in the M5. This leads to the suspicion that out crossing was done with a mutation, which appears dominant in heterozygous plants.

As a conclusion, one could suggest that Curly and Bushy phenotypes which show several characteristics of KNOX overexpression, could be mild and severe versions of the same point mutation. This is suggested because the Curly and the Bushy phenotype share some characteristics like dwarfism and adventitious shoots. On the other hand the flowering of the Curly plants occurs very early whereas the Bushy plants seem to be delayed in flowering (data not shown). Also a significant difference was observed regarding the number and size of the developed cauline leaves. In case of Curly there are less cauline leaves, which were only found at the base of the stem. Bushy plants show a greater number of cauline leaves than the wildtype, with a round shape and an unusual size. Additionally, several lines of the M5 generation looked like a hybrid between Bushy and Curly, regarding the size of the plant body. The final conclusion is displayed in figure 53. The Curly phenotype is the prime candidate for a phenotype regarding a MPB2C mutation. The 11% of plants genotyped wt, which showed a Bushy and Curly phenotyp in M5 generation could derived from unintended cross-pollination events with wildtype plants. The collected data from the MPB2C TILLING studies seem to fit to the predicted model, but could not be verified due to the inconsistency between the phenotyp and genotype.

Thus, new MPB2C TILLING lines should be established and verified. If these plants show again Bushy/Curly phenotypes we can assume that inconsistancies were caused by PCR-contaminations and cross-pollination. Furthermore these plants should be controled on the mRNA level. To see if KNB36 is responsible for KNOX protein regulation in the SAM, KNB36 overexpression mutant should be crossed with homozygotic MPB2C TILLING lines. The observed MPB2C TILLING phenotype shouldbe rescued.

7. ***Conclusion – Cell-to-cell transport as an essential element of tissue specific regulation processes.***

MPB2C is expressed within primordial protrusions during the formation of the leaf primordia. KNB36 and HD proteins such as KN1, STM and KNAT1/BP are known to be expressed specifically within meristems, but not in primordial tissues. As a result of higher levels of GA outside of the meristem, cells initiate. It becomes clear that KNOX factors, which are known to down-regulate levels of GA, have to be downregulated in differentiating tissues. Based on our model this might be achieved by MPB2C and KNB36. We could show that KNB36 is present/active along with the KNOX proteins in the shoot apical meristem (SAM).
In this environment KNB36 might modulate the levels of KNOX factors, and maybe also cyclins by submitting the interacting proteins into the 26S proteasome dependent protein degradation pathway. Both KNB36 and MPB2C are also expressed in tissues adjacent to the meristematic tissues where they maybe define a meristematic border. MPB2C blocks KNOX protein movement from meristematic cells to adjacent primordial ones and KNB36 triggers the degradation of the complex.
KNB36 is also suggested to move from cell to cell and could possibly move into the meristematic layers to form a morphogenic gradient regulating the presence of HD proteins.
At this point it should be noted that levels of overexpressed MPB2C seem to decrease in the presence of KNB36. Whether KNB36 alone triggers degradation of MPB2C and how efficient this regulation is in comparison to degradation within a trimeric complex with KNOX factors remains to be investigated.
However, MPB2C seems to be a factor limiting the movement of class I KNOX proteins like At STM and At KNAT1 in the meristems. To find further support for this notion, additional experiments in transgenic lines overexpressing or silencing MPB2C and KNB36 have to be carried out and phenotypes analysed for an impaired function of HD proteins.

Supplemental figure 2: Interaction Model including KNB36, MPB2C and KN1

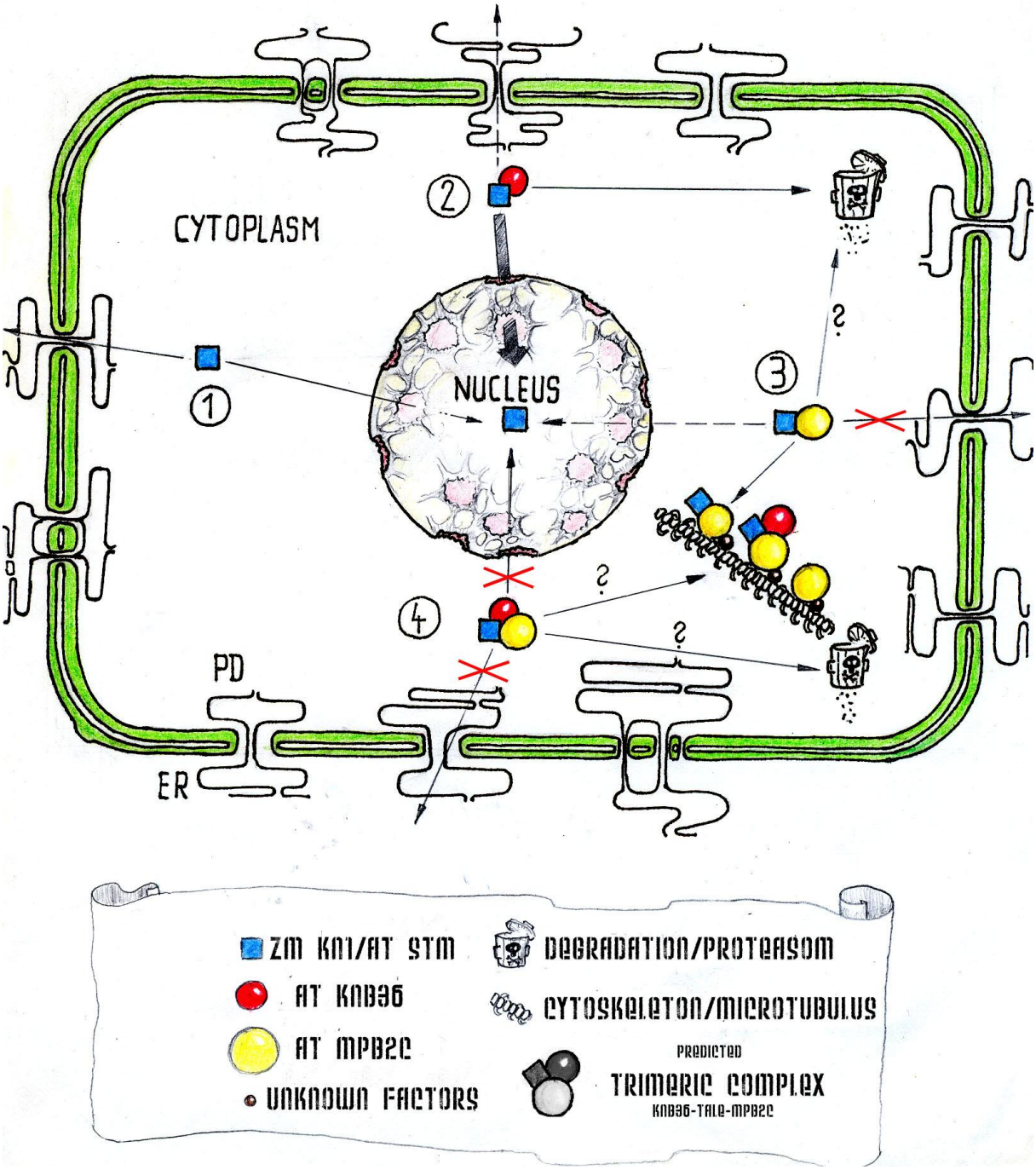

IV. MATERIAL & METHODS

1. Optimized Methods

1.1. Cloning of the BINARY vectors:

The subcloning of the diverse inserts into the pENTR/D-TOPO (Invitrogen) donor vector was amongst others done by René Ladurner**,** Claudia Blaukopf and Niko Winter.

At KNB36 genomic ORF was PCR amplified with specific primers **FK230** 5`(5´-CACCATGAACACTGAAATGGAAG-3´) and **FK187** 3´(5´-CGGCGGATCCGCTTGCTCAATGCTAGG-3´) and cloned into pENTR/D-TOPO GATEWAY® donor vector **(#161, #21**) (Invitrogen, KanR, reading frame A).

MPB2C cDS was amplified with specific primers **FK227** 5´(5´-CACCATGTATGAGCAGCAGCAAC-3´) and **FK228** 3´(5´-ATAATATGTAAAGGCTAGTGATTG-3´) and cloned also in pENTR/D- TOPO GATEWAY® donor vector **(#2**; **#X**) (Invitrogen, KanR, reading frame A).

The At KNB36 promoter region was amplified with primers **FK231** 5´(5´-CACCCCTTTCTCGATGCAGTGATCC-3´) and **FK250** 3´(5´-TTCAGTGTTCATCAAAACT-3´) and cloned in pENTR/D- TOPO GATEWAY® donor vector (#162) (Invitrogen, KanR, reading frame A).

The At MPB2C promoter region was amplified with primers **FK298** 5´(5´-CTCCAAAAATGTATATATAG
ATATATAGATTC-3´) and **FK299** 3´(5´ -CTTCTTCGTCCTCCGTATAATAGATCTG-3´) and cloned in pENTR4 GATEWAY® donor vector (#1.1,#2.1) (Invitrogen, KanR, reading frame A) by Niko Winter.

Supplemental table1: Overview of designed Binary Vectors

Term	Expressed Construct	Binary Vector	Restistance: Bacteria
pA	$PRO_{At\ KNB36}$:GUS - EgfpER	pKGWFS7	Spectionmycin
pB	PRO_{35S}:At KNB36 - mGFP5 - 6xHIS	pEarly Gate 103	Kanamycine
pD	PRO_{35S}:At KNB36 - TAP	pEarly Gate 205	Kanamycine
pE	PRO_{35S}:GUS - TAP	pEarly Gate 206	Kanamycine
pF	PRO_{hsp}:At KNB36	pMDC30	Kanamycine
pG	PRO_{hsp}:At MPB2C	pMDC30	Kanamycine
pH	PRO_{35S}:At MPB2C - mGFP5 - 6xHIS	pEarly Gate 103	Kanamycine
pI	PRO_{35S}:MPB2C - TAP	pEarly Gate 205	Kanamycine
pJ	PRO_{35S}:At KNB36 - 10xALA - mRFP1	pMDC32	Kanamycine
p1/1;p2/1	$PRO_{At\ MPB2C}$:GUS - EgfpER	pKGWFS7	Spectionmycin

1.1.1 Generation of the PRO_{35S}:At KNB36-mGFP5-6xHis overexpression construct

The pENTR/D-TOPO clones #161 and #21 were inserted into electro competent E.coli strain TOP 10 via electroporation and selected on full media plates containing kanamycine. After inoculation of grown colonies in LB^{KAN} the plasmids were extracted via Plasmid-Miniprep (clean). The correct donor vector backbone was confirmed via PvuI/HpaI diagnostic digest and subsequent examination via agarose gel electrophoresis. The reading frame, the orientation and also the identity of the insert were confirmed by sequencing the plasmid with **M13** forward and reverse primer.
After excision of the kanamycin resistance gene via RcaI restriction digest the approach was loaded on a 1.5% agarose gel (Figure 3). The plasmid DNA of the correct size was cut out from gel and purified via QIAEX II gel extraction kit. The concentration of the gained purified DNA was determined by loading 1µl on a 1% agarose control gel.
GATEWAY® recombination of the confirmed clone **#161** was done into binary vector pEarly Gate 103 (Early et al., 2006) which provides overexpression and a C-terminal mGFP5 fusion. Subsequently chemo-competent E.coli strain TOP 10 was transformed with 1µl Gateway approach via heat shock transformation. 100µl bacteria as well as positive and negative controls were plated on selection plates containing kanamycin and grown for 24 hours at 37°C. After detecting positive colonies via colony-PCR using primers **FK177** 5`(5`-A ATGGAAGAAGACGCAGGGAATGGAGGA-3´) and **FK178** 3`(5`-CCTCAT TGCTCAATGCTAGGATTCTGAAT-3´) they were inoculated in LB^{KAN} and confirmed after extraction via EcoRI diagnostic digest (Supp. Figure 3).
Both identified positive clones (#B2; #B9) showed the mGFP5 signal after transfer in *Arabidopsis thaliana* ecotype Columbia using the biolistic particle delivery system (Gold particle were coated with 1µg extracted plasmid DNA).

Supplemental figure 3: pB2/pB9

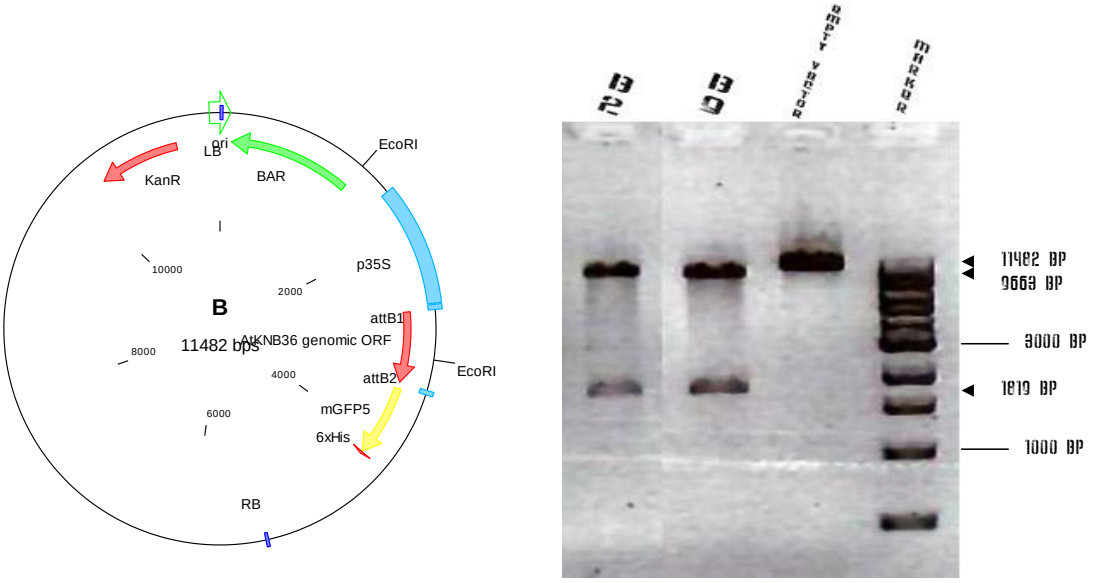

1.1.2 Generation of the $\underline{PRO_{35S}}$:At MPB2C-mGFP5-6xHis overexpression construct

The pENTR/D-TOPO clones #X and #2 were inserted into electro competent E.coli strain TOP 10 via electroporation and selected on full media plates containing kanamycin. After inoculation of grown colonies in LB^{KAN} the plasmids were extracted via Plasmid-Miniprep (clean). The correct donor vector backbone was confirmed via PvuI/HpaI diagnostic digest and subsequent examination via agarose gel electrophoresis. The reading frame, the orientation and also the identity of the insert were confirmed by sequencing the plasmid with M13 forward and reverse primer.
After excision of the kanamycin resistance gene via RcaI restriction digest the approach was loaded on a 1.5% agarose gel. The plasmid DNA of the correct size was cut out from gel and purified via QIAEX II gel extraction kit. The concentration of the gained purified DNA was determined by loading 1µl on a 1% agarose control gel.
GATEWAY® recombination of the confirmed clone **#X** was done into binary vector pEarly Gate 103 (Early et al., 2006) which provides overexpression and a C-terminal mGFP5 fusion. Subsequently chemo-competent E.coli strain TOP 10 was transformed with 1µl Gateway approach via heat shock transformation. 100µl bacteria as well as positive and negative controls were plated on selection plates containing kanamycin and grown for 24 hours at 37°C. After detecting positive colonies via colony-PCR using **FK227** 5´ (5´-CACCATGTATGAGCAGCAGCAAC-3´) and **FK228** 3´(5´-ATAATATGTAAAGGCTAGTGATTG-3´) they were inoculated in LB^{KAN} and confirmed after extraction via XhoI diagnostic digest. (Supp. Figure 4) Two of the four positive clones (#H4; #H6) were tested in transient overexpression systems using the biolistic particle delivery system. Construct #H4 and #H6 showing the mGFP5 signal after transfer in Arabidopsis thaliana ecotype col0 (Gold particle were coated with 1µg extracted plasmid DNA).

Supplemental figure 4:pH4/pH6

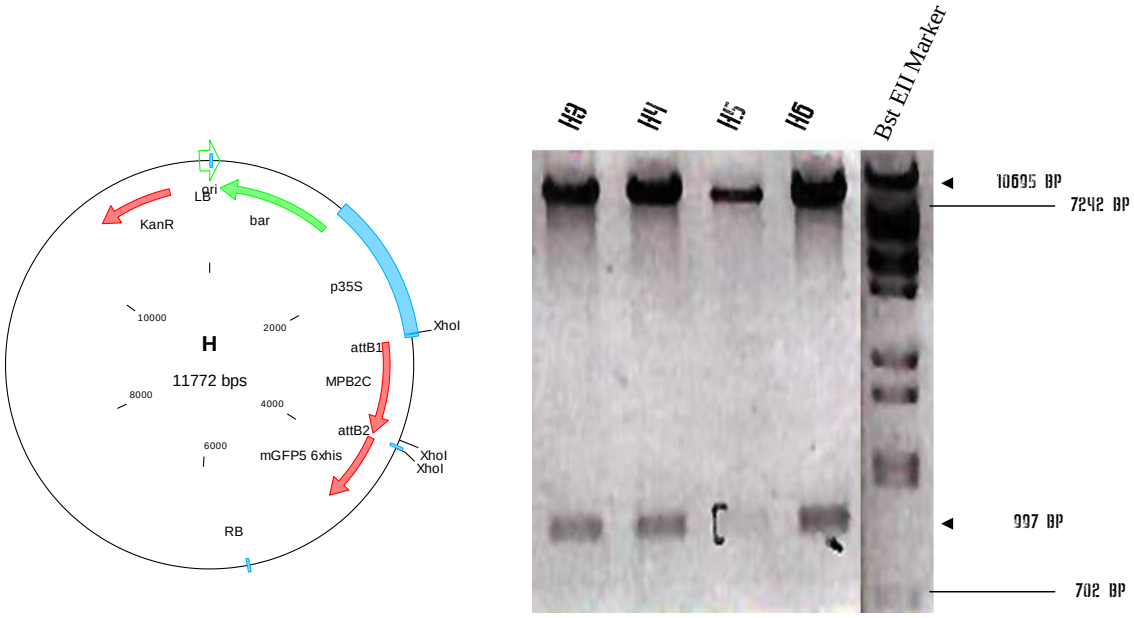

1.1.3 Generation of the PRO_{35S}:At KNB36-mRFP1 overexpression construct

The At KNB36 CDS was PCR amplified and fused to mRFP1 using a 10xALA linker and cloned into pUC vector by Dr. Friedrich Kragler. After confirmation of in vivo functionality via particle bombardment the At KNB36-10xALA-mRFP1 fragment was cut out via NcoI/XbaI restriction from pUC vector. After cutting pENTR4 vector with the same enzymes, fragments were loaded on a 1.5% Agarosegel. The correct bands were purified from gel with QIAEX II Gel Extraction Kit. After measuring the DNA concentration, fragments were ligated and inserted into electro competent E.coli strain TOP 10 via electroporation and selected on full media plates containing kanamycin. After inoculation of grown colonies in LB^{KAN} the plasmids were extracted via Plasmid-Miniprep (clean). The successful cloning was confirmed by NcoI/XbaI diagnostic digestion in 9 out of 11 colonies and the gained construct termed **#163.**

The pENTR4 clones #163.7 and #163.9 were chosen for GATEWAY® recombination and linearized within the Kanamycine resistance gene with PvuI and subsequently loaded on a 1.5% agarose gel. The plasmid DNA of the correct size was cut out from gel and purified via QIAEX II gel extraction kit. The concentration of the gained purified DNA was determined by loading 1µl on a 1% agarose control gel.

GATEWAY® recombination of clone **#7** and **#9** was done into binary vector pMDC32 (Curtis and Grossniklaus et al., 2003) which provides the CaMV 35S promoter. Subsequently chemo-competent E.coli strain TOP 10 was transformed with 1µl Gateway approach via heat shock transformation. 100µl bacteria as well as positive and negative controls were plated on selection plates containing kanamycin and grown for 24 hours at 37°C. Grown colonies were inoculated in LB^{KAN} and confirmed after extraction via EcoRI diagnostic digest (Supp. Figure 5). Of the 5 positive clones were found (#J7.2; #J7.3; #J7.4; #J9.1; #J9.2) 2 clones were tested in transient overexpression systems using the biolistic particle delivery system. Construct **#J7.2** as **#J9.2** showed the mRFP1 signal after transfer in Arabidopsis thaliana ecotype col0 (Gold particle were coated with 1µg extracted plasmid DNA).

Supplemental figure 5: pJ7.2

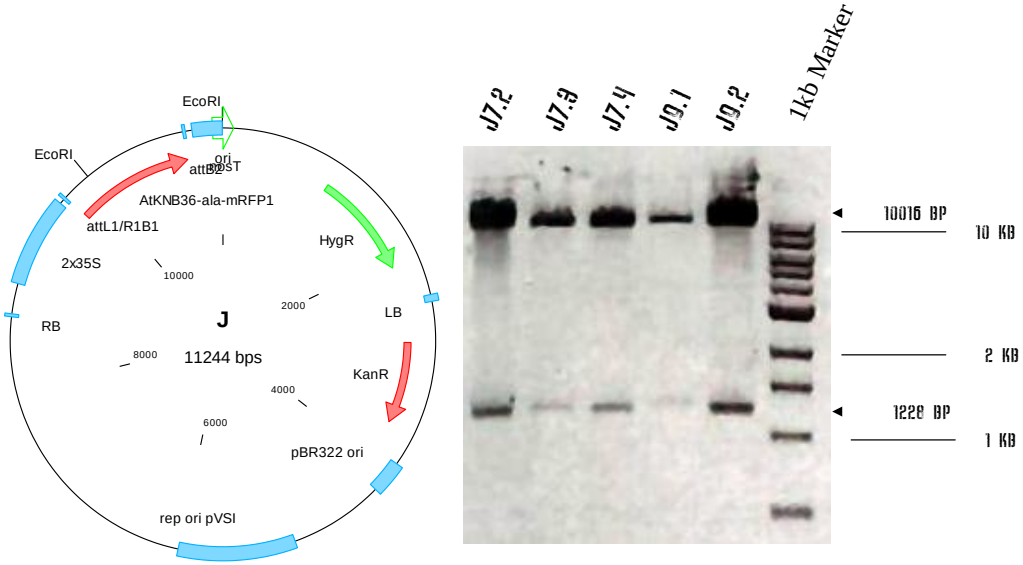

1.1.4 Generation of the PRO_{hsp}:At MPB2C heat inducible construct

The pENTR/D-TOPO clones #X and #2 were inserted into electro competent E.coli strain TOP 10 via electroporation and selected on full media plates containing kanamycin. After inoculation of grown colonies in LB^{KAN} the plasmids were extracted via Plasmid-Miniprep (clean). The correct donor vector backbone was confirmed via PvuI/HpaI diagnostic digest and subsequent examination via agarose gel electrophoresis. The reading frame, the orientation and also the identity of the insert were confirmed by sequencing the plasmid with M13 forward and reverse primer.

After excision of the kanamycin resistance gene via RcaI restriction digest the approach was loaded on a 1.5% agarose gel. The plasmid DNA of the correct size was cut out from gel and purified via QIAEX II gel extraction kit. The concentration of the gained purified DNA was determined by loading 1µl on a 1% agarose control gel.

GATEWAY® recombination of the confirmed clone **#X** was done into binary vector pMDC30 (Curtis and Grossniklaus et. al., 2003) which provides heat shock inducible expression. Subsequently chemo-competent E.coli strain TOP 10 was transformed with 1µl Gateway approach via heat shock transformation. 100µl bacteria as well as positive and negative controls were plated on selection plates containing hygromycin and grown for 24 hours at 37°C. After detecting positive colonies via colony-PCR using **FK227** 5´ (5´-CACCATGTATGAGCAGCAGCAAC-3´) and **FK228** 3´(5´-ATAATATGTAAAGGCTAGTGATTG-3´) they were inoculated in LB^{KAN} and confirmed after extraction via XhoI diagnostic digest (Suppl. Figure 6). One of the four positive clones (#G6) was tested and verified in transgen plants by Niko Winter via PCR amplification from genomic DNA with the primers **FK355** 5´(5´CTAATATATTTACACAAGACTGG-3´) and **FK228** 3´(5´-ATAATATGTAAAGGCTAGTGATTG-3´).

Supplemental figure 6: pG6

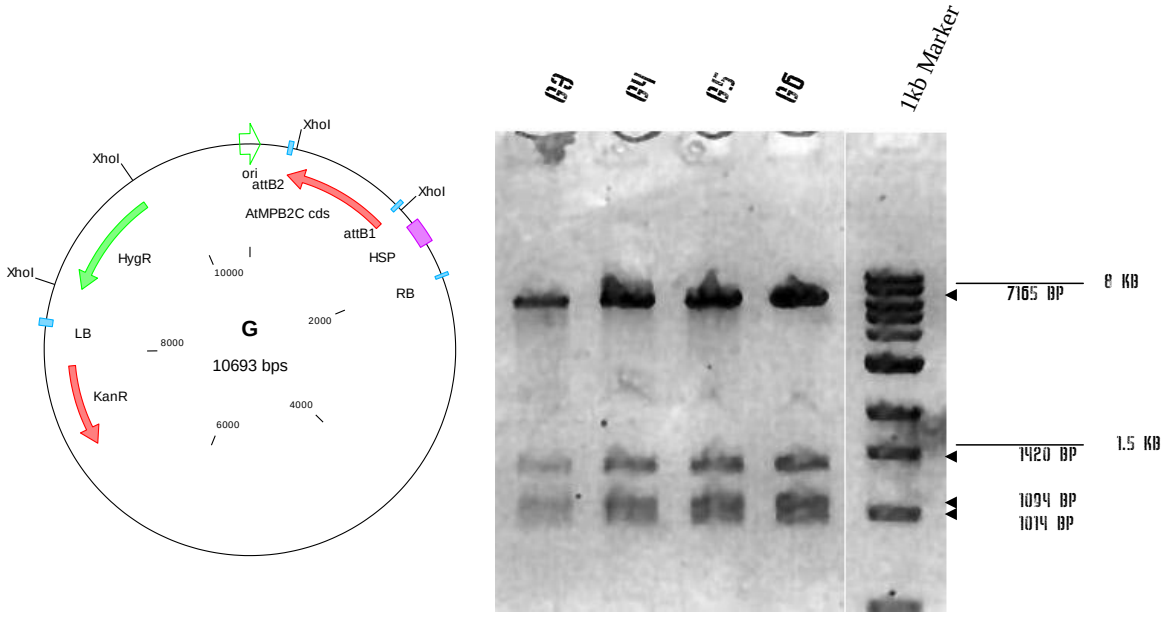

1.1.5 Generation of the PRO_{hsp}:At KNB36 heat inducible construct

The pENTR/D-TOPO clones #161 and #21 were inserted into electro competent E.coli strain TOP 10 via electroporation and selected on full media plates containing kanamycin. After inoculation of grown colonies in LB^{KAN} the plasmids were extracted via Plasmid-Miniprep (clean). The correct donor vector backbone was confirmed via PvuI/HpaI diagnostic digest and subsequent examination via agarose gel electrophoresis. The reading frame, the orientation and also the identity of the insert were confirmed by sequencing the plasmid with M13 forward and reverse primer.

After excision of the kanamycine resistance gene via RcaI restriction digest, the approach was loaded on a 1.5% agarose gel. The plasmid DNA of the correct size was cut out from gel and purified via QIAEX II gel extraction kit. The concentration of the gained purified DNA was determined by loading 1µl on a 1% agarose control gel.

GATEWAY® recombination of the confirmed clone **#161** was done into binary vector pMDC30 (Curtis and Grossniklaus et al., 2003) which provides heat shock inducible expression. Subsequently chemo-competent E.coli strain TOP 10 was transformed with 1µl Gateway approach via heat shock transformation. 100µl bacteria as well as positive and negative controls were plated on selection plates containing Hygromycin and grown for 24 hours at 37°C. After detecting positive colonies via colony-PCR using primers **FK177** 5`(5`-A ATGGAAGAAGACGCAG GGAATGGAGGA-3´) and **FK178** 3`(5`-CCTCAT TGCTCAATGCTAGGATTCTGAAT-3´) they were inoculated in LB^{KAN} and confirmed after extraction via EcoRI diagnostic digest (Suppl. Figure 7). One positive clone was found (#F4) and verified via PCR amplification with specific primers **FK355** 5´(5´-CTAATATATTTACACAAGACTGG-3´) and **FK178** 3`.

Supplemental figure 7: pF4

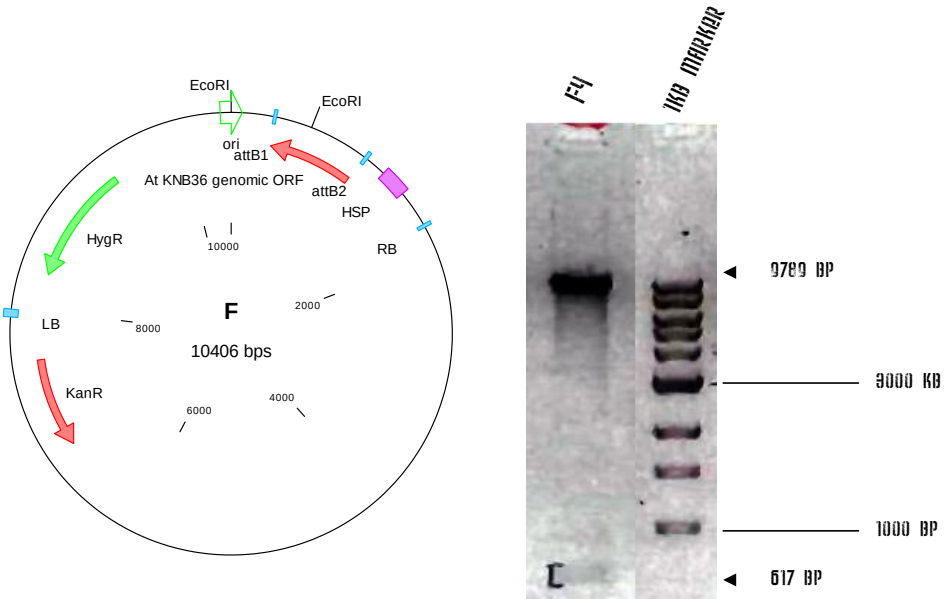

1.1.6 Generation of the $PRO_{At\ KNB36}$:EgfpER-GUS construct for expression analysis

The pENTR/D-TOPO clones #162 was inserted into electro competent E.coli strain TOP 10 via electroporation and selected on full media plates containing kanamycin. After inoculation of grown colonies in LB^{KAN} the plasmids were extracted via Plasmid-Miniprep (clean). The correct donor vector backbone was confirmed via PvuI/HpaI diagnostic digest and subsequent examination via agarose gel electrophoresis. The reading frame, the orientation and also the identity of the insert were confirmed by sequencing the plasmid with M13 forward and reverse primer.

An excision of the kanamycine resistance gene via restriction digest was not needed because the binary recipient vector differs regarding to the resistance gene for bacterial selection. The concentration of the DNA was determined by loading 1µl on a 1% agarose control gel.

GATEWAY® recombination of the confirmed clone **#162** was done into binary vector pKGWFS7 (Karimi et al., 2002) which is constructed for promoter analysis. This vector contains the coding sequence of a Enhanced green-fluorescence protein linked to the endoplasmatic rediculum (EgfpER). Subsequently chemo-competent E.coli strain TOP 10 was transformed with 1µl Gateway approach via heat shock transformation. 100µl bacteria as well as positive and negative controls were plated on selection plates containing Spectinomycin and grown for 24 hours at 37°C. After detecting positive colonies via colony-PCR using primers **FK231** 5´(5´-CACCCCTTTCTCGATGCAG
TGATCC-3´) and **FK250** 3´(5´-TTCAGTGTTCATCAAAACT-3´) they were inoculated in LB^{SPEC} and confirmed after extraction via PstI diagnostic digest (Suppl. Figure 8). One positive clone was found (#A4) and verified after inserting into Arabidopsis thaliana ecotype col0 via GUS stain. (described in details below)

Supplemental figure 8: pA4

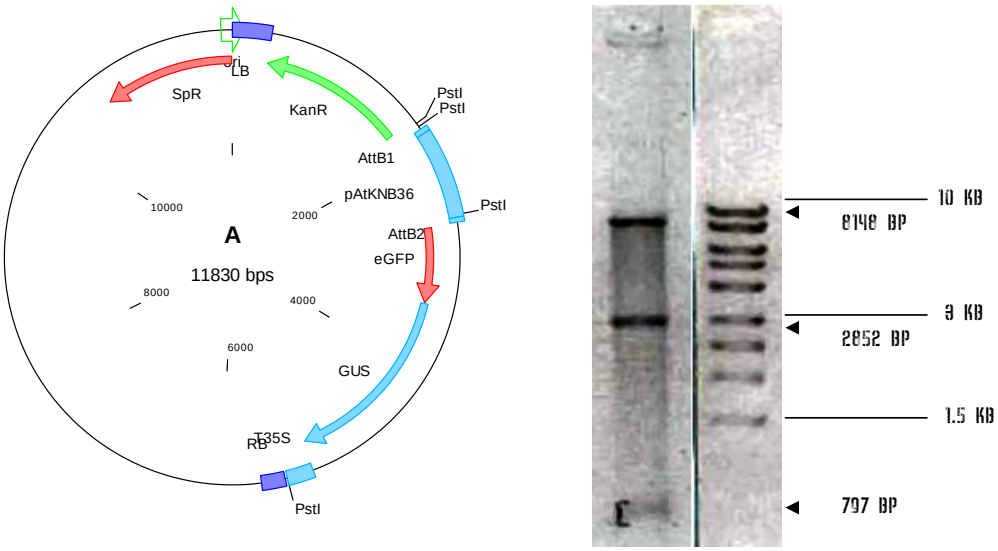

1.1.7 Generation of the PRO $_{At\ MPB2C}$:EgfpER-GUS construct for expression analysis

Cloning was done by Niko Winter who also did Arabidopsis thaliana transformation and verification of this construct.

The promoter region of At MPB2C was PCR amplified with the primers **FK298** 5´(5´-CTCCAAAAATGTATA TATAGATATATAGATTC-3´) and **FK299** 3´(5´-CTTCTTCGTCCTCCGTATAATAGATCTG-3´) using *A.thaliana* Columbia wt genomic DNA as a template. After inserting the 487 bp PCR product into TOPO vector pCR2.1-TOPO, the promoter region was cloned into pENTR4 Gateway donor vector.

Two resulting clones were sequenced and subsequently cloned into binary vector pKGWFS7 (Karimi et al., 2002) after linearization in the Kanamycin resistance gene via PvuI.

After transformation of E.coli TOP10 were selected with spectinomycin and positive colonies confirmed via NcoI restriction (Suppl. Figure 9). Two positive clones were found (#1/1-C, #2/1-C) and verified after inserting into Arabidopsis thaliana ecotype col0 via GUS stain.

Supplemental figure 9: p1/1-C & p2/1-C

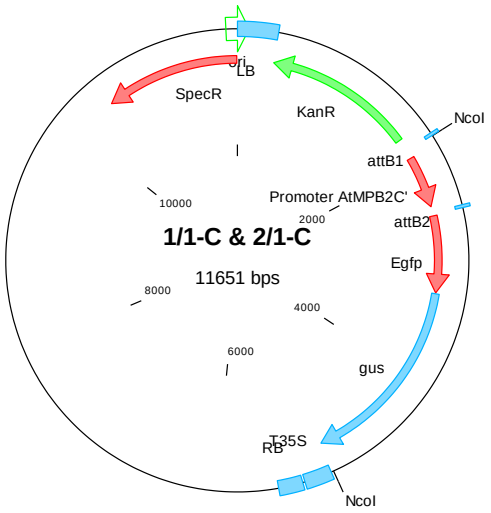

1.1.8 Generation of the PRO_{35S}:At MPB2C-TAP TAG construct

The pENTR/D-TOPO clones #X and #2 were inserted into electro competent E.coli strain TOP 10 via electroporation and selected on full media plates containing kanamycin. After inoculation of grown colonies in LB^{KAN} the plasmids were extracted via Plasmid-Miniprep (clean). The correct donor vector backbone was confirmed via PvuI/HpaI diagnostic digest and subsequent examination via agarose gel electrophoresis. The reading frame, the orientation and also the identity of the insert were confirmed by sequencing the plasmid with M13 forward and reverse primer.

After excision of the kanamycin resistance gene via RcaI restriction digest the approach was loaded on a 1.5% agarose gel. The plasmid DNA of the correct size was cut out from gel and purified via QIAEX II gel extraction kit. The concentration of the gained purified DNA was determined by loading 1µl on a 1% agarose control gel.

GATEWAY® recombination of the confirmed clone **#X** was done into binary vector pEarly Gate 205 (Early et al.,2006) which provides overexpression and a C-terminal TAP-tag fusion. Subsequently chemo-competent E.coli strain TOP 10 was transformed with 1µl Gateway approach via heat shock transformation. 100µl bacteria as well as positive and negative controls were plated on selection plates containing kanamycin and grown for 24 hours at 37°C. After detecting positive colonies via colony-PCR using **FK227** 5´ (5´-CACCATGTATGAGCAGCAGCAAC-3´) and **FK228** 3´(5´-ATAATATGTAAAGGCTAGTGATTG-3´) they were inoculated in LB^{KAN} and confirmed after extraction via XhoI diagnostic digest (Suppl. Figure 10). One of the four found positive clones (#I3) verified via PCR after transformation of Arabidopsis thaliana ecotype col0 with primers **FK156** 5`(5´-CCTTCGCAAGACCCTTCCTC-3´) and **FK228** 3´(5´-ATAATATGTAAAGGCTAGTGATTG-3´) and RT-PCR after using primer **FK398** 3`(5`GACTTCCCCGCGGAATTCGC-3´).

Supplementa figure10 : pI3

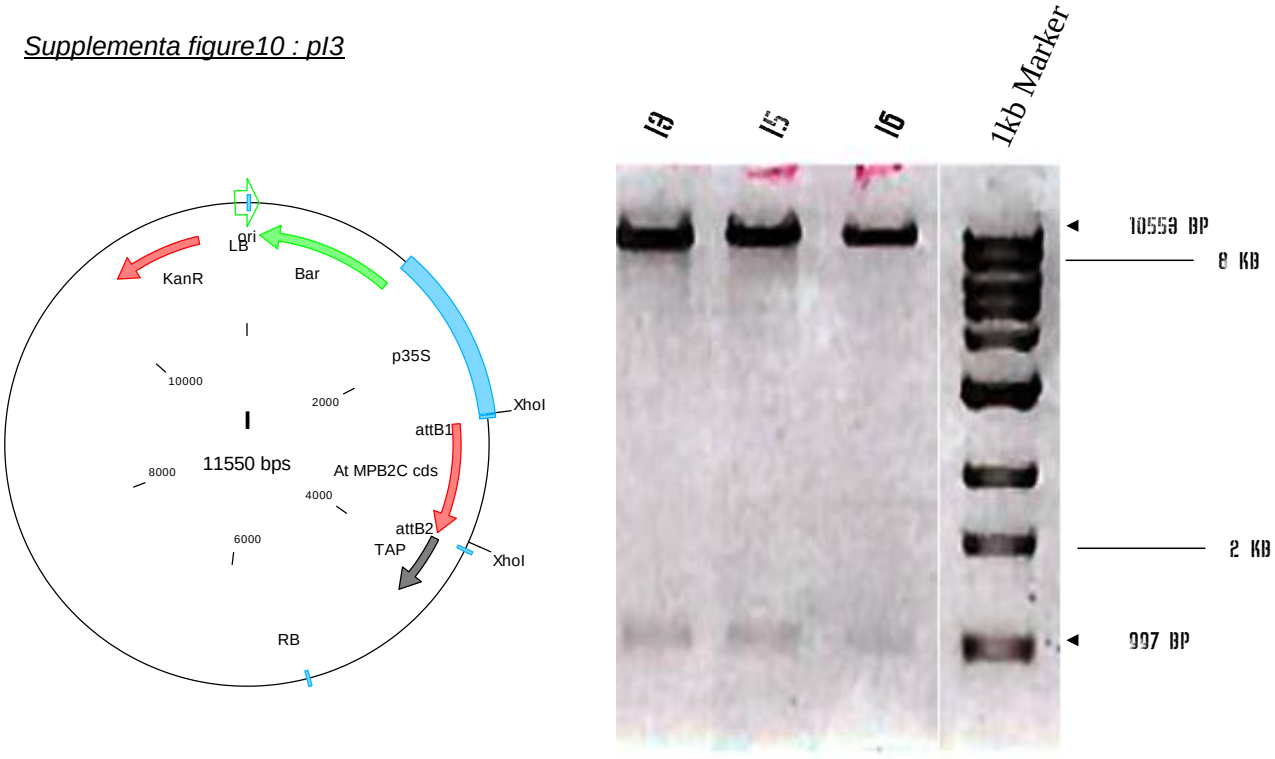

1.1.9 Generation of the PRO_{35S}:At KNB36-TAP TAG construct

The pENTR/D-TOPO clones #161 and #21 were inserted into electro competent E.coli strain TOP 10 via electroporation and selected on full media plates containing kanamycine. After inoculation of grown colonies in LB^{KAN} the plasmids were extracted via Plasmid-Miniprep (clean). The correct donor vector backbone was confirmed via PvuI/HpaI diagnostic digest and subsequent examination via agarose gel electrophoresis. The reading frame, the orientation and also the identity of the insert were confirmed by sequencing the plasmid with M13 forward and reverse primer.

After excision of the Kanamycin resistance gene via RcaI restriction digest the approach was loaded on a 1.5% agarose gel (Figure 11). The plasmid DNA of the correct size was cut out from gel and purified via QIAEX II gel extraction kit. The concentration of the gained purified DNA was determined by loading 1µl on a 1% agarose control gel.

GATEWAY® recombination of the confirmed clone **#161** was done into binary vector pEarly Gate 205 (Early et al.,2006) which provides overexpression and a C-terminal TAP-tag fusion. Subsequently chemo-competent E.coli strain TOP 10 was transformed with 1µl Gateway approach via heat shock transformation. 100µl bacteria as well as positive and negative controls were plated on selection plates containing kanamycin and grown for 24 hours at 37°C. After detecting positive colonies via colony-PCR using primers **FK177** 5`(5`-A ATGGAAGAAGACGCAG GAATGGAGGA-3´) and **FK178** 3`(5`-CCTCAT TGCTCAATGCTAGGATTCTGAAT-3´) they were inoculated in LB^{KAN} and confirmed after extraction via EcoRI diagnostic digest (Suppl. Figure 11).
Both of the 2 identified positive clones (#D7; #D9) were verified via PCR transformation of Arabidopsis thaliana ecotype col0 with primers **FK156** 5`(5´-CCTTCGCAAGACCCTTCCTC-3´) and **FK178** 3`(5`-CCTCAT TGCTCAATGCTAGGATTCTGAAT-3´) and RT-PCR after using primer **FK398** 3`(5`GACTTCCCCGCGGAATTCGC-3´).

Supplemental figure 11: pD7

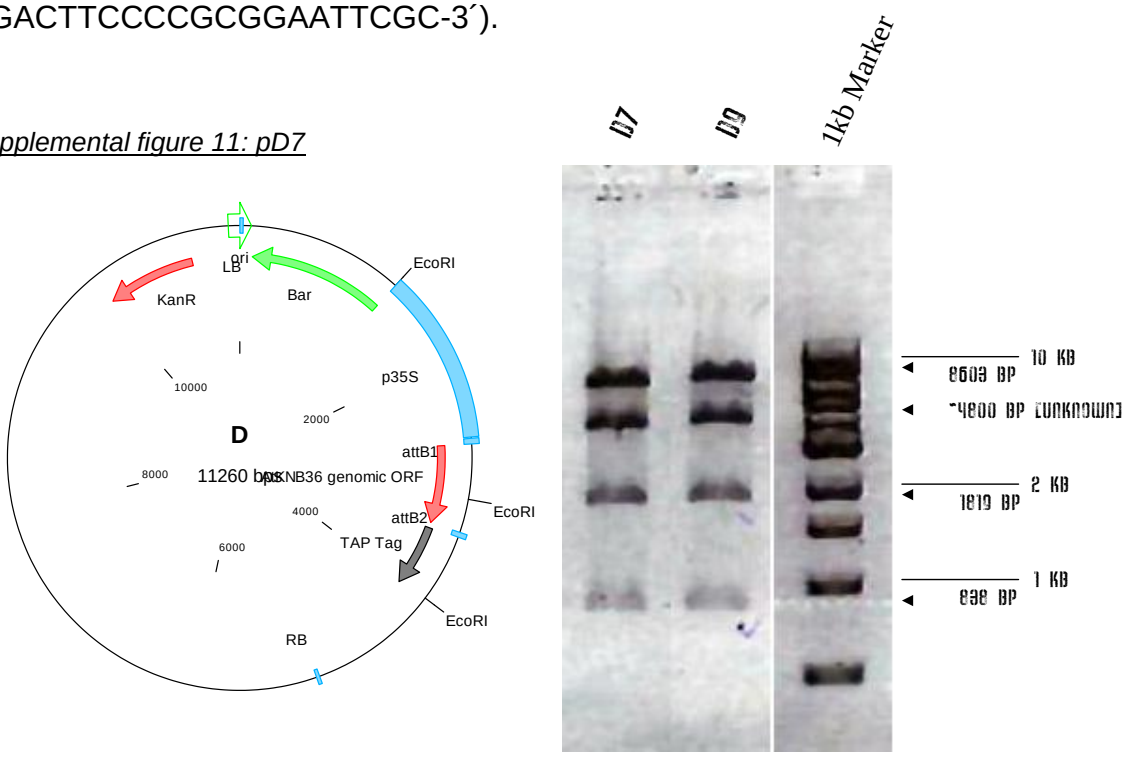

1.1.10 Generation of the PRO_{35S}:GUS-TAP TAG control construct

This construct was designed only for control purposes. The glucuronisidase coding gene derives from a pENTR-GUS donor vector (Invitrogen).
The donor vector was inserted into electro competent E.coli strain TOP 10 via electroporation and selected on full media plates containing kanamycin. After inoculation of grown colonies in LB^{KAN} the plasmids were extracted via Plasmid-Miniprep (clean). The correct donor vector backbone was confirmed via PvuI/HpaI diagnostic digest and subsequent examination via agarose gel electrophoresis.

After excision of the kanamycine resistance gene via RcaI restriction digest, the approach was loaded on a 1.5% agarose gel. The plasmid DNA of the correct size was cut out from gel and purified via QIAEX II gel extraction kit. The concentration of the gained purified DNA was determined by loading 1µl on a 1% agarose control gel.

GATEWAY® recombination of the donor entry clone was done into binary vector pEarly Gate 103 and pEarly Gate 205 (Early et al., 2006) to provide controls for the At MPB2C and At KNB36 overexpression constructs regarding to phenotype, microscopy and trichome rescue analysis. This control construct also serves as a positive control of the transgenic plants transformed with pKGWFS7 containing the At MPB2C and At KNB36 promoter region.
The chemo-competent E.coli strain TOP 10 was transformed with 1µl Gateway approach via heat shock transformation. 100µl bacteria as well as positive and negative controls were plated on selection plates containing kanamycin and grown for 24 hours at 37°C. After detecting positive colonies they were inoculated in LB^{KAN} and confirmed after extraction via BspHI diagnostic digest (Suppl. Figure 12). Of four investigated colonies, 1 positive clone could be identified (#E6) and verified after transformation in plants via GUS staining. E6 is a pEarly Gate 205 vector containing the GUS coding gene under the CaMV 35S promoter. No positive colonies could be gained in case of pEarly Gate 103.

Supplemental figure 12: pE6

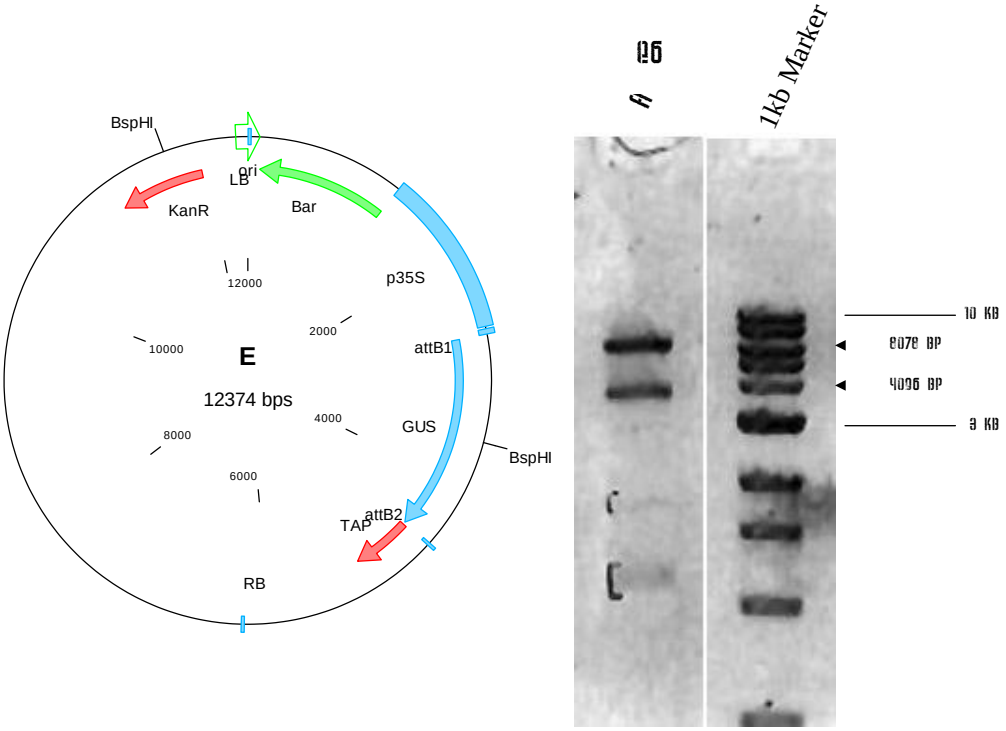

1.2. Production of Transgenic Plants

Protocol: Agrobacterium-mediated transformation/floral dip (Clough and Bent et al., 1998)

1.2.1 Conditions for growth of the Target Plants

All plants were growing under the same conditions in controlled environment with a light intensity in the range of 800 to 1000 µmol m^{-2} s^{-1} and temperatures with 22˚C for 16h light.
Used Pots (D=6cm/12cm) and screening trays (~24x30cm) were filled with a mixture of soil and silica sand in a ratio of 2:1. Soil and sand were sterilized before use by autoclaving. The used ecotypes of our model organism *Arabidopsis thaliana* were *Col 0, Ws* and also *Col 0* plants harbouring the Pro_{RbcS}*::GFP-GL1-KN1*$_{HD}$ construct and termed as *GL1-KN1HD* (Suppl.table 3). The GL1-KN1HD plants were selected in the previous generation on germination plates containing Hygromycin [50mg/l] to confirm the genetic background.
Before sowing 20-25 seeds per 12cm pot, they were synchronised for 12h at 4°C. To obtain more floral buds per plant, inflorescences were clipped 1 or 2 times to synchronise flowering and encourage formation of secondary bolts. Plants were dipped approximately 4-8 days after clipping, when most blossoms were nearly open.

1.2.2 Protocol for culture of Agrobacterium tumefaciens

Agrobacterium tumefaciens strain AGL1 carrying our produced binary vectors (Suppl.table 1) was inoculated from -80°C stock (culture in Glycerol [100%] in a ratio of 1:1) into 8 ml LB media, containing an appropriate amount of antibiotic (LB^{AB}) as described below. The cultures were grown o/n at 30°C under constant motion. For better results all used flasks were always covered with aluminium foil to shade the growing agrobacteria. After transferring the 8ml o/n-culture into 200ml LB^{AB}, bacteria were grown to stationary phase indicated by an OD_{600} of approximately 1.0. Subsequent centrifugation (30min /4300rpm /RT) took place in a SORVALL RC5C using a F14S carbon Rotor (Rotor code 10). After resuspension of the pellet in 250ml Sucrose (5%) by intense vortexing, bacteria were left at 30°C and under constant motion until an OD_{600} of approximately 0.8.

1.2.3 Floral Dip transformation of Arabidopsis

Shortly before starting the procedure L77 Silvet was added to the cultures to a final concentration of 0.02% (→50µl L77 per 250ml inoculum). For the floral dip, the culture was decanted into plastic boxes or glass beakers with appropriate dimensions to fit with the diameter of the pots. To prevent soil and plants from slipping into the culture, we used a Parafilm strip which we placed gently in the middle of the pots where it can be comfortable fixed with the fingers at the side of the pots. Furthermore the pots containing the target plants were inverted into the inoculum such that all above-ground tissues were submerged. To prevent severe injury of the inflorescence the plants were dipped in a rotary motion and removed after 5-10 seconds. After removing the parafilm strip the plants were covered with a blue plastic dome to maintain humidity and protection from light. To optimize the environment for an efficient bacterial infection, plants were left in a low light location until retuning the pots into the grow chambers and removing the dome after 24 hours.

1.2.4 Harvesting of the seeds and selection of putative positive transformants

Dipped plants were grown for several weeks until the siliques were brown. All seeds deriving from single pots were harvested together through gently pulling of the dry inflorescences so that the seeds can easily be colleted on a piece of paper. Remaining plant parts were removed through gentle blowing. The first gained seeds (TP) were stored in micofuge tubes but later we exchanged from tubes to paper envelopes.
Antibiotic/herbicide – application to identify positive seedlings in the T1 generation differs regarding to the inserted construct (Suppl.table 2) Seeds of putative positive transformants harbouring the BASTA resistance gene were synchronised at 4°C for approximately 12h and dibbled subsequently directly on soil in large screening trays. 2-3 weeks after germination, plants and wild type controls were screened by spraying twice with BASTA Solution [200mg/l]. BASTA showed no effect on putative positives whereas untransformed plants and controls turned brown within days and died rapidly. Seeds which should harbour a Kanamycin or Hygromycin resistance gene were sterilized and poured on germination plates (standard protocol). Putative positives could be easily detected by analysing the morphology of the developing seedlings. In case of a Kanamycine selection, resistant plants develop complete normal whereas sensitive plants and wild type controls fail to develop leaves and roots. Additional cotyledons turn out to be white. Germination plates including Hygromycin were additional shaded 2 days after germination for the following 2 days. Here putative positives show expected hypocotyl elongation whereas sensitive plants retarded.
After positive transformants were identified on the selection plates or screening trays, plantlets were transferred into pots containing heavily moistened soil. Positive transgenic plants were confirmed in T0 and T1 generation using different methods regarding to the genetic modification. Data and verification results can be seen in chapter “Results”.

Supplemental table 2: Resistance of the produced transgenic plants

Term	Expressed Construct	Binary Vector	Restiance: Plant
A4	$p_{At\ KNB36}$::EgfpER - GUS	pKGWFS7	Kanamycine
B2;B9	p_{35S}::At KNB36 - mGFP5 - 6xHIS	pEarly Gate 103	BASTA*
D7	p_{35S}::At KNB36 - TAP	pEarly Gate 205	BASTA*
E6	p_{35S}::GUS - TAP	pEarly Gate 206	BASTA
F4	p_{hsp}::At KNB36	pMDC30	Hygromycine
G6	p_{hsp}::At MPB2C	pMDC30	Hygromycine
H4;H6	p_{35S}::At MPB2C - mGFP5 - 6xHIS	pEarly Gate 103	BASTA*
I3	p_{35S}::MPB2C - TAP	pEarly Gate 205	BASTA*
J7	p_{35S}::At KNB36 - 10xALA - mRFP1	pMDC32	Hygromycine
1/1;2/1	$p_{At\ MPB2C}$::EgfpER - GUS	pKGWFS7	Kanamycine

**marked lines harbour a Hygromycin resistance gene too if the genetic background is GL1-KN1HD!*

Supplemental table 3: Confirmed and verified transgenic plant lines

		Nr. of Confirmed Independend Transgenic Lines	
Term	Expressed Construct	Genetic background: Col0	Genetic background: GL1-KN1HD
A4	$p_{At\ KNB36}$::EgfpER - GUS	12	0
B2;B9	p_{35S}::At KNB36 - mGFP5 - 6xHIS	3	18
D7	p_{35S}::At KNB36 - TAP	7 [5]	0(4)*
E6	p_{35S}::GUS - TAP	6	0
F4	p_{hsp}::At KNB36	5	0**
G6	p_{hsp}::At MPB2C	5	0**
H4;H6	p_{35S}::At MPB2C - mGFP5 - 6xHIS	9 [4]	7 [7]
I3	p_{35S}::MPB2C - TAP	36 [4]	14 [8]
J7	p_{35S}::At KNB36 - 10xALA - mRFP1	25	0**

Note: All seeds/seedlings were selected with an appropriate antibiotic/herbicide and verified via PCR with insert specific primers or via confocal microscopy in case of mGFP5/mRFP1 tagged lines. No positive transgenic plants could be established in Ws background. Genomic verifications of transgenic plants carrying H4, H6, I3 and E6 and also the confirmation of mGFP5/mRFP1 signals of several lines were partly done by Niko Winter.

Numbers in square brackets refer to RT-PCR confirmed lines. These RT-PCR experiments were partly done by Shoudong Zhang.

** indicates plant lines which show BASTA resistance but could not be verified by PCR or RT-PCR.*

*** indicates lines which could not be generated because of a resistance conflict which made selection of the T0 plants impossible because the Hygromycin resistance gene which was needed for T0 selection can already be found in plants harbouring the Pro_{RbcS}:GFP-GL1-$KN1_{HD}$ construct*

1.3. In Situ Localisation of GUS Activity & Tissue Embedding

1.3.1 Plant Material

Examined plant lines were produced as described in chapter “production of transgenic plants”.
A4 plants ($p_{At\ KNB36}$::EgfpER – GUS) of the T0 generation derived from the agrobacteria transformed parental plants (TP), were selected on germination plates and positives transferred on soil. Plants were verified through staining different organs of 4 weeks old plants following *Staining & Clearing Procedure 1* and subsequent clearing according to same procedure.
1-1 and 2-1 plants ($p_{At\ MPB2C}$::EgfpER – GUS) were produced and selected in a similar way by Niko Winter. 3 day old T1 Seedlings of these lines were verified using *Staining & Clearing Procedure 2* followed by clearing according to the same protocol.

All examined plants were growing under the same conditions in controlled environment with a light intensity in the range of 800 to 1000 µmol m^{-2} s^{-1} and temperatures of 22˚C for 16h light.

To investigate seedlings, T1 seeds were collected and dried in paper envelopes at 37°C for several days. After drying, seeds were synchronised at 4°C for approximately 12 hours and dibbled on water saturated filter paper placed in sterile Petri dishes. Dishes were sealed with parafilm and placed in the grown chamber. Seedlings were stained 3 days after germination. The segregating T1 seedlings were sorted after staining regarding whether GUS expression is visible or not.

Plants which served the examination of mature organs, like stem, florescence or siliques, derive from T1 seeds grown on selection plates and were later transferred to single pots. After confirmation of the correct expression pattern, seeds of these plants were used to establish T2 generation. To examine the GUS expression pattern in cotyledons in later stages, in the first leaves and during secondary root formation, single individuals of each line were stained after a period of 16 days of development on the selection plates.

1.3.2 Preparation of Solutions

(Note: All staining solutions should be prepared fresh and used immediately! All work has to be done on ice /°4C°! Exceptions are denoted.)

Staining Solution 1

- 100mM sodium phosphate buffer (PH7)
- 10mM Na_2EDTA (PH8)
- 1mM 5-bromo-4-chloro-3-indolyl-ß-glucuronic acid (X-Gluc in DMF; fresh)
- 0,1% Triton-X100

For a 1ml approach mix 50µl X-Gluc dissolved in DMF [20mM] with 100µl sodium phosphate buffer (pH7) [1M], 20µl Na_2EDTA (pH8) [0,5M], 10µl Triton-X100 (10%) and add 820µl ddH_2O

Staining Solution 2

- 50mM sodium phosphate buffer
- 0,5mM potassium ferrocyanide: $K_4Fe(CN)_6$
- 2mM 5-bromo-4-chloro-3-indolyl-ß-glucuronic acid (X-Gluc in DMSO; fresh)
- 0,1% Triton-X100

For a 1ml approach mix 96µl X-Gluc dissolved in DMSO [20mM] with 50µl sodium phosphate buffer (pH7) [1M], 100µl $K_4Fe(CN)_6$ [5mM] , 10µl Triton-X100 (10%) and add 744µl ddH_2O in a autoclaved glass beaker. Adjust pH to 7.2. (Pautot et al., 2001)

Staining Solution 3

- 50mM sodium phosphate buffer
- 2mM potassium ferrocyanide: $K_4Fe(CN)_6$
- 2mM potassium ferricyanide: $K_3Fe(CN)_6$
- 2mM 5-bromo-4-chloro-3-indolyl-ß-glucuronic acid (X-Gluc in DMSO; fresh)
- 0,1% Triton-X100

For a 1ml approach mix 96µl X-Gluc dissolved in DMSO [20mM] with 50µ sodium phosphate buffer (pH7) [1M], 20µl $K_4Fe(CN)_6$ [100mM], 20µl $K_3Fe(CN)_6$ [100mM], 10µl Triton-X100 (10%) and add 804µl ddH_2O. Adjust pH to 7.2. (Vitha et. al., 1995; Sessions et al., 1999)

Clearing solution 1

Mix Acetic acid and Ethanol (96%) in a ratio of 1:1.

Clearing solution 2

Here a simplified version of Herr´s liquid (lactic acid, chloral hydrate, phenol crystals, clove oil, xylene mixed in a ratio of 2:2:2:2:1 (J.M.Herr, 1971)) containing only lactic acid saturated with chloral hydrate (Lux et al., 2005; J.M. Herr Jr. 1993) was used. This clearing fluid ("Herr´s light") was produced through dissolving chloral hydrate in a glass beaker containing an adequate amount of lactic acid until limits of solubility were reached. This was done at room temperature.

1x Pipes buffer (1000ml)

Mix 37.86g Pipes, 3.804g EGTA and 0.241g $MgSO_4$ and add 800 ml ddH_2O. After adjusting pH to 6.8 add ddH_2O to 1000 ml.

Triple Fix

- 1,5% Glutaraldehyd
- 1% Paraformaldehyd
- 2 % Acrolein
- 84mM Pipes buffer
- 0.05% Tween 20

For a 200ml approach mix 12ml Glutaraldehyd (25%) with 20ml Paraformldehyd (10%), 168ml 1x pipes buffer, 100µl Tween 20 and check if pH is 6.8. Add Acrolein as the last component after Trible Fix was aliquoted in vials (see procedure) to 2% of volume. Note that Acrolein is heavily toxic and should only be handled under the hood, wearing gloves, a mask and protective overalls.

1.3.3 Staining and Clearing Procedures

Method I

Plant tissues were collected after 8 hours light and placed in 6 well microtiter plates. After addition of Staining Solution 1 samples were infiltrated under vacuum for 3min. The stain was carried out for 12 hours at 37°C in a light protected environment. After staining, staining solution was removed and replaced by Clearing Solution 1 by pipetting. Clearing took place at room temperature for 48 hours (Pautot et al., 2001).

Method II

Plant tissues were collected after 8 hours light and permeabilised in Acetone (80%) under vacuum for 10-15 min until tissues sunk down (If tissues remained on the surface the infiltration had to be repeated!). Subsequently samples were left in Acetone (80%) at -20°C for 1 hour.to facilitate the X-Gluc uptake (Hemerly et al., 1993).

Here we tested different duration times (1hour – 72hours) depending on tissue size (seedlings / adult tissues) We agree with Scarpella et.al., 2004 that a acetone-incubation for longer than 1 hour damages the tissues, so the signal can spread in the adjacent tissues which can result in an increasing lack of quality and sharpness. Solely a period of 24 hours should not been exceeded, otherwise the signal strength decreases obvious. Staining was done in 24 well microtiter plates (seedlings) / 6 well microtiterplates (adult tissues). The Acetone (80%) was removed and replaced by Staining Solution 2 by pipetting. This solution contains potassium Ferricyanid and potassium Ferrocyanide in a concentration of 2mM. Higher concentrations accelerate the oxidative dimerization of the reaction intermediate into the blue insoluble product and thereby reduce diffusion of the intermediately at the expense of sensitivity (Lojda, 1970, Scarapella et.al., 2004).
Subsequently the samples were infiltrated under vacuum for 10 min. The stain has been carried out for different durations between 6 hours and 24 hours. The best results were archived with a staining period of 12 hours at 37°C in the dark. Afterwards tissues were rinsed in Ethanol (70%) (Vitha et.al.,1995) for 30 min and subsequently cleared in Clearing Solution 1 for 12 hours at 4°C. Clearing Solution 1 was removed, tissues rinsed and stored at 4°C in Ethanol (70%).
Alternatively tissues were also rinsed in Ethanol (70%) after staining (30min) and cleared in “Herr´s light” for 12 hours at RT. Note that impurities can cause unspecific blue staining if tissues cleared too long in “Herr´s light”. After the tissue became obvious transparent, samples were immediate analysed by microscopy or stored in Ethanol (70%) (J.M.Herr. jr. 1993).

Method III (recommended)

Plant tissues were collected after 8 hours light, placed in 6/24 well microtiterplates and permeabilised in Acetone (80%) through vacuum infiltration for 15 min. (repeated if tissues remaining at the surface!). Subsequently samples were placed at -20°C for 1hour (Hemerly et al., 1993). After rinsing the tissues 2 times for 5 minutes in Sodium Phosphate Buffer [1M], Staining Solution 3 was added to samples and infiltration was done for 15 min. After infiltration tissues were incubated for 12 hours at 37°C in a light protected environment. Subsequently tissues were dehydrated in gradual steps with ethanol series (10, 30, 50 and 70%) to 70% and either incubated in clearing solution 1 for 6 -12 hours at 4°C or in Clearing Solution 2 at RT for 2-6 hours, depending on the tissue quality and size. Best quality was archived if microscopic analysis was done immediately after clearing! Storage took place after rinsing in Ethanol (70%) at 4°C.

1.3.4 Microscopy

For microscopy analysis tissues were transferred after clearing on a slide and treated with a drop Glycerol (10% or 50%) (Vitha et.al., 1995) or a drop of lactic acid saturated with chloral hydrate. (Depended on clearing method) (J.M. Herr Jr. 1993)

Pictures were taken with:

-Coolpix 3200 camera (Nikon)
-SP500UZ camera (Olympus)
-Stereomicroscope : Zeiss Discovery. V12
-Axiomicroscope : Zeiss Imager. M1

Following programs were in use to image and process pictures:

-MTB2004KONFIGURATION (Zeiss;Microtoolbox 2004, Konfigurationsprogramm version 1.2.0.9)
-AXIOVISION (Zeiss;Version AxioVS40 V 4.5.0.0)
-PHOTOSHOP (Adobe; version 7.0

1.3.5 Embedding

To localize the GUS activity in sections, tissues were transferred from staining solution into plastic vials containing 5-10 ml Triple Fix (w/o Acrolein). Subsequently Acrolein was added to 2% of volume and swirled.
Tissues were infiltrated under vacuum for ~30 min until they sink down. Subsequently vials were left at 4°C for 24 hours under constant movement. The Triple Fix was removed and tissues are rinsed with 10ml Pipes buffer [100mM] (2x) and incubated in Pipes buffer [100mM] for 2 additional hours. (After this step, tissues can also be stored in Pipes buffer [100mM] at 4°C)

To proceed with embedding, tissues were dehydrated in gradual steps (10, 30, clearing solution 1, 70, 90 and 100% Ethanol for 30 min/step) and embedded in Technovit 7100 (Heraeus, Kulzer; Haslab GmbH) according to the manufacturer's instructions:

- Mix Basislösung and 100% Ethanol in a ratio of 1:1
- Fix tissues in this solution for 60 min (24 hours are possible) at room temperature
- Mix 100ml Basislösung with 1 g Härter 1to produce the Vorbereitungslösung
- Infiltrate tissues in Vorbereitungslösung 1 -12 (6) hours (Duration depends on tissue size)
- Mix 15 ml Vorbereitungslösung with 1ml Härter II
- Fill solution into histoform (PCR-eppendorf tube), place tissues in solution and position correctly
- CLOSE histoform and make sure that histoform is air-tight, otherwise hardening will fail!!
- Leave histoform o/n at the bench upside down

2. Primer list

2.1 Primers for TOPO cloning

At KNB36 genomic ORF (Primer for insert cloning):
FK230 5`(5´-CACCATGAACACTGAAATGGAA G-3´)
FK187 3´(5´-CGGCGGATCCGCTTGCTCAATGCTAGG-3´)

At KNB36 genomic ORF (Primer for insert verification):
FK177 5`(5`-A ATGGAAGAAGACGCAGGGAATGGAGGA-3´)
FK178 3`(5`-CCTCAT TGCTCAATGCTAGGATTCTGAAT-)

AtKNB36 promoter region (Primer for insert cloning):
FK231 5´(5´-CACCCCTTTCTCGATGCAGTGATCC-3´)
FK250 3´(5´-TTCAGTGTTCATCAAAACT-3´)

At MPB2C cDNA (Primer for insert cloning):
FK227 5´(5´-CACCATGTATGAGCAGCAGCAAC-3´)
FK228 3´(5´-ATAATATGTAAAGGCTAGTGATTG-3´)

At MPB2C promoter region (Primer for insert cloning):
FK298 5´(5´-CTCCAAAAATGTATATATAGATATATAGATTC -3´)
FK299 3´(5´ -CTTCTTCGTCCTCCGTATAATAGATCTG-3´)

2.2 Primers for transgen plant confirmation

Verification of the At MPB2C - TAP (line I_3; in combination with FK 227) and Verification of the At KNB36 - TAP (line D_7; in combination with FK 177):
FK398 3`(5`-GACTTCCCCGCGGAATTCGC-3´)

Verification of the PRO_{hsp}:At MPB2C (line G_6; combination with FK228) and Verification of the PRO_{hsp}:At KNB36 (line F_4; combination with FK178):
FK355 5´(5´-CTAATATATTTACACAAGACTGG-3´)

Verification of the PRO_{35S}:At MPB2C (line H_6 & I_3; combination with FK228) and Verification of the PRO_{35S} At KNB36 (line B_2, B_9 & D_7; in combination with FK 178):
FK156 5`(5´- CCTTCGCAAGACCCTTCCTC-3´)

Standardization of the At KNB36/At MPB2C promoter (A_4) verification (RT-PCR)
At Actin (TAIR acc' At3g18780)
FK424 5´(5´- GGAAGGATCTGTACGGTAAC- 3´)
FK425 3`(5`- TGTGAACGATTCCTGGACCT-3´)

2.3 Primers for At MPB2C TILLING analysis

Analysis of TILLING line #72928 and line #96221
FK293 5´ (5´- GGTTTCGAGGGGATTGCAG-3´)
FK295 3´(5´- CCTATGCAACCAAGCTACAG-3´)

Analysis of TILLING line #91258
FK296 5´ (5´- GGA AGA AAT GCT TCT CAA AC -3´)
FK297 3´(5´- GTG TCC GAT AAT TGT AAC TG -3´)

2.4 Primers for RT-PCRs

At STM (TAIR acc# At1g62360)
FK350 (5´-GGGGACCACTTTGTACAAGAAAGCTGGGTCAAGCATGGTGGAGGAGATGTG- 3´)

At KNAT1 (TAIR acc# At4g08150)
FK352 (5´- GGGGACCACTTTGTACAAGAAAGCTGGGTCTGGACCGAGACGATAAGGTCC- 3´)

At Ga2Ox4 (TAIR acc# At1g47990)
FK354 (5´- CCACATGCCATCTGAATTGGAC - 3´)

At UBQ4 (TAIR acc# At5g20620)
FK345 (5´- ACCAGGTGAAGATCTCACCTC- 3´)

At MPB2C: (TAIR acc# At5g08120)
FK228 (5´- ATA ATATGTAAAGGCTAGTGATTG- 3´)

3. Standard Methods

Agarose Gel Electrophoresis

- Transfer X µl DNA in a Eppendorf tube (1µ for DNA/RNA concentration check)
- Add 2µl 6X Loading Dye Solution (Fermentas)
- Add Xµl ddH_2O (to a final volume of 5µl for DNA/RNA concentration check)
- Load on a X% Agarosegel (Standard 1%)
- Add 5µl [0,1µg/µl] of a appropriate Marker in separate slots(100bp / 1kb)
- Fill 1X TAE Buffer (in case of RNA 1X TBE Buffer) apparatus
- Run gel electrophoresis with 100V* for approximately 40 min *

Protocol: Molecular Cloning, Cold Spring Harbor Press
Note: Use RNAse free Buffers for analysis of RNA! For analysis of restriction approaches 20µl /slot were loaded.
*depends on the product length and kind of further procedures

Biolistic Particle Delivery System (Bombardment)

Gold coating:

- transfer 1µg* (Combinations: 0.5+0,5**) Vector DNA into a new Eppendorf tube (Endvolume:10µl)
- add 50µl* gold particles
- vortex 30 sec
- add $CaCl_2$ [2,5M]
- vortex 1 min
- add 25µl Spermidine [0,1M]
- vortex 10min at 4°C or 3x 30 sec at RT
- 1min at RT
- centrifuge 5 sec
- remove supernatant
- add 150µl EtOH 99% (stored at -20°C)
- vortex briefly
- centrifuge 5
- remove supernatant
- resuspend in 60µl EtOH 99%
- store at 4°C

*In case of binary vecors 2µg (Combinations 1+1) were in use and gold particles were reduced to 25µl.
** Combined binary vecors and smaller ones like pUC in a ratio of 4:1 µg

Bombardment:

Note: all steps of cleaning & loading were done under the internal hood!

- mark pots of the target plants / Petri dishes with wet paper covered single leafs
- start apparatus (Biolistic PDS-1000-He apparatus (BioRad))
- clean loading discs, rapture discs and stopping screens in EtOH 99%
- vortex Eppendorf tubes containing particles for ~5min
- transfer 10µl of each construct /combination on a loading disc & let it dry

- install dried carrier disc (direction!), rapture disc (450psi for At) and stop disc
- place pots in the lowest position / single leavs (adaxial) in position 3 from bottom
- establish vacuum until 23 pounds per square inch (psi) (leaves)/ 27 psi (plants in pots) are reached
- activate particle pressure delivery
- deactivate vacuum pump
- spray plant with H_2O and cover plants with a dome to keep humidity

Microscopy & Image Processing:

Images of expressed fluorescent proteins or microinjected probes were obtained with a Leica SP1 confocal microscope. GFP, mRFP1 and DsRED fluorescent probes were excited at 476/488 nm and 568 nm, respectively. GFP was detected at 500-520 nm (green), mRFP1 and DsRED at 610-630 nm (red) and chloroplast fluorescence at 680-710 nm (blue). All tissues/cells harbouring green and red fluorescent probes were scanned also in sequential mode switching between the 476/488 nm and 568 nm laser excitations and according detection channels to ensure specific identification of red and green fluorescent signal.

Protocol: Dr.Kragler

Diagnostic Digest /Restriction assay

Restriction Approach: ∑ 20µl		
Amount	**Content**	**Concentration**
7.9µl	ddH_2O	
2µl	Buffer	
10µl	Template	
0.1µl	Enzyme	[10U/µl]

- Mix up the components in the assigned order in a 1,5 ml Eppendorf tube
- Digestion takes place at 37°C for 3 hours

DNA Isolation from Plant Tissue

- Remove leaf tissue of an approximate size of 2x4 mm from target plant (use a fresh razor blade!)
- Transfer the isolated tissue immediately into 1.5 ml Eppendorf tube
- Grind tissue with staff grinder until homogenized (fast!)
- Add 600 µl Extraction buffer
- Spin down (3 min/13.000 rpm/RT)
- Transfer 500 µl supernatant into new 1.5 ml Eppendorf tube
- Add 500 µl Isopropanol (2-propanol)
- Mix by inverting
- Precipitate at -20°C for 10 min
- Spin down (5 min/13.000 rpm /RT)
- Discard supernatant
- Add 500 µl EtOH (96%)
- Vortex briefly
- Spin down (5 min/ 13.000 rpm / RT)
- Discard supernatant

- Add 500 µl EtOH (96%)
- Vortex briefly
- Spin down (5 min/ 13.000 rpm /RT)
- Discard supernatant
- Dry pellet at RT
- Dissolve pellet in 100 µl ddH_2O
- Add 1µl RNAse A

DNA Purification via Chloroform/Phenol Extraction

- Cut out gel slice which contain PCR product with a common razor blade
- Transfer gel slice into an 2ml Eppendorf tube
- Weigh DNA fragment (The weight should not exceed 250mg! Otherwise you have to part it)
- Add 500 µl NaCl [0,4M]
- Heat up the sample to 80°C for 10 min (→also preheat the Phenol which will needed in next step!)
- Add 500 µl preheated, buffered & water saturated Phenol; pH 7.8 (→ stored @4°C)
- Vortex vigorously (→ Check if agarose is complete dissolved, if not repeat heating step!)
- Spin down (5 min /13.000 rpm/RT)
- Transfer agarose free supernatant into a new 1.5 Eppendorf tube
- Add 500 µl Phenol/Chloroform/Isoamylalkohol (with a ratio of 25:24:1)
- Vortex vigorously
- Spin down (5 min /13.000 rpm/RT)
- Transfer supernatant (top phase) into new 1.5 Tube
- add 500 µl Chloroform
- Vortex vigorously
- Spin down (5 min /13.000 rpm/RT)
- Transfer supernatant into new 1.5 Tube
- Add EtOH (96%) equal to sample volume
- Mix it by inverting
- Incubate at 4°C for 1 hour
- Spin down (30 min/13.000 rpm/4°C)
- Discard supernatant (→Be careful: pellets near invisible and easy become lost!)
- Add EtOH (70%) equal to sample volume
- Mix it by inverting
- Spin down (5 min /13.000 rpm/RT)
- Discard supernatant
- Add EtOH (96%) equal to sample volume
- Mix it by inverting
- Spin down (5 min /13.000 rpm/RT)
- Discard supernatant
- Dry pellet at RT
- add 20 µl ddH_2O or 1xTE Buffer (to lower salt concentration)

DNA Purification with QIAEX II Gel Extraction Kit

Note: Purifications were done according to manufacturers instructions.

GATEWAY Recombination

- Make sure that the AB-resistance gene of donor vector differs from destination vector. Otherwise linearize the donor vector in the resistance gene via enzyme digestion
- The concentration of donor and destination vector should be 1:1.
- The amount of the donor vector should be around 150ng.
- The amount of the destination vector should be between 100ng and 300ng.
- The end volume of each approach should not excess 10µl. Do not to forget a positive controls for each recombination (e.g. GUS as insert)

Sup. Table: Used Ratios: Donor vector : Destination vector

Construct Nr.:	Donor vector	Insert	Amount	Concentration	Destination vector	Amount	Concentration
A	#162	pAtKNB36	0.5µl	265ng/µl	pKGWFS7	0.65µl	150ng/µl
B	#161	AtKNB36 genomic ORF	2.7µl	20ng/µl	pEARLY GATE 103	1.3µl	75ng/µl
C	+control	GUS	2µl	50ng/µl	pEARLY GATE 103	1.3µl	75ng/µl
D	#161	AtKNB36 genomic ORF	3.7µl	20ng/µl	pEARLY GATE 205	0.3µl	300ng/µl
E	+control	GUS	2.0µl	50ng/µl	pEARLY GATE 205	0.3µl	300ng/µl
F	#161	AtKNB36 genomic ORF	3.8µl	20ng/µl	pMDC30	0.2µl	500ng/µl
G	#X	AtMPB2C cDS	3.8µl	20ng/µl	pMDC30	0.2µl	500ng/µl
H	#X	AtMPB2C cDS	2.7µl	20ng/µl	pEARLY GATE 103	1.3µl	75ng/µl
I	#X	AtMPB2C cDS	3.7µl	20ng/µl	pEARLY GATE 205	0.3µl	75ng/µl
J	#163	AtKNB36cDS-ala-mRFP1	5µl	20ng/µl	pMDC32	1µl	100ng/µl

- Mix the correct amounts of destination and donor vector in a 1.5ml Eppendorf tube
- Thaw LR clonase on ice and vortex after it becomes liquid
- Add buffer and ddH_2O to a endvolume of 8µl as described in the table below
- Add LR clonase at
- Vortex
- Spin down for several seconds
- Incubate for 60min at RT (alternative o/n)
- Add 1µl protein kinase A to each approach to stop the recombination reaction
- Use 1µl of the GATEWAY® approach for heat shock transformation into 50µl super chemo-competent Top 10 (KIT). Note that the DNA amount in the approach belongs to the concentration of the destination vector.
- Include a negative control in the transformation (only Destination vecor)

GATEWAY® Approach: ∑ 10µl		
Amount	**Content**	**Concentration**
Xµl	Donor vector (pENTR)	[100-300ng]
Xµl	Destination vector (Binary)	[150ng]
2µl	5x LR Clonase reaction buffer	
Xµl	ddH_2O	
2µl	LR Clonase	

- To check if colonies are positive they were picked from plate and verified via colony PCR (described below)
- Positive clones were verified a in a second round via diagnostic digests and finally via particle delivery.

Protocol: Invitrogen GATEWAY® Technology

Ligation

Ligation Approach: ∑ 30µl		
Amount	**Content**	**Concentration**
7.2ml	ddH_2O	
3µl	10x T4 Ligase buffer	[10mM]
8.3µl	KNB36 cDNA	[12ng/µl]
10µl	pENTR4	[5ng/µl]
1.5µl	T4 Ligase	

- Mix up the components in the assigned order in a 1,5 ml Eppendorf tube
- Ligation at 16°C for o/n
- Use 5µl for Transformation approach (Electroporation) into Top10/Top10F´

Note: Ratio of INSERT (KNB36 cDNA):VECTOR (pENTR4) should be 2:1 (100ng:50ng)

Plasmid DNA Extraction (Miniprep Fast)

- Add an adequate amount of RNAse A to buffer P3
- transfer 2ml o/n culture into a 2ml Eppendorf tube
- centrifuge (1min/13000rpm/RT)
- discard supernatant
- resuspend pellet in 300ml buffer P1
- add 300µl buffer P2
- add 300ml buffer P3
- incubate 5min on ice
- centrifuge (10min/13.000rpm/4°C)
- transfer 850µl supernatant into a new Eppendorf tube
- add 650ml Isopropanol
- incubate 20min at -20°C
- centrifuge (25min/13.000rpm/4°C)
- remove supernatant
- wash pellet with EtOH (70%)
- wash pellet with EtOH (96%)
- dry pellet
- resuspend in 30µl ddH_2O

Note: Check possible contaminations of RNA on agarose gel (inhibit enzymes/compete on gold particles) and add additional RNAse A if clean DNA is required!

Protocol: Veerle De Wever

Plasmid DNA Extraction (Miniprep Clean)

- transfer o/n culture into Eppendorf tube
- centrifuge 10 sec
- discard supernatant (If you have more then 2 ml repeat step)
- pellet + 200µl lysis buffer
- resuspend pellet (→ " rag rattern " or vortex)
- add 400µl alakaline SDS
- invert Eppendorf tube 3x
- add 300µlNaOAc [3M]
- invert Eppendorf tube 3x (optional: incubate 5´on ice)
- centrifuge 15min full speed
- remove pellet (contains proteins, cell wall components) with toothpick
- supernatant + 600µl Isopropanol (optional: incubate 10´at -20°C)
- centrifuge 15min full speed
- discard supernatant (DNA in pellet)
- resuspend pellet in 400µl NH_4Ac [2,5M]
- add 1µl RNAse A
- 30 min RT (shake)
- centrifuge 5 min full speed
- transfer supernatant to new Eppendorf tube
- add 200µl Isopropanol
- invert Eppendorf tube
- 10 min –20°C
- centrifuge 15 min full speed (4°C) (DNA in pellet)
- carefully discard supernatant
- wash pellet 1x with pre chilled EtOH 70%
- centrifuge 5 min full speed (4°C)
- discard supernatant
- wash pellet 1x with pre chilled EtOH 96%
- centrifuge 5 min full speed (4°C)
- dry pellet (maximum 10 min)
- resuspend pellet in 30 µl ddH_2O
- store at –20°C (use 2 µl for diagnostic digests)

Precipitation of Plasmid DNA

- transfer DNA in H_2O into an Eppendorf tube
- add 3 Vol EtOH [96%]
- add 1/10 Vol NaOAc [3M]
- adjust pH to 5,2
- incubate o/n at -20°C or alternative 1 hour @ -80°C
- centrifuge (15min/13000 rpm/4°C)
- wash pellet with 70% EtOH (-20°C)
- centrifuge (5min/13000 rpm/RT) (repeat this step 2 times)
- wash pellet with 96% EtOH (-20°C)
- centrifuge 5min/13000 rpm/RT
- dry pellet
- resuspend pellet in 10-30µl ddH_2O (depends on futher use)

Protocol: Dr. Kragler

Preparation of an X% agarose gel

- Weigh Xg Agarose
- Add 100 ml 1X TAE Buffer in a glass beaker (1X TBE Buffer if analysing RNA)
- Heat up solution in a microwave oven until the agarose becomes completely dissolved
- Cool down to approximately 40 °C
- Add 5 µl Ethidium Bromide [5 mg/ml] and
- Cast solution into tray

Plasmid DNA Extraction (Midiprep)

Note: Purifications were done according to manufacturers instructions.

Production of Electro competent E.Coli Top 10 / Top 10 F´

- Prepare 2x50 ml o/n cultures (E.coli Top10/Top10F`),
- 1.5 l LB
- 0.5 l Glycerol (10%)
- 2.5 l ddH_20 (ion free water!)
- Check if centrifugation tubes are autoclaved and centrifuge is reserved
- Precool Rotor GSA or F14S
- Dilute 2x 50ml bacteria with 1200ml LB (split in 2x600ml)
- Put it on 37°C (shake) until OD600 = 0.8-1.0
- Split cultures to 6x200 ml
- Centrifuge (20min/3700rcf/4°C) (precooled rotor GSA or F14S, code 10) with SORVALL RC5C
- Wash pellet with 200ml ddH_2O
- Centrifuge (20min/3700rcf/4°C) with SORVALL RC5C
- Wash pellet with 100ml ddH_2O
- Centrifuge (20min/3700rcf/4°C) with SORVALL RC5C
- Wash pellet with 50ml ddH_2O (transfer to falcon tubes)
- Centrifuge (20min/3700rcf/4°C) with swinging bucked centrifuge
- Wash pellet with 50ml Glycerol (10%)
- Centrifuge (20min/3700rcf/4°C) with swinging bucked centrifuge
- Resuspend pellet in 1ml Glycerol (10%) (work@4°C until this step)
- Transfer 100µl aliquots to separate Eppendorf tubes
- Shock freeze with liquid N_2
- Store @ -80°C

Outcrossing of Background Mutations

- isolate the anthers of the donor plant with a foreceps (make sure that the pollen is mature →yellow)
- choose a nearly opened flower of the recipient plant
- open the blossom carefully with a foreceps
- remove the anthers and filaments of the recipient plant. (it is necessary that the carpel/stigma of the recipient plant stays intact!)
- Pollinate the stigma of the recipient plant with the pollen of the donor plant
- mark the pollinated blossom carefully

  Note: The crossing events taken place under a stereomicroscope

.

RNA Isolation from Plant Tissue

- Harvest 0.2g plant material and shockfreeze in liquid N2
- Homogenize plant material in precooled mortar
- Transfer homogenized material to E. tube
- Add 500µl RNA extraction buffer
- Add 500µl PCI (Phenol/Chloroform/Isoamylalkohol)
- Vortex & keep on ice (until sample show yellow colouring)
- Centrifuge (5min/ 13000rpm/ RT)
- Transfer supernatant to fresh prechilled (4°C) Eppendorf tube
- OPTIONAL: add 400 µl RNA extraction buffer to remaining PCI phase & vortex
- OPTIONAL: centrifuge (5min/ 13000rpm/ RT) & unify this supernatant with the first one
- Add 400 µl PCI to ~900µl sup. →vortex
- Centrifuge (5min/ 13000rpm/ 4°C)
- Transfer ~800µl supernatant into fresh Eppendorf tube
- Add 400 µl PCI to ~800µl sup. →vortex
- Centrifuge (5min/ 13000rpm/ 4°C)
- Transfer ~700µl supernatant into fresh Eppendorf tube **(Work RNAse free beyond this point!)**
- Add 1µ DNAse [2U/µl]
- Incubate 10 – 20 min @ 37°C
- Add 1/3 vol 10M LiCl
- Precipitate o/n @ 4°C
- Centrifuge (10min/ 13000rpm/ 4°C)
- Wash pellet with 2,5 M LiCl
- Centrifuge (5min/ 13000rpm/ 4°C)
- Wash pellet with 80 % EtoH (prechilled)
- Wash pellet with 96 % EtoH (prechilled)
- Dry (avoid overdrying!)
- Dissolve in 20 µl DEPC-H_2O
- Incubate 10 – 20 min @ 37°C
- Inactivate DNAse 10min @ 75°C
- Store @ -20 °C

Protocol: Allison C. Mallory, Bartel Lab Whitehead Institute

Reverse Transcriptase Reaction

- Incubate 10µl total RNA (1µg) at 65°C for 5 min to destroy RNA secondary structure
- Transfer RNA immediately to ice
- Mix it with 10µl reaction solution containing:

RT reaction mixture: ∑ 10µl		
Amount	**Content**	**Provider**
1µl	dNTP´s [10mM]	
4µl	5x AMV Reverse Transcriptase Buffer	Promega
2µl	Dithioreithol [100mM]	
0,5µl	RNAsin[40U/µl]	
0,5µl	reverse primer [10pmol]	
0,25µl	AMV Reverse Transcriptase [10U/µl]	Promega
1,75µl	ddH_2O	

- Incubate it at 42°C for 2 hours
- Add 1µl AMV Reverse Transcriptase[10U/ml]
- Incubate at 42°C for 1hour

Seed Sterilisation

- Transfer seeds into 2ml Eppendorf tube
- Add 1ml EtoH (70%)
- Remove the fluid carefully after ~2min, using a pipette
- Add 1ml Bleach mix
- Invert tube several times
- Remove the liquid carefully after 5-10min, using a pipette
- Wash the seeds with ddH_20 three times until no foam is seen
- Label the full media plates with a permanent marker
- Spread the ddH_20 including the sterilized seeds on plate using a pipette
- Sealing the plates with a stripe of Parafilm

Note: The whole process, including the preparation of solutions was done under the hood. All tools came in use were sterilized with EtoH (96%) and breamed with a Bunsen burner.

Standard, Colony and RT PCR Approach

-Standard PCR

[functional for genomic At KNB36 with FK 177/FK 178 →673bp fragment]

Standard PCR Approach: ∑ 20µl		
Amount	**Content**	**Provider**
Xµl *	template	
2µl	10X Advantage 2 PCR Buffer	Clontech
0.4µl	dNTP [10 mM]	Fermentas
1µl	Primer 1 [10 pM]	FK
1µl	Primer 2 [10 pM]	FK
Xµl	ddH2O	
0.1µl	Advantage 2 Polymerase Mix	Clontech

	Denaturation		Annealing		Extension	
Cycles	Temp	Time	Temp	Time	Temp	Time
1	95°C	1 min	-	-	-	-
5	95°C	1 min	-	-	68°C	45 sec
30	95°C	30 sec	55°C	45 sec	68°C	1 min
1	95°C	-	-	-	68°C	3 min

*For standard PCR 5 µl genomic template were used.
Note: As a Robocycler was used, so it was necessary to add mineral oil to every sample to prevent evaporation. To separate the mineral oil from the gained PCR products, the 2 phases were transferred on a piece of clean Parafilm with an adequate size. After banking the Parafilm the aqueous phase separates immediately from the oil.

-Colony PCR

[functional for At KNB36 genomic with FK 177/FK 178 →673bp fragment]

- Resuspend colony in 20µl LB
- Use 2 µl as template in PCR reaction

Colony PCR Approach: ∑ 50µl		
Amount	**Content**	**Provider**
2µl	template	
5µl	10X Advantage 2 PCR Buffer	Clontech
1µl	dNTP [10 mM]	Fermentas
2,5µl	Primer 1 [10 pM]	FK
2,5µl	Primer 2 [10 pM]	FK
36.75µl	ddH2O	
0.25µl	Advantage 2 Polymerase Mix	Clontech

	Denaturation		Annealing		Extension	
Cycles	Temp	Time	Temp	Time	Temp	Time
30	95°C	45sec	50°C	1.25 min	68°C	1 min

-RT-PCR

RT PCR Approach: ∑ 20µl		
Amount	**Content**	**Provider**
5µl	RT reaction	
2µl	10X Advantage 2 PCR Buffer	Clontech
0.4µl	dNTP [10 mM]	Fermentas
1µl	Primer 1 [10 pM]	FK
1µl	Primer 2 [10 pM]	FK
0.5µl	ddH2O	
0.1µl	Advantage 2 Polymerase Mix	Clontech

Note: Used temperature program depends on primer, product length and kind of used DNA.

Transformation of E.coli Top 10 /Top 10 F´ via Electroporation

- Transfer 2µl vector into a new Eppendorf tube
- Add 50µl electro-competent E.coli Top10
- Mix carefully by pipetting
- Transfer content into a pre cooled cuvette
- Electroporate (1,8kV/ 200Ω/25µF) time constant should be~4,5
- Add 1ml SOC
- Mix carefully by pipetting
- Transfer the content into a new Eppendorf tube
- Incubate 1hour on 37°C (shake!)
- Transfer the content on LB ^{AMP} [100µg/ml] plates (Note: use 100µl for plate pouring)
- Incubate o/n on 37°C

Transformation of E.coli Top 10 /Top 10 F´ via Heat Shock

- Prepare heat blocks to 42°C / 37°C
- Transfer 40µl chemo competent bacteria into an 1.5ml Eppendorf tube
- Add 1µ DNA
- Mix carefully with a pipet (do not pump up and down)
- Put on ice for 30 min
- Put on 42°C for 30 sec
- Put immediately back on ice
- Add 250µ SOC (should have RT!)
- Incubate for 1 hour @ 37°C for regeneration (shake)
- Use ~20µl per sample for inoculation in 5ml LB^{AB}
- Use ~100µl to spread it out on a plate

Verification Approach for MPB2C TILLING Lines MPB2C [94728]

Model for the verification of line CS94728

The point mutation and the resulting base pair exchange removesthe recognition site for the enzyme NLaIV at the position bp 366 (corresponding to the At MPB2C CDS; TAIR acc. # At5g08120).

Sup. figure: Recognition sides of Nla IV within the PCR amplified fragment of AtMPB2C

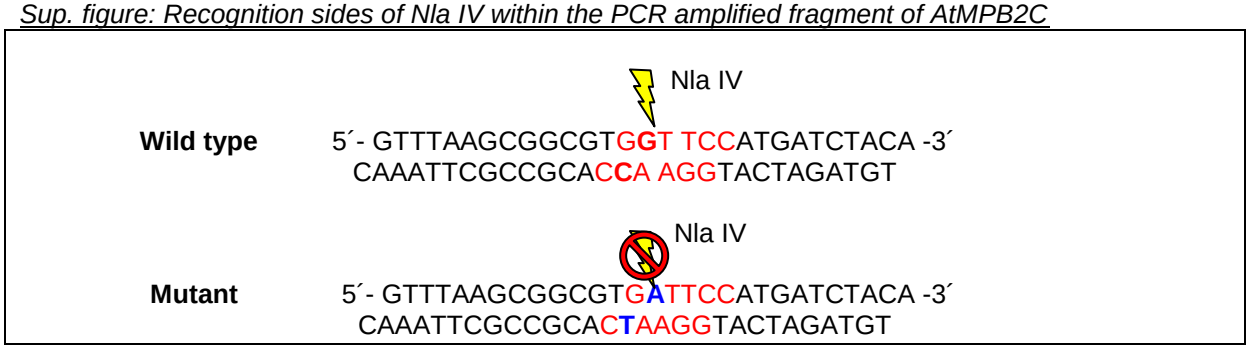

Sup. Figure: The predicted restriction pattern (NlaIV)

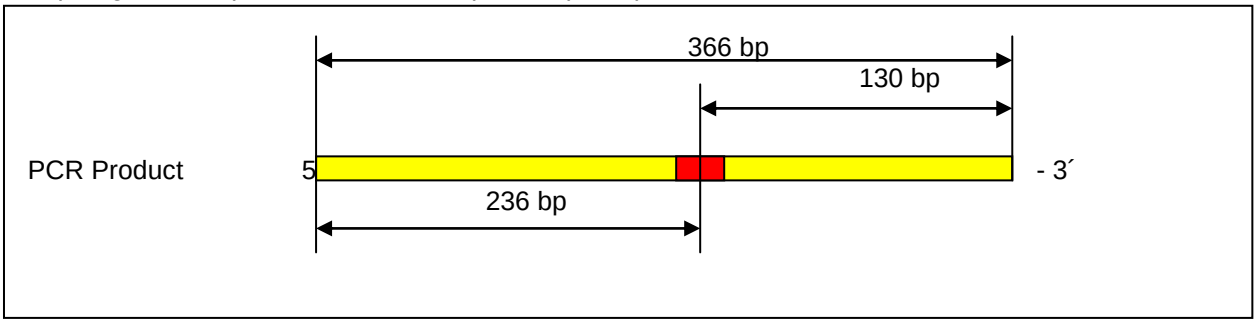

Sup. Figure: Representative figure of restricted 366bp MPB2C fragments

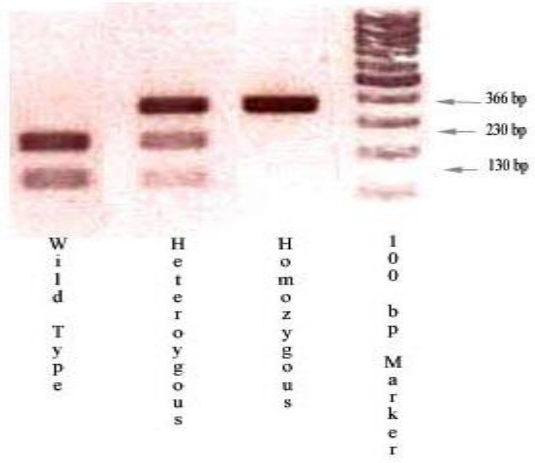

Verification Approach for MPB2C TILLING Lines MPB2C [91285]

The point mutation and the resulting base pair exchange removes the recognition site for the enzyme DdeI at the position bp 428 (corresponding to the AtMPB2C CDS; TAIR acc. # At5g08120) in a way that it makes a restriction impossible. Note that the enzyme cuts within the wild type DNA 2 times, producing a small additional fragment (48bp)

Sup. Figure: Recognition sides of DdeI within the PCR amplified fragment of At MPB2C

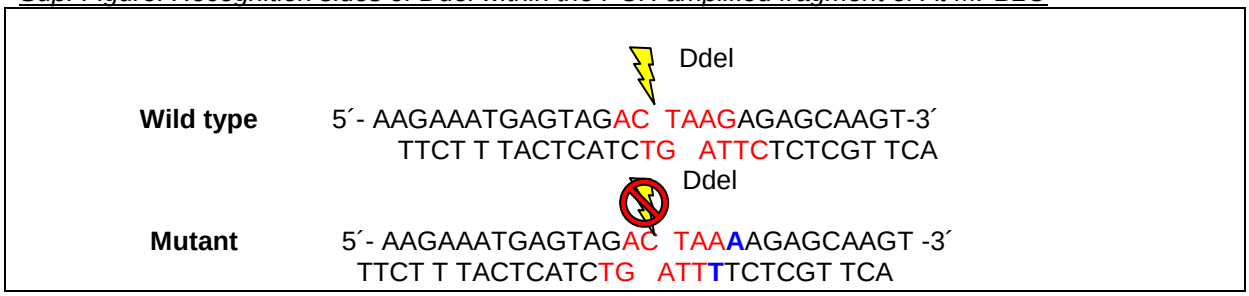

Sup. Figure: The predicted restriction pattern (DdeI)

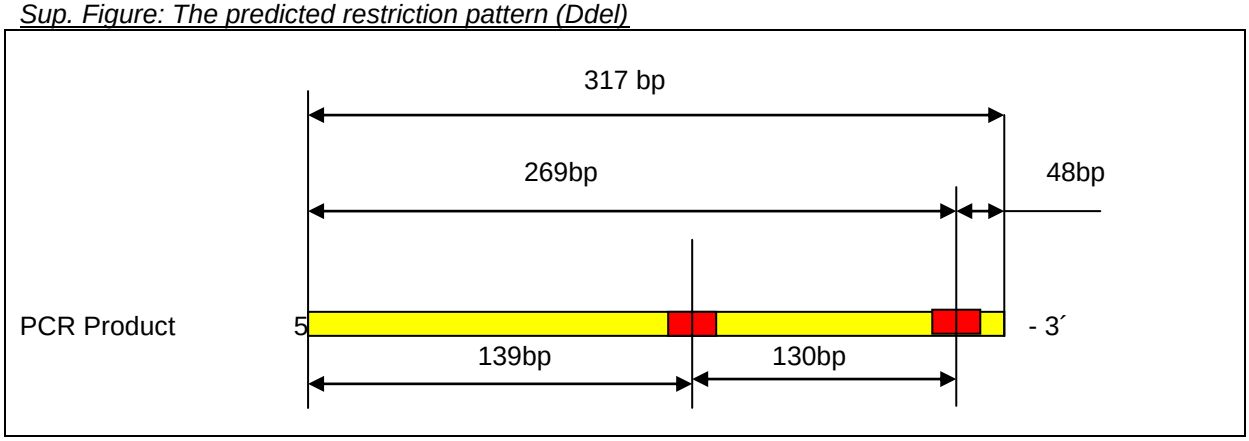

4. Antibiotics and Organisms

--Antibiotics (used concentrations)--

- KAN (Kanamycine) 1µl KAN [50µg/µl] for 1ml LB (LB^{KAN}: [50µg/ml])
- SPEC (Spectinomycine) 1µl SPEC [50µg/µl] for 1ml LB (LB^{SPEC}: [50µg/ml])
- HYG (Hygromycine) 1µl HYG [20µg/µl] for 1ml LB (LB^{HYG}: [20µg/ml])
- AMP (Ampiciline) 1µl AMP [100µg/µl] for 1ml LB (LB^{AMP}: [100µg/ml])
- BASTA (Phosphinothrizine) spray solution [200µg/ml H_2O]

--Bacteria (used strains)—

- Escherichia Coli TOP 10
- Escherichia Coli TOP 10 F`
- DB3.1
- Agrobacterium thumefaciens AGL1

--Plants (used ecotypes)--

- Arabidopsis thaliana ecotype Col0 (col0)
- Arabidopsis thaliana ecotype Wassilewskija (Ws)
- Nicotiana tabacum
- Nicotiana benthamian

5. Buffers & Solutions

(Note: All solutions have been autoclaved- exceptions are denoted!)

Bleach Mix

- 0.5ml SDS (10%), 3,8ml Bleach (from 13% Stock)
- Fill up ddH_2O ad 10ml (store@2-8°C)

Bombardment: $CaCl_2$ [2,5M] 100ml

- Dissolve 36,8g $CaCl_2$ in 100ml ddH_2O

Bombardment: Spermidine [0,1M]

- 0.5g Spermidine in 3.5ml ddH_2O
- Aliquot in 200µl parts & store at -80°C

Bombardment: Gold particles

- Dissolve 60mg in 1ml ddH_2O (stored at 4°C)

DNA Extraction Buffer

- Weigh 2.433g Tris Base (=200mM), 1.461g NaCl (=250mM), 0.936g EDTA (=25mM), 0.5g SDS (=0.5%)
- Dissolve in ddH_2O ad 100ml
- Adjust pH to 8.8 (store@RT)

Full media plates (plants) 1000ml

- Mix um 4g MS B5, 1g Succrose, 0.5g MES and dilute it with dH_2O
- Adjust pH to 7.5 with KOH
- For production of plates add 6g plantager/l to a 1l glass bottle
- Transfer the solution into the glass bottle (RT: does not dissolve completly!)
- Fill up dH_2O ad 1000ml

LB-Medium (Bacteria) 1000ml

- Weigh 10g Bacto-typtone, 5g Yeast extract, 5g NaCl
- Dissolve in ddH_2O ad 1000ml (store@RT)

Miniprep clean: **Lysis Buffer** 10ml

- Mix up 2ml glucose [5%], 2ml EDTA [50mM], 0,25ml Tris-base [1M] pH8 and 5,75ddH_2O

Miniprep clean: **Glucose [5%]** 100ml

- Weigh 5g Glucose
- Fill up ddH_2O ad 100ml

Miniprep clean: **Tris-Cl [1M]** 1000ml

- Weight 121.14g Tris-base
- Dilute in 500ml ddH_2O
- Adjust pH to 8 with HCL
- Fill up H_2O to 1000ml

Miniprep clean: **NH4Ac [2,5M]** 100ml

- Weigh 19.27g NH_4Ac and dilute in 100ml ddH_2O

Miniprep clean: **Alkaline SDS** 10ml

- Mix up 7ml ddH_2O with 2ml 1N NaOH and 1ml 10 % SDS
  Note: should be prepared fresh before using!

Miniprep clean: **NaOH [1N]** 100ml

- Weigh 4g NaOH and dilute in 100 ml ddH_2O

Miniprep clean: **SDS (10%)** 100ml

- Weigh 10g SDS
- Fill up ddH_2O ad 100ml

Miniprep fast: **resuspension buffer P1** 100ml

- Weigh 0.6gTris-base (=50mM) and 3.72g EDTA (=10mM)
- Dissolve in ~70ml ddH_2O
- Adjust pH to 8.0 with HCL
- Fill up ddH_2O ad 100ml (store@2-8°C)

Miniprep fast: **lysis buffer P2** 100ml

- Weigh 7.99g NaOH (=200mM) and 1g SDS (1%)
- Fill up H_2O ad 100ml (store@RT)

Miniprep fast: **neutralisation buffer P3** 100ml

- Weigh 29.44g CH_3COOK (=3M)
- Dissolve in ~70ml H_2O
- Adjust pH to 5.5
- Fill up H_2O ad 100ml (store@2-8°C/RT)

NaCl [0.4M] 100ml

- Weigh 2,34g NaCl
- Fill up ddH_2O ad 100ml
-

RNA Extraction Buffer 2.2ml (all components RNAse free!!!)

- Mix 1000µl NaOAc [3M], 1000µl SDS (10%) and 200µl EDTA [0,5M]
  Prepare it **always fresh**, use only DEPC-ddH2O and do not autoclave solution!

RNA Extraction: **SDS (10%)** 100ml

- Weigh 10g SDS
- Fill up DEPC-ddH_2O ad 100ml

RNA Extraction : **EDTA [0.5M]** 100ml

- Weigh 18.61g EDTA
- Fill up DEPC-ddH_2O ad 100ml

RNA Extraction: **DEPC-H2O** (RNAse free water)

- 1ml DEPC in 1000ml ddH_2O (o/n @RT)
- Autoclave twice!! DEPC will be heatinactivated

RNA Extraction: **NaOAc [3M]** 100ml

- Dissolve 40,8g NaOAc in 40ml DEPC-ddH2O
- Adjust pH to 4,8-5,2
- Add H_2O ad 100ml

RNA Extraction: **LiCl [2,5M]** 10ml

- 1.059g in 10ml DEPC-ddH_2O

RNA Extraction: **LiCl [10M]** 10ml

- 4,239g in 10ml DEPC-ddH_2O

SOB Medium (1000ml)

- Weigh 20g Bacto-tryptone, 5g Yeast extract, 0.588g NaCl and 0.186g KCl
- Dissolve in 500ml ddH2O
- Adjust pH to 7.0 with NaOH
- Fill up H2O ad 1000ml (store@4°C)

SOC Medium (100ml)

- Mix 98ml SOB with 1ml Mg stock [2M] and 1ml Glucose D(+) Monohydrate [2M] (store@4°C)

SOC: **Mg stock [2M]** 100ml

- Weigh 20.33g $MgCl_2.6H_2O$ and 24.65g $MgSO_4.7H_2O$
- Dissolve in ddH_2O ad 100ml

SOC: **Glucose [2M]** 100ml

- Weigh 39.63g Glucose D(+) Monohydrate
- Dissolve in ddH_2O ad 100ml

Staining: **X-Gluc [20mM]** ~10ml

- Weigh 100mg X-Gluc substrate
- Dissolve in 9,6 ml DMF or DMSO to obtain a 20mM stock (10.42mg/ml) (store@-20°C)

Staining: **Sodium Phospate Buffer [1M]** 250ml

- Weigh 34.50g Na_2HPO_4
- Dissolve in 200ml ddH_2O
- Adjust pH to 7.0 (Preferably with a 1M monobasic sodium phosphate solution)
- Add ddH_2O to 250ml end volume (store@RT)

Staining**: Triton-X100 (10%)** 50ml

- Dilute 5ml Triton-X100 (100%) in 45ml ddH_2O (store@RT)

Staining: **Na_2EDTA [0,5M]** 500ml

- Weigh 93.06g Na_2EDTA
- Dissolve in 400ml ddH_2O
- Adjust pH with NaOH to 8.0
- Fill up ddH_2O ad 500ml

Staining: **$K_4Fe(CN)_6$ [100mM] / [5mM]** 100ml

- Weigh 4.2241g $K_4Fe(CN)_{6.}3H_2O$
- Dissolve in 100ml ddH_2O to obtain a 100mM stock solution (store@4°C)
- Dilute 5ml of the 100mM stock in 95ml ddH_2O to obtain a 5mM solution (store@4°C)

Do not autoclave!

Staining: **$K_3Fe(CN)_6$ [100mM]** 100ml

- Weigh 3.2926g $K_3Fe(CN)_{6.}3H_2O$
- Dissolve in 100ml ddH_2O to obtain a 100mM stock solution (store@4°C)

Do not autoclave!

Staining: **Paraformaldehyd (10%)** 500ml

- Weigh 5g Paraformaldehyd
- Dilute in 500ml Pipes Buffer (Heat the solution during solution process to 70°C (Hood!!)
- Add some drops of NaOH[1M] to boost solubility.
- Adjust pH to 6.8

TAE 50X Buffer 1000ml

- Weigh 242g Tris-base
- Dissolve in a mix of 57.1ml Glacial Acetic Acid and 100ml EDTA [0.5M]
- Adjust pH to 8.5
- Fill up H_2O ad 1000ml (store@RT)

TAE 1X Buffer 20 l

- Mix 400ml TAE 50X Buffer with 19,6 l dH_2O (store@RT)

TBE 1X Buffer 1000ml

- Weigh 108g Tris-base, 9.3g EDTA and 55g H_3BO_3
- Dissolve in 500ml ddH_2O
- Adjust pH to 8,5
- Fill up H_2O ad 1000ml (store@RT)

6. Chemicals

Chemical/Material	Supplier
1,5ml Polypropylene tubes	Eppendorf
100bp DNA Ladder	Fermentas
10kb DNA Ladder	Fermentas
10x T4 Ligase buffer	New England Biolabs
15 ml Tube	Falcon
1kb DNA Ladder	New England Biolabs
24 well microtiterplate	NUNC
2ml Polypropylene tubes	Eppendorf
2-propanol (Isopropanol)	J.T.Baker
5x AMV Reverse Transcriptase Buffer	Promega
5x LR Clonase reaction buffer	Invitrogen
6 well mirotiterplate	NUNC
6X Loading Dye Solution	Fermentas
Acetaldehyd	SIGMA
Acetic Acid	J.T.Baker
Acetone	J.T.Baker
Acrolein	Fluka
Acrolein (M=56.06g/M)	Sigma Aldrich
Agarose	Biozym
Ampiciline	Sigma
AMV Reverse Transcriptase [10U/µl]	Promega
BASTA	Raiffeisen Warehouse
Bleach (Hypochlorid)	Colgate-palmolive
BstEII DNA Ladder	Fermentas
Buffered & water saturated Phenol	Sigma
CaCl2 (Calziumchlorid-2-hydrat) [M=147.2g/M]	Riedel - de Häen
Centrifuge (max 16.1 rcf)	Eppendorf
Centrifuge RC5C (max 20000 rpm)	SORVAL
CH3COOK (Potassium Acetate) [M=98.15g/mol]	Riedel-de Häen
Chloral Hydrate (2,2,2-trichloroethane-1,1-diol) [M=165.5g/M]	AppliChem
Chloroform	Sigma
Cuvette	J.T.Baker
DEPC (Diethylpyrocarbonate)	Sigma
DMF (Diethylformamid)	AppliChem
DMSO (Dimethylsulfoxide)	Merck
DNAse	Ambion
dNTP´s [10 mM]	Fermentas
DTT (Dithioreithol) [100mM]	Scharlau
EDTA (Ethylendiamin tetraacetic acid) [M=372.24g/M]	AppliChem
EGTA [M=380.35g/M]	Sigma
Enzyme Buffer Tango (yellow)	Fermentas
Enzyme DdeI [10U]	Fermentas
Enzyme NLaIV [10U]	Fermentas
Ethidium Bromide	Sigma
EtOH (Ethanol) 96%	J.T.Baker
EtOH (Ethanol) 99%	J.T.Baker
Formaldehyd [M=30.03g/M]	Sigma
Gel Extraction Kit	Sigma
Generuler 100bp DNA Ladder	Fermentas
Glucose D(+) Monohydrate [M=198.17g/M)	Fermentas
Glutaraldehyd	AppliChem
Glycerol (99%)	Riedel - de Häen

Gold particles (1µm; store@RT)	BIORAD
HCl (Hydrochlorid Acid)	J.T.Baker
Hygromycin	Sigma
$K_3[Fe(CN_)_6].3H2O$ (Kaliumhexacyanoferrat(III)) [M=329.26]	Merck
$K_4[Fe(CN)_6].3H2O$ (Kaliumhexacyanoferrat(II) Trihydrat) [M=422.41]	Merck
Kanamycin	Sigma
KCl (Kaliumcloride) [M=74.56g/M]	Merck
KOH (Potassiumhydroxide) [M=56,11g/M]	Merck
L77 Silwet	Lehle Seeds
Lactic Acid (2-hydroxypropanoic acid) [M=90.08g/M]	Merck
LiCl (Lithium cloride anhydrous) [M=42.39g/M]	Fluka
Loading Discs (Bombardment)	BIORAD
LR Clonase	Invitrogen
Macrocarrier (Bombardment)	BIORAD
MES(morpholino ethane sulfonic acid) [M=213g/M]	Sigma
$MgCl_2.6H2O$ (Magnesiumdicloride Hexahydate (M=203.31g/M]	Riedel - de Häen
$MgSO_4$ (Magnesium sulfate) [120.36g/M]	Riedel - de Häen
$MgSO_4.7H2O$ (Magnesium sulfate heptahydrate [M=246.48g/M]	Riedel - de Häen
MS (Murashige and Skook salt)	Duchefa Biochemie
Na_2EDTA (Disodium Ethylendiamin tetraacetic acid) [M=372.24g/M]	Riedel-de Häen
Na_2HPO_4 (Disodium hydrogen phosphate) [M=141.96g/M]	Riedel-de Häen
NaCl (Natriumchloride) [M=58,44g/M]	Riedel - de Häen
NaOAc	Sigma
NaOH (Sodium Hydorxide) [M=39.997g/M]	Riedel - de Häen
NH_4Ac (Ammoniumacetate) [M=77.08g/M]	Merck
Parafilm	Pechiney
PCI (Phenol/Chloroform/Isoamylalcohol)	AppliChem
PCR: Robocycler 40	Stratagene
PCR: Robocycler Gradient 96	Stratagene
Phenol (water saturated)	AppliChem
Phytagel	SIGMA
PIPES (Piperazine-N,N´- bis(2-etanesulfonic acid) [M=346.3g/M]	Sigma
Protein Kinase A	Invitrogen
RNAse A	Roche
RNAsin [40U/µl]	Promega
Rotor F14-6x250g)	Fiberlite
Rupture Discs 450 psi (Bombardment)	BIORAD
Safranin O	Sigma
SDS (Sodium Dodecyl Sulfate) (M=288.4g/M)	QIAEX II
Spectinomycin	SIGMA
Spermidine	BIORAD
Stopping Screen (Bombardment)	BIORAD
Succrose [M=342,3g/M]	GERBU
T4 Ligase	New England Biolabs
Taq Advantage 2 PCR Buffer10X	BD Clontech
Taq Advantage 2 Polymerase Mix	BD Clontech
Technovit 7100	Heraeus, Kulzer
Tris-base (Tris(hydroxymethyl)-aminomethan) [M=121.14g/M]	AppliChem
Triton-X100	Serva
Tween 20	Sigma
X-gluc(5-bromo-4-chloro-3-indolyl-ß-glucuronic acid) [M=521.8g/M]	Fermentas

References

1. Ananda K. Sarkar, Marijn Luijten, Shunsuke Miyashima3, Michael Lenhard, Takashi Hashimoto, Keiji Nakajima3, Ben Scheres2, Renze Heidstra2 & Thomas Laux.(2007). Conserved factors regulate signalling in Arabidopsis thaliana shoot and root stem cell organizers. Nature 411:414-446
2. Aoki, K., Kragler, F., Xoconostle-Cazares, B., and Lucas, W.J. (2002). A subclass of plant heat shock cognate 70 chaperones carries a motif that facilitates trafficking through plasmodesmata. Proc Natl Acad Sci U S A 99, 16342-16347.
3. Baluska, F., Cvrckova, F., Kendrick-Jones, J., and Volkmann, D. (2001). Sink plasmodesmata as gateways for phloem unloading. Myosin VIII and calreticulin as molecular determinants of sink strength? Plant Physiol 126, 39-46.
4. Baluska, F., Samaj, J., Napier, R., and Volkmann, D. (1999). Maize calreticulin localizes preferentially to plasmodesmata in root apex. Plant J 19, 481-488.
5. Bellaoui, M., Pidkowich, M.S., Samach, A., Kushalappa, K., Kohalmi, S.E., Modrusan, Z., Crosby, W.L., and Haughn, G.W. (2001). The Arabidopsis BELL1 and KNOX TALE homeodomain proteins interact through a domain conserved between plants and animals. Plant Cell 13, 2455-2470.
6. Bhatt, A.M., Etchells, J.P., Canales, C., Lagodienko, A., and Dickinson, H. (2004). VAAMANA--a BEL1-like homeodomain protein, interacts with KNOX proteins BP and STM and regulates inflorescence stem growth in Arabidopsis. Gene 328, 103-111.
7. Blackman, L.M., Harper, J.D., and Overall, R.L. (1999). Localization of a centrin-like protein to higher plant plasmodesmata. Eur J Cell Biol 78, 297-304.
8. Botha CEJ, Hartley BJ, Cross RHM. (1993). The ultrastructure and computer-enhanced digital image analysis of plasmodesmata at the Kranz mesophyll-bundle sheath interface of Themeda triandra var. imberbis (Retz) A. Camus in conventionally-fixed leaf blades. Ann. Bot. 72:255–61
9. Botha, C.E., and Cross, R.H. (2000). Towards reconciliation of structure with function in plasmodesmata-who is the gatekeeper? Micron 31, 713-721.
10. Brand, U., Fletcher, J.C., Hobe, M., Meyerowitz, E.M., and Simon, R. (2000). Dependence of stem cell fate in Arabidopsis on a feedback loop regulated by CLV3 activity. Science 289, 617-619.
11. Brand, U., Grunewald, M., Hobe, M., and Simon, R. (2002). Regulation of CLV3 expression by two homeobox genes in Arabidopsis. Plant Physiol 129, 565-575.
12. Burglin, T.R. (1997). Analysis of TALE superclass homeobox genes (MEIS, PBC, KNOX, Iroquois, TGIF) reveals a novel domain conserved between plants and animals. Nucleic Acids Res 25, 4173-4180.
13. Byrne, M.E., Groover, A.T., Fontana, J.R., and Martienssen, R.A. (2003). Phyllotactic pattern and stem cell fate are determined by the Arabidopsis homeobox gene BELLRINGER. Development 130, 3941-3950.
14. Chan, R.L., Gago, G.M., Palena, C.M., and Gonzalez, D.H. (1998). Homeoboxes in plant development. Biochim Biophys Acta 1442, 1-19.

15. Chen, H., Banerjee, A.K., and Hannapel, D.J. (2004). The tandem complex of BEL and KNOX partners is required for transcriptional repression of ga20ox1. Plant J 38, 276-284.
16. Citovsky, V., Knorr, D., Schuster, G., and Zambryski, P. (1990). The P30 movement protein of tobacco mosaic virus is a single-strand nucleic acid binding protein. Cell 60, 637-647.
17. Citovsky, V., Wong, M.L., Shaw, A.L., Prasad, B.V., and Zambryski, P. (1992). Visualization and characterization of tobacco mosaic virus movement protein binding to single-stranded nucleic acids. Plant Cell 4, 397-411.
18. Clark, S.E., Jacobsen, S.E., Levin, J.Z., and Meyerowitz, E.M. (1996). The CLAVATA and SHOOT MERISTEMLESS loci competitively regulate meristem activity in Arabidopsis. Development 122, 1567-1575.
19. Clark, S.E., Running, M.P., and Meyerowitz, E.M. (1993). CLAVATA1, a regulator of meristem and flower development in Arabidopsis. Development 119, 397-418.
20. Clark, S.E., Williams, R.W., and Meyerowitz, E.M. (1997). The CLAVATA1 gene encodes a putative receptor kinase that controls shoot and floral meristem size in Arabidopsis. Cell 89, 575-585.
21. Comai, L., and Henikoff, S. (2006). TILLING: practical single-nucleotide mutation discovery. Plant J 45, 684-694.
22. Cooper, B., Hutchison, D., Park, S., Guimil, S., Luginbuhl, P., Ellero, C., Goff, S.A., and Glazebrook, J. (2003). Identification of rice (Oryza sativa) proteins linked to the cyclin-mediated regulation of the cell cycle. Plant Mol Biol 53, 273-279.
23. Crawford, K.M., and Zambryski, P.C. (2000). Subcellular localization determines the availability of non-targeted proteins to plasmodesmatal transport. Curr Biol 10, 1032-1040.
24. Curtis, M.D., and Grossniklaus, U. (2003). A gateway cloning vector set for high-throughput functional analysis of genes in planta. Plant Physiol 133, 462-469.
25. Deom, C.M., Lapidot, M., and Beachy, R.N. (1992). Plant virus movement proteins. Cell 69, 221-224.
26. Ding B, Kwon MO, Warnberg L. (1996). Evidence that actin ®laments are involved in controlling the permeability of plasmodesmata in tobacco mesophyll. Plant Journal 10: 157-164.
27. Ding B, Lucas WJ. (1996). Secondary plasmodesmata: biogenesis, special functions and evolution. In: Smallwood M, Knox JP, Bowles DJ, eds, Membranes: specialized functions in plants. Oxford: BIOS Scienti®c Publishers, 489-506.
28. Ding, B., Haudenshield, J.S., Hull, R.J., Wolf, S., Beachy, R.N., and Lucas, W.J. (1992). Secondary plasmodesmata are specific sites of localization of the tobacco mosaic virus movement protein in transgenic tobacco plants. Plant Cell 4, 915-928.
29. Dolan, L., Janmaat, K., Willemsen, V., Linstead, P., Poethig, S., Roberts, K., and Scheres, B. (1993). Cellular organisation of the Arabidopsis thaliana root. Development 119, 71-84.
30. Earley, K.W., Haag, J.R., Pontes, O., Opper, K., Juehne, T., Song, K., and Pikaard, C.S. (2006). Gateway-compatible vectors for plant functional genomics and proteomics. Plant J 45, 616-629.
31. Gehring, W.J., Affolter, M., and Burglin, T. (1994). Homeodomain proteins. Annu Rev Biochem 63, 487-526.

32. Gerdes, H.H., Bukoreshtliev, N.V., and Barroso, J.F. (2007). Tunneling nanotubes: a new route for the exchange of components between animal cells. FEBS Lett 581, 2194-2201.
33. Gisel, A., Hempel, F.D., Barella, S., and Zambryski, P. (2002). Leaf-to-shoot apex movement of symplastic tracer is restricted coincident with flowering in Arabidopsis. Proc Natl Acad Sci U S A 99, 1713-1717.
34. Hackbusch, J., Richter, K., Muller, J., Salamini, F., and Uhrig, J.F. (2005). A central role of Arabidopsis thaliana ovate family proteins in networking and subcellular localization of 3-aa loop extension homeodomain proteins. Proc Natl Acad Sci U S A 102, 4908-4912.
35. Haywood, V., Kragler, F., and Lucas, W.J. (2002). Plasmodesmata: pathways for protein and ribonucleoprotein signaling. Plant Cell 14 Suppl, S303-325.
36. Heinlein, M., and Epel, B.L. (2004). Macromolecular transport and signaling through plasmodesmata. Int Rev Cytol 235, 93-164.
37. Heinlein, M., Padgett, H.S., Gens, J.S., Pickard, B.G., Casper, S.J., Epel, B.L., and Beachy, R.N. (1998). Changing patterns of localization of the tobacco mosaic virus movement protein and replicase to the endoplasmic reticulum and microtubules during infection. Plant Cell 10, 1107-1120.
38. Henikoff, S., Till, B.J., and Comai, L. (2004). TILLING. Traditional mutagenesis meets functional genomics. Plant Physiol 135, 630-636.
39. Hepler P. (1982). Endoplasmic reticulum in theformation of the cell plate and plasmodesmata. Protoplasma 111:121–33
40. Itaya A, Hickman H, Bao Y, Nelson R, Ding B. (1997). Cell-to-cell trafficking of cucumber mosaic virus movement protein:green fluorescent protein fusion produced by biolistic gene bombardment in tobacco. Plant J. 12:1223–30
41. Jasinski, S., Piazza, P., Craft, J., Hay, A., Woolley, L., Rieu, I., Phillips, A., Hedden, P., and Tsiantis, M. (2005). KNOX action in Arabidopsis is mediated by coordinate regulation of cytokinin and gibberellin activities. Curr Biol 15, 1560-1565.
42. Jones, M.G.K. (1976). The origin and development of plasmodesmata. lntercellular Communication in Plants: Studies on Plasmodesmata, B.E.S. Gunning and A.W. Robards, eds (New York: Springer-Verlag), pp. 81-105.
43. Karimi, M., Inze, D., and Depicker, A. (2002). GATEWAY vectors for Agrobacterium-mediated plant transformation. Trends Plant Sci 7, 193-195.
44. Kayes, J.M., and Clark, S.E. (1998). CLAVATA2, a regulator of meristem and organ development in Arabidopsis. Development 125, 3843-3851.
45. Kerstetter, R., Vollbrecht, E., Lowe, B., Veit, B., Yamaguchi, J., and Hake, S. (1994). Sequence analysis and expression patterns divide the maize knotted1-like homeobox genes into two classes. Plant Cell 6, 1877-1887.
46. Kim, I., Kobayashi, K., Cho, E., and Zambryski, P.C. (2005b). Subdomains for transport via plasmodesmata corresponding to the apical-basal axis are established during Arabidopsis embryogenesis. Proc Natl Acad Sci U S A 102, 11945-11950.
47. Kim, J.Y. (2005). Regulation of short-distance transport of RNA and protein. Curr Opin Plant Biol 8, 45-52.
48. Kim, J.Y., Rim, Y., Wang, J., and Jackson, D. (2005a). A novel cell-to-cell trafficking assay indicates that the KNOX homeodomain is necessary and sufficient for intercellular protein and mRNA trafficking. Genes Dev 19, 788-793.
49. Kragler F. (1998a). Plasmodesmata: Dynamics, Domains and Patterning. Annals of Botany 81: 1-10

50. Kragler F. (1998b). Cell-to-cell transport of proteins: requirement for unfolding and characterization of binding to a putative plasmodesmal receptor
51. Kragler, F., Curin, M., Trutnyeva, K., Gansch, A., and Waigmann, E. (2003). MPB2C, a microtubule-associated plant protein binds to and interferes with cell-to-cell transport of tobacco mosaic virus movement protein. Plant Physiol 132, 1870-1883.
52. Kragler, F., Monzer, J., Xoconostle-Cazares, B., and Lucas, W.J. (2000). Peptide antagonists of the plasmodesmal macromolecular trafficking pathway. Embo J 19, 2856-2868.
53. Lachaud S, Maurousset L. (1996). Occurrence of plasmodesmata between differentiating vessels and other xylem cells in Sorbus torminalis L. Crantz and their fate during xylem maturation. Protoplasma 191:220-226.
54. Larkin, J.C., Oppenheimer, D.G., Pollock, S., and Marks, M.D. (1993). Arabidopsis GLABROUS1 Gene Requires Downstream Sequences for Function. Plant Cell 5, 1739-1748.
55. Laux, T., Mayer, K.F., Berger, J., and Jurgens, G. (1996). The WUSCHEL gene is required for shoot and floral meristem integrity in Arabidopsis. Development 122, 87-96.
56. Lee, J.Y., Taoka, K., Yoo, B.C., Ben-Nissan, G., Kim, D.J., and Lucas, W.J. (2005). Plasmodesmal-associated protein kinase in tobacco and Arabidopsis recognizes a subset of non-cell-autonomous proteins. Plant Cell 17, 2817-2831.
57. Lewis, E.B. (1978). A gene complex controlling segmentation in Drosophila. Nature 276, 565-570.
58. Liu, J., Van Eck, J., Cong, B., and Tanksley, S.D. (2002). A new class of regulatory genes underlying the cause of pear-shaped tomato fruit. Proc Natl Acad Sci U S A 99, 13302-13306.
59. Liu, L., White, M.J., and MacRae, T.H. (1999). Transcription factors and their genes in higher plants functional domains, evolution and regulation. Eur J Biochem 262, 247-257.
60. Long, J.A., Moan, E.I., Medford, J.I., and Barton, M.K. (1996). A member of the KNOTTED class of homeodomain proteins encoded by the STM gene of Arabidopsis. Nature 379, 66-69.
61. Lucas WJ, Ding B, Van Der Schoot C. (1993). Tansley Review No. 58: Plasmodesmata and the supracellular nature of plants. New Phytol. 125:435–76
62. Lucas, W.J., and Wolf, S. (1993). Plasmodesmata: the intercellular organelles of green plants. Trends Cell Biol 3, 308-315.
63. Lucas, W.J., Bouche-Pillon, S., Jackson, D.P., Nguyen, L., Baker, L., Ding, B., and Hake, S. (1995). Selective trafficking of KNOTTED1 homeodomain protein and its mRNA through plasmodesmata. Science 270, 1980-1983.
64. Lucas, W.J., Yoo, B.C., and Kragler, F. (2001). RNA as a long-distance information macromolecule in plants. Nat Rev Mol Cell Biol 2, 849-857.
65. Magnani, E., and Hake, S. (2008). KNOX lost the OX: the Arabidopsis KNATM gene defines a novel class of KNOX transcriptional regulators missing the homeodomain. Plant Cell 20, 875-887.
66. Mese, G., Richard, G., and White, T.W. (2007). Gap junctions: basic structure and function. J Invest Dermatol 127, 2516-2524.
67. Oparka KJ, Duckett CM, Prior DAM, Fisher DB. (1994). Real-time imaging of phloem unloading in the root tip of Arabidopsis. Plant J. 6:759–66

68. Oparka, K.J. (2004). Getting the message across: how do plant cells exchange macromolecular complexes? Trends Plant Sci 9, 33-41.
69. Oparka, K.J., Roberts, A.G., Boevink, P., Santa Cruz, S., Roberts, I., Pradel, K.S., Imlau, A., Kotlizky, G., Sauer, N., and Epel, B. (1999). Simple, but not branched, plasmodesmata allow the nonspecific trafficking of proteins in developing tobacco leaves. Cell 97, 743-754.
70. Oppenheimer, D.G., Herman, P.L., Sivakumaran, S., Esch, J., and Marks, M.D. (1991). A myb gene required for leaf trichome differentiation in Arabidopsis is expressed in stipules. Cell 67, 483-493.
71. Overall RL, Blackman LM. (1996). A model of the macromolecular structure of plasmodesmata. Trends Plant Sci. 1:307–11
72. Reichelt, S., Knight, A.E., Hodge, T.P., Baluska, F., Samaj, J., Volkmann, D., and Kendrick-Jones, J. (1999). Characterization of the unconventional myosin VIII in plant cells and its localization at the post-cytokinetic cell wall. Plant J 19, 555-567.
73. Reiser, L., Modrusan, Z., Margossian, L., Samach, A., Ohad, N., Haughn, G.W., and Fischer, R.L. (1995). The BELL1 gene encodes a homeodomain protein involved in pattern formation in the Arabidopsis ovule primordium. Cell 83, 735-742.
74. Reiser, L., Sanchez-Baracaldo, P., and Hake, S. (2000). Knots in the family tree: evolutionary relationships and functions of knox homeobox genes. Plant Mol Biol 42, 151-166.
75. Revel, J.P., and Karnovsky, M.J. (1967). Hexagonal array of subunits in intercellular junctions of the mouse heart and liver. J Cell Biol 33, C7-C12.
76. Robards AW. (1968). A new interpretation of plasmodesmatal ultrastructure. Protoplasma 72:315–23
77. Robertson, J.D. (1963). The Occurrence Of A Subunit Pattern In The Unit Membranes Of Club Endings In Mauthner Cell Synapses In Goldfish Brains. J Cell Biol 19, 201-221.
78. Ruiz-Medrano, R., Xoconostle-Cazares, B., and Kragler, F. (2004). The plasmodesmatal transport pathway for homeotic proteins, silencing signals and viruses. Curr Opin Plant Biol 7, 641-650.
79. Rustom, A., Saffrich, R., Markovic, I., Walther, P., and Gerdes, H.H. (2004). Nanotubular highways for intercellular organelle transport. Science 303, 1007-1010.
80. Scarpella, E., Francis, P., and Berleth, T. (2004). Stage-specific markers define early steps of procambium development in Arabidopsis leaves and correlate termination of vein formation with mesophyll differentiation. Development 131, 3445-3455.
81. Schoof, H., Lenhard, M., Haecker, A., Mayer, K.F., Jurgens, G., and Laux, T. (2000). The stem cell population of Arabidopsis shoot meristems in maintained by a regulatory loop between the CLAVATA and WUSCHEL genes. Cell 100, 635-644.
82. Scofield, S., Dewitte, W., and Murray, J.A. (2007). The KNOX gene SHOOT MERISTEMLESS is required for the development of reproductive meristematic tissues in Arabidopsis. Plant J 50, 767-781.
83. Serikawa, K.A., Martinez-Laborda, A., and Zambryski, P. (1996). Three knotted1-like homeobox genes in Arabidopsis. Plant Mol Biol 32, 673-683.
84. Smith, H.M., Boschke, I., and Hake, S. (2002). Selective interaction of plant homeodomain proteins mediates high DNA-binding affinity. Proc Natl Acad Sci U S A 99, 9579-9584.

85. Smith, H.M., Campbell, B.C., and Hake, S. (2004). Competence to respond to floral inductive signals requires the homeobox genes PENNYWISE and POUND-FOOLISH. Curr Biol 14, 812-817.
86. Somerville, C.R and Meyerowith, E.M. (2003).The Arabidopsis Book. American Society fo Plant Biologiests, Rockville, DOI 10.1199/tab.9999.
87. Stadler, R., Lauterbach, C., and Sauer, N. (2005). Cell-to-cell movement of green fluorescent protein reveals post-phloem transport in the outer integument and identifies symplastic domains in Arabidopsis seeds and embryos. Plant Physiol 139, 701-712.
88. Steeves, T.A., and Sussex, I.M. (1989). Patterns in Plant Development (Cambridge, MA: Cambridge University Press).
89. The Plant Journal 15(3): 367-381
90. Till, B.J., Colbert, T., Codomo, C., Enns, L., Johnson, J., Reynolds, S.H., Henikoff, J.G., Greene, E.A., Steine, M.N., Comai, L., and Henikoff, S. (2006). High-throughput TILLING for Arabidopsis. Methods Mol Biol 323, 127-135.
91. Till, B.J., Colbert, T., Tompa, R., Enns, L.C., Codomo, C.A., Johnson, J.E., Reynolds, S.H., Henikoff, J.G., Greene, E.A., Steine, M.N., Comai, L., and Henikoff, S. (2003). High-throughput TILLING for functional genomics. Methods Mol Biol 236, 205-220.
92. Till, B.J., Reynolds, S.H., Greene, E.A., Codomo, C.A., Enns, L.C., Johnson, J.E., Burtner, C., Odden, A.R., Young, K., Taylor, N.E., Henikoff, J.G., Comai, L., and Henikoff, S. (2003b). Large-scale discovery of induced point mutations with high-throughput TILLING. Genome Res 13, 524-530.
93. Turner, A., Wells, B., and Roberts, K. (1994). Plasmodesmata of maize root tips: structure and composition. J Cell Sci 107 (Pt 12), 3351-3361.
94. Vitha, S., Benes, K., Phillips, J.P., and Gartland, K.M. (1995). Histochemical GUS analysis. Methods Mol Biol 44, 185-193.
95. Vollbrecht, E., Veit, B., Sinha, N., and Hake, S. (1991). The developmental gene Knotted-1 is a member of a maize homeobox gene family. Nature 350, 241-243.
96. Waigmann, E., and Zambryski, P. (1994). Plasmodesmata. Gateways for rapid information transfer. Curr Biol 4, 713-716.
97. Waigmann, E., Lucas, W.J., Citovsky, V., and Zambryski, P. (1994). Direct functional assay for tobacco mosaic virus cell-to-cell movement protein and identification of a domain involved in increasing plasmodesmal permeability. Proc Natl Acad Sci U S A 91, 1433-1437.
98. White RG, Badelt K,Overall RL,Vesk M. (1994). Actin associated with plasmodesmata. Protoplasma 180:169–84
99. Winter, N., Kollwig, G., Zhang, S., and Kragler, F. (2007). MPB2C, a Microtubule-Associated Protein, Regulates Non-Cell-Autonomy of the Homeodomain Protein KNOTTED1. Plant Cell.
100. Wolf S, Deom CM, Beachy RN, Lucas WJ.(1989). Movement protein of tobacco mosaic virus modifies plasmodesmata size exclusion limit. Science 246:377–79
101. Wolf, S., Deom, C.M., Beachy, R.N., and Lucas, W.J. (1989). Movement protein of tobacco mosaic virus modifies plasmodesmatal size exclusion limit. Science 246, 377-379.
102. Yahalom A, Lando R, Katz A, Epel BL. (1998). Acalcium-dependent protein kinase is associated with maize mesocotyl plasmodesmata. J. Plant Physiol. 153:354–62

103. Yoo, B.C., Kragler, F., Varkonyi-Gasic, E., Haywood, V., Archer-Evans, S., Lee, Y.M., Lough, T.J., and Lucas, W.J. (2004). A systemic small RNA signaling system in plants. Plant Cell 16, 1979-2000.
104. Zambryski, P. (2004). Cell-to-cell transport of proteins and fluorescent tracers via plasmodesmata during plant development. J Cell Biol 164, 165-168.
105. Zambryski, P., and Crawford, K. (2000). Plasmodesmata: gatekeepers for cell-to-cell transport of developmental signals in plants. Annu Rev Cell Dev Biol 16, 393-421.

ACKNOWLEDGEMENTS

Allen voran möchte ich von ganzem Herzen Dewi Kamitz danken, die mich als langjährige Freundin nicht nur hilfreich durchs Studium sondern auch durch eine sehr schwierige Zeit begleitet hat. Danke für die vielen Stunden des Zuhörens

Zu großem Dank bin ich ebenfalls Fritz Kragler verpflichtet, der mir die Möglichkeit gab im Rahmen dieser Arbeit die Erfahrung zu machen was es heißt Wissenschaftler bzw. Forscher zu sein. Danke auch für die Nachsicht und die Fairness die du mir gegenüber bewiesen hast.

Im weiteren möchte ich einige Namen anführen ohne deren Unterstützung geistiger wie auch körperlicher Natur, Protokolle, Tipps & Tricks, Ideen und aufbauende Worte ich die praktische Arbeit im Labor niemals bewältigt hätte: Niko Winter, Veerle de Wever, Daniela Fichtenbauer, Eva Klopf, Andreas Rötzer und Kornelia Pranjic.

Zum Abschluss noch einige Namen von Leuten die meine Psyche intakt gehalten oder mich anderwärtig tatkräftigst unterstützt haben: Meine Mutter & mein Vater ohne die wohl gar nichts gegangen wäre. Norwin Kollwig, Astrid Meingaßner, Andrea Heitzer, Bettina Strobel & Christine Scheffknecht, Georg Feichtinger und Ara Hacobian.

Da es ein „wenig“ länger gedauert hat diese Arbeit zu vollenden, ist wohl jedem klar dass ich diese Liste wohl beliebig fortsetzen kann. Aus diesem Grunde spreche ich hiermit auch allen nicht angeführten Personen meinen aufrichtigen Dank aus. Ohne euch alle wäre ich nicht da wo ich jetzt bin.

CURRICULUM VITAE

PERSONAL DETAILS

Name:	Gregor Kollwig
Date of birth:	17.03.1980
Place of birth:	St.Pölten
Nationality:	Austria

EDUCATION

2006 – 2007	Diplomathesis at the MFPL Vienna / Univ. Doz. Dr. Kragler
1999 - 2006	Study of Biology/Genetics at the University of Vienna
1994 – 1999	HTBLuVA Mödling / Matura in Mechatronic
1990 – 1994	Secondary modern school Neulengbach
1986 – 1990	Primary school Neulengbach

INTERNSHIP & ADDITIONAL WORK

07/2000	Internship at BAXTER AG Austria / Section for Biochemical control
04/2008 – 04/2009	Ludwig Boltzmann Institute for Experimental and Clinical Traumatology Austrian Cluster for Tissue Regeneration – Molecularbiology/ Mag. Feichtinger; Establishment of a GATEWAY based vector library
04/2010 –	Max F. Perutz Laboratorys / Univ. Doz. Dr. Kragler; Establishment of doublehaploid pollen in cooperation with Rijk Zwaan

PUBLICATION

2007 Nikola Winter,* Gregor Kollwig,* Shoudong Zhang and Friedrich Kragler (2007) “MPB2C, a Microtubule-Associated Protein, Regulates Non-cell-Autonomy of the Homeodomain Protein KNOTTED1”. Plant Cell. (*equal contributions)